

สำนักหอสมุดกลาง พระจอมเกล้าลาดกระบัง

AN EXPERIMENTAL PERFORMANCE STUDY OF  
A RANQUE-HILSCH VORTEX TUBE



เลขหม.....  
เลขทะเบียน..... 35749  
วัน, เดือน, ปี..... - ๒๕๔๓

A THESIS SUBMITTED IN PARTIAL FULFILLMENT  
OF THE REQUIREMENT FOR THE DEGREE OF  
MASTER OF ENGINEERING IN MECHANICAL ENGINEERING  
SCHOOL OF GRADUATE STUDIES  
KING MONGKUT'S INSTITUTE OF TECHNOLOGY LADKRABANG

2000

ISBN 974-622-904-4

This material is reserved for educational use only, not allowed for commercial use.

Forbidden to modify the content, and cite the document when use.



**COPYRIGHT 2000**

**SCHOOL OF GRADUATE STUDIES**

**KING MONGKUT'S INSTITUTE OF TECHNOLOGY LADKRABANG**

This material is reserved for educational use only, not allowed for commercial use.

Forbidden to modify the content, and cite the document when use.

หัวข้อวิทยานิพนธ์	การศึกษาสมรรถนะเชิงทดลองของท่อ Ranque-Hilsch vortex
นักศึกษา	นาย สมิทธิ์ เอี่ยมสอาด
รหัสประจำตัว	41062008
ปริญญา	วิศวกรรมศาสตรมหาบัณฑิต
สาขาวิชา	วิศวกรรมเครื่องกล
พ.ศ.	2543
อาจารย์ผู้ควบคุมวิทยานิพนธ์	ผศ.ดร.พงษ์เจต พรหมวงศ์

### บทคัดย่อ

วิทยานิพนธ์ฉบับนี้ ได้ทำการศึกษาถึงสมรรถนะเชิงทดลองของท่อ Ranque-Hilsch vortex ในการลดลงของอุณหภูมิที่ท่อด้านอากาศเย็นได้สูงสุด โดยทำการพิจารณาถึงการปรับเปลี่ยนขนาดค่าต่างๆของท่อวอร์เทกซ์ คือ อัตราส่วนขนาดแผ่นออริฟิส ( $d/D$ ) และจำนวนหัวฉีดที่ทางเข้าท่อวอร์เทกซ์ ที่มีผลต่อค่าการลดลงของอุณหภูมิในการนำความเย็นและการกระจายอุณหภูมิภายในผนังท่อวอร์เทกซ์ โดยพบว่าที่ขนาดค่าอัตราส่วนรูแผ่นออริฟิสที่ ( $d/D$ ) เท่ากับ 0.5, ที่จำนวนหัวฉีดที่ทางเข้าสู่ท่อวอร์เทกซ์เท่ากับ 4 รู, ที่ค่าการปรับวาล์วควบคุมให้ได้ค่าอัตราส่วนมวลของอากาศเย็น ( $\mu_c$ ) เท่ากับ 0.328 และที่ขนาดเส้นผ่านศูนย์กลางของท่อวอร์เทกซ์เท่ากับ 16 mm จะให้ค่าการลดลงของอุณหภูมิด้านอากาศเย็นสูงสุดเท่ากับ  $-30^{\circ}\text{C}$  และการเพิ่มขึ้นของอุณหภูมิด้านอากาศร้อนสูงสุดเท่ากับ  $78^{\circ}\text{C}$  โดยจะมีแนวโน้มการกระจายของอุณหภูมิที่ผนังท่อมากขึ้นตามค่าอัตราส่วนมวลของอากาศเย็น ( $\mu_c$ ) และจะมีค่าลดลงของอุณหภูมิที่ค่าอัตราส่วนมวลของอากาศเย็นเข้าใกล้ 1 และได้ทำการศึกษาการวิเคราะห์ตัวแปรไร้มิติและความคล้ายทางรูปร่าง ในการช่วยหาสมการในการจะหาค่าช่วงการทำงานของท่อวอร์เทกซ์ในการผลิตอากาศเย็นได้สูงสุด

<b>Thesis Title</b>	An Experimental Performance Study of a Ranque-Hilsch Vortex Tube
<b>Student</b>	Mr. Smith Eiamsa-ard
<b>Student ID.</b>	41062008
<b>Degree</b>	Master of Engineering
<b>Programme</b>	Mechanical Engineering
<b>Year</b>	2000
<b>Thesis Advisor</b>	Asst.Prof.Dr. Pongjet Promvonge

### ABSTRACT

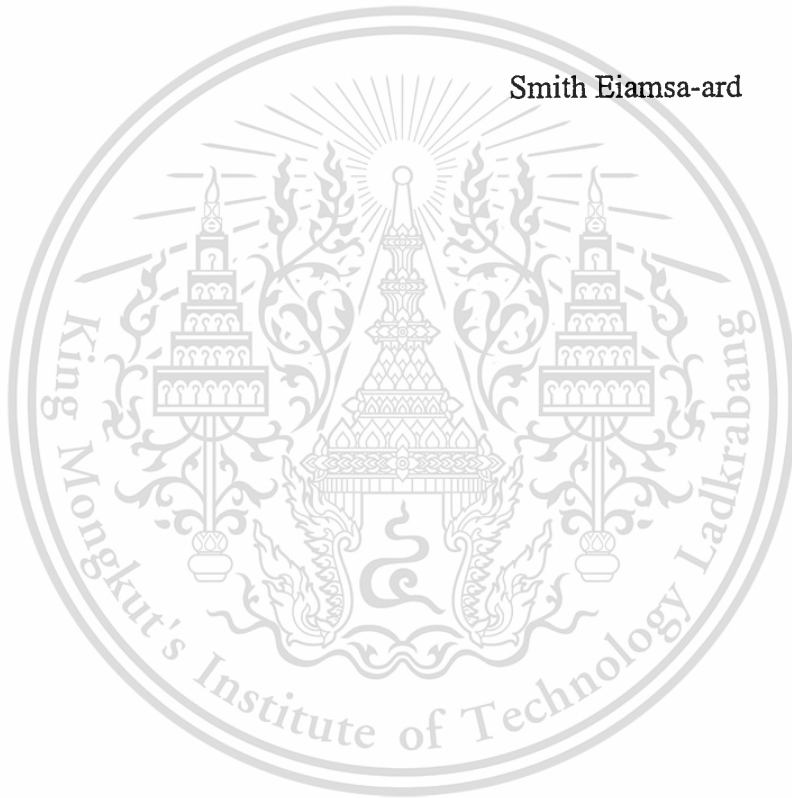
The thesis presents the experimental performance study of a Ranque-Hilsch vortex tube with a view to obtaining a maximum temperature difference at the cold tube. To investigate the effect of the various parameters on the temperature difference, the experiments were made by varying the ratio of orifice to tube diameters and the number of the inlet nozzles of the tube. From experimental results, the maximum temperature reduction at the cold side and the maximum increase in temperature at the hot side in comparison with the inlet temperature are  $-30^{\circ}\text{C}$  and  $78^{\circ}\text{C}$  respectively, for the orifice plate ratio ( $d/D$ ) of 0.5, 4 inlet nozzles, the cold mass fraction ( $\mu_c$ ) of 0.328 and diameter of the vortex tube of 16 mm. In addition, wall temperature distribution tends to increase proportionally to the cold mass fraction ( $\mu_c$ ) but tends to decline as the cold mass fraction approaches to unity.

The dimensional analysis and the similarity geometry were carried out to yield the empirical correlation for use in a vortex tube design with optimal performance.



I would like to dedicate all of the excellence and the efforts at this study work to everyone whose names were mentioned above. Without their encouragement and great assistance, this thesis might have remained only on dream. May the merit accrued from this meritorious deed increase their paramis and perfection's and bring them limitless blessing of good health and happiness. May The Triple Gems, Our Lord Buddha and all of the Holy things in the universe bless them with excellent hearth, wealth greatest wisdom, happiness, prosperity, success, security and good luck through their loves.

Smith Eiamsa-ard



This material is reserved for educational use only, not allowed for commercial use.

Forbidden to modify the content, and cite the document when use.

# CONTENTS

	Page
<b>THAI ABSTRACT .....</b>	<b>I</b>
<b>ENGLISH ABSTRACT .....</b>	<b>II</b>
<b>ACKNOWLEDGMENTS .....</b>	<b>III</b>
<b>LIST OF FIGURES .....</b>	<b>VII</b>
<b>LIST OF TABLES .....</b>	<b>X</b>
<b>NOMENCLATURE.....</b>	<b>XI</b>
<b>CHAPTER 1 INTRODUCTION.....</b>	<b>1</b>
1.1 Background of the Ranque-Hilsch Vortex Tube .....	1
1.2 The Work of Ranque-Hilsch Vortex Tube .....	1
1.3 Objectives of the Study.....	2
1.4 The Hypothesis of the Study.....	3
1.5 The Procedure of the Study.....	3
1.6 The Scopes of the Research .....	3
1.7 The Expected Results.....	3
<b>CHAPTER 2 LITERATURE REVIEW.....</b>	<b>4</b>
2.1 Introduction.....	4
2.2 The Past Research Work.....	4
2.3 The Application of Research Study to Industrial Development.....	15
<b>CHAPTER 3 THEORY AND MECHANISM OF THE RANQUE-HILSCH</b>	
<b>VORTEX TUBE.....</b>	<b>18</b>
3.1 Ranque-Hilsch Vortex Tube .....	18
3.2 Types of Vortex Tubes .....	18
3.2.1 Counter Flow Vortex Tube .....	18
3.2.2 Uni-Flow Vortex Tube.....	20
3.3 Hypothesis on the Mechanism of the Vortex Separation Effect.....	20
3.4 Thermodynamics: The First and Second Laws in Vortex tube .....	21
3.4.1 First Law Analysis .....	21

# CONTENTS (CONTINUED)

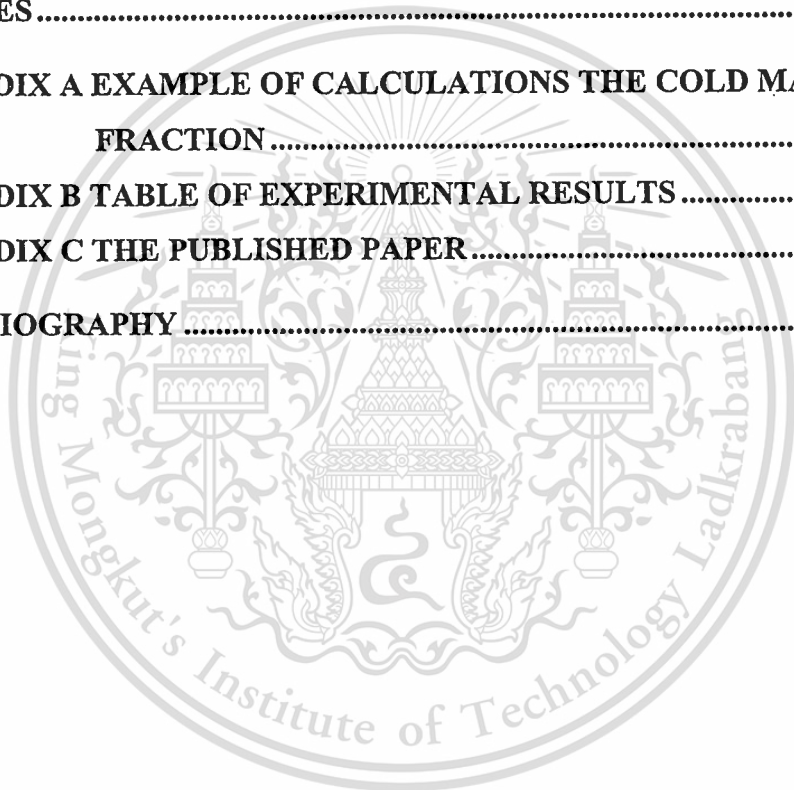
	Page
3.4.2 Second Law Analysis.....	22
3.5 Parameter Indicating Vortex Tube Performance .....	24
3.5.1 Cooling Air Ratio per unit of Air Inlet in the Vortex Tube.....	24
3.5.2 Cooling Efficiency in Thermodynamics of the Vortex Tube .....	25
3.5.3 Coefficient of Performance.....	27
<b>CHAPTER 4 EXPERIMENTAL APPARATUS AND PROCEDURE .....</b>	<b>29</b>
4.1 Experimental Set-Up.....	29
4.2 Equipment and Measurement Device .....	30
4.2.1 The Hot and the Cold of the Vortex Tube.....	30
4.2.2 Nozzles at the Inlet of the Vortex Chamber.....	31
4.2.3 Orifice Plates.....	32
4.2.4 Cone Valve.....	33
4.2.5 Air Compression .....	33
4.2.6 Measurement Devices .....	34
4.2.6.1 The Flow Measuring Devices .....	34
4.2.6.2 Temperature Measuring Devices .....	35
4.3 Procedure of Experimentation .....	36
<b>CHAPTER 5 EXPERIMENTAL RESULTS AND DISCUSSION .....</b>	<b>38</b>
5.1 Insulated and Non-Insulated Vortex Tube.....	38
5.2 Inlet Pressure of Insulated Vortex Tube .....	40
5.3 Wall Temperature Distribution along the Insulated Vortex Tube .....	42
5.4 Parametric Study of the Insulated Vortex Tube.....	43
5.4.1 The Influence of the Orifice Plates Size .....	43
5.4.2 The Influence of the Number of Inlet Nozzles.....	44
5.5 Comparison with Previous Work.....	46
5.6 Empirical Relationship of the Insulated Vortex Tube .....	48
5.7 Rate of Cooling and Coefficient of Performance .....	53

This material is reserved for educational use only, not allowed for commercial use.

Forbidden to modify the content, and cite the document when use.

# CONTENTS (CONTINUED)

	Page
<b>CHAPTER 6 CONCLUSION AND RECOMMENDATION .....</b>	<b>55</b>
6.1 Research Summary .....	55
6.2 Recommendation .....	56
<b>BIBLIOGRAPHY .....</b>	<b>57</b>
<b>APPENDICES .....</b>	<b>62</b>
<b>APPENDIX A EXAMPLE OF CALCULATIONS THE COLD MASS         FRACTION .....</b>	<b>63</b>
<b>APPENDIX B TABLE OF EXPERIMENTAL RESULTS .....</b>	<b>69</b>
<b>APPENDIX C THE PUBLISHED PAPER .....</b>	<b>84</b>
<b>AUTHOR BIOGRAPHY .....</b>	<b>91</b>



# LIST OF FIGURES

Figure	Page
1.1 The Ranque-Hilsch vortex tube .....	1
1.2 Operation of vortex tube (a) Counter flow vortex, (b) Uni-flow vortex or parallel flow vortex. ....	2
2.1 Hilsch vortex tube in 1947.....	6
2.2 Vortex chamber by Martynovskii and Alekseev (1956).....	6
2.3 Uni-flow vortex tube type (a) Hot wire anemometer for measurements velocity and temperature (b) Vortex chamber by Lay (1959) .....	6
2.4 Streamline of uni-flow vortex tube by Cockerill. (1994) .....	10
2.5 Simulation of 3-Dimension velocity by David and Bart (1995).....	10
2.6 Grid with representation of the arithmetic mean of the relation after the correlation from Keys (Frohlingdorf and Unger, 1999) .....	11
2.7 Contour of Velocity of Bruun vortex tube by the CFX code (Frohlingdorf and Unger, 1999) .....	11
2.8 Contour of total temperature and velocity of Eckert and Hartnett vortex tube by the ASM (Promvonge, 1999).....	12
2.9 Contour of total temperature and velocity of Bruun vortex tube by the ASM (Promvonge, 1999) .....	12
2.10 Vortex tube appliance and air conditioning in the work of cooler Exair Co., (1998).....	15
2.11 Cooling in different processes (Newman Tools Inc.,1998) .....	16
3.1 Counter flow vortex tube type .....	18
3.2 Vortex tube with 1, 2 and 4 inlet nozzles.....	19
3.3 Flow pattern in a counter flow vortex tube type .....	19
3.4 Uni-flow vortex tube type or parallel flow vortex tube type .....	20
3.5 Uni-flow vortex tube type or parallel flow vortex tube type .....	20
3.6 Temperature distribution in the vortex tube.....	21
3.7 Diagram of thermodynamic in the vortex tube.....	23
3.8 Mass, pressure and temperature at the inlet and exit of the hot and cold tube .....	24
3.9 T-s isentropic process diagram .....	26

This material is reserved for educational use only, not allowed for commercial use.

Forbidden to modify the content, and cite the document when use.

# LIST OF FIGURES (CONTINUED)

Figure	Page
4.1 The working system of the Ranque-Hilsch vortex tube.....	29
4.2 The Ranque–Hilsch vortex tube.....	30
4.3 Hot tube and the cold tube . ....	31
4.4 The vortex chamber with 1, 2 and 4 inlet nozzles. ....	32
4.5 The orifice plates with the ratio ( $d / D$ ) equivalent to $0.4D$ to $0.9D$ .....	32
4.6 The cone valve controlling the flow was equipped with the hot tube connection.	33
4.7 The orifice meter.....	35
4.8 Thermocouple type K .....	35
4.9 The insulated at the Ranque –Hilsch vortex tube. ....	35
4.10 The set of Ranque-Hilsch vortex tube apparatus. ....	36
5.1 Temperature differences at various cold mass fractions between insulated and non-insulated tubes for inlet pressure at 3.5 bar .....	39
5.2 Effect of inlet pressures on the increasing temperature at the hot tube and the temperature reduction at the cold tube.....	41
5.3 Location of temperature to be measured in the insulated vortex tube.. ....	42
5.4 Axial wall temperature distribution .. ....	42
5.5 Influence of the orifice plates size on temperature reduction.....	44
5.6 Influence of the number of the inlet nozzles on temperature reduction... ..	45
5.7 Comparison of temperature reduction in the cold tube among the present work, Hilsch work (1947) and Stephan work (1983).....	46
5.8 Comparison of the non-dimensional temperature reduction at the cold tube among the present work, Hilsch’s and Stephan’s work.....	47
5.9 Dimension of the vortex tube.....	49
5.10 Temperature reduction at various orifice plates of $0.4D$ to $0.5D$ and for 2 and 4 inlet nozzles.. ....	51
5.11 Non-dimensional temperature reduction at various orifice plates of $0.4D$ to $0.5D$ and for 2 and 4 inlet nozzles.....	51
5.12 The temperature reduction in the cold tube with the inlet pressure at 2.0, 3.0 and 3.5 bars .....	53

This material is reserved for educational use only, not allowed for commercial use.

Forbidden to modify the content, and cite the document when use.

# LIST OF TABLES

Table	Page
2.1 Summary of experimental studies.....	13
2.2 Summary of computer numerical studies .....	14
4.1 Summary of the data of the Ranque–Hilsch vortex tube. ....	34
5.1 Comparison of the present tube with Hilsch’s tube and Stephan’s tube.....	45
5.2 Summary of different independent parameter equations. ....	47
5.3 Summary of independent variables.....	47



# NOMENCLATURE

$m_i$	Mass flow rate of air at the inlet vortex tube
$m_c$	Mass flow rate of cold air at the exit of the cold tube
$m_h$	Mass flow rate of hot air at the exit of the hot tube
$P_i$	Pressure at the inlet of the vortex tube
$P_c$	Pressure at the exit of the cold tube
$P_h$	Pressure at the exit of the hot tube
$T_i$	Temperature at the inlet of the vortex tube
$T_c$	Temperature at the exit of the cold tube
$T_h$	Temperature at the exit of the hot tube
$T_0$	Stagnation temperature at the inlet air
$T_{jt}$	Joule Thomson
$(\Delta T)_c$	Difference of temperature reduction
$(\Delta T)_{isen}$	Difference of temperature reduction in isentropic process
$C.O.P$	Coefficient of performance
$Q_c$	Cooling rate per unit of air inlet in the vortex tube
$w$	Mechanical energy in cooling per unit of air inlet the tube
$\Delta P$	Pressure drop at orifice plate
$\rho_1$	Density at the pre-orifice plates entry
$C$	Coefficient of discharge
$E_M$	Mechanical energy flux
$h_0$	Stagnation enthalpy
$d/D$	Diameter ratio of orifice plate
$k$	Conductivity
$c_p$	Specific heat at pressure constant
$c_v$	Specific heat at volumn constant
$L_h$	Length of the hot tube

This material is reserved for educational use only, not allowed for commercial use.

Forbidden to modify the content, and cite the document when use.

$L_c$	Length of the cold tube
$D$	Diameter of the vortex tube
$N$	Number of the inlet nozzles
$T$	Thickness of the vortex chamber
$t$	Thickness of orifice plate
$Ma$	Mach number
$Re$	Reynolds number
$Eu$	Euler's number

### Greek Symbols

$\mu_c$	Cold mass fraction.
$\mu$	Dynamic viscosity
$\delta$	Diameter of nozzle
$\epsilon$	Expandability factor
$\gamma$	Specific density
$\eta_c$	Cooling efficiency

### Abbreviations

k- $\epsilon$ model	k-Epsilon model
RSM	Reynolds Stress model
ASM	Algebraic Reynolds Stress model
LDV	Laser Dropper Velocimetry
CFX	Code system CFX

# CHAPTER 1

## INTRODUCTION

### 1.1 Background of the Ranque-Hilsch Vortex Tube

Vortex flows or swirl flows have been of considerable interest over the past decades because of their occurrence in industrial applications, such as furnaces, gas-turbine combustors and dust collectors (Gupta *et al.*, 1984). Vortex (or high swirl) can also produce a hot and a cold stream in a Ranque-Hilsch vortex tube (Promvonge, 1997, 1999). The vortex tube has been used in industrial applications of cooling and heating processes because of a simple, compact, light and quiet (in operation) device as shown in Fig. 1. (Bruno 1992, 1993). The physical phenomena of energy separation in vortex tube has not been well explained by attempts, both theoretical and experimental, to describe the phenomenon. The present survey has come across many of experimental researches but few of numerical simulations of such flows. Since vortex flow phenomenon taking place in a vortex tube is compressible and complex, the simulation and solution of turbulent vortex flows is a difficult and challenging task.

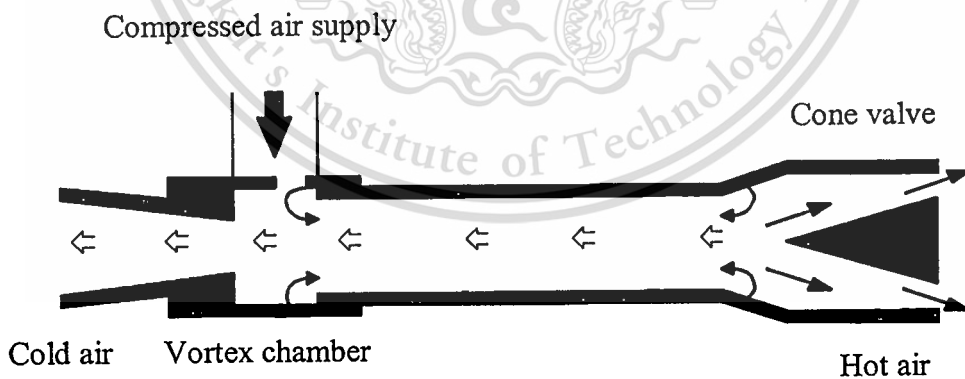


**Figure 1.1** The Ranque-Hilsch vortex tube

### 1.2 The Work of Ranque-Hilsch Vortex Tube

Ranque-Hilsch vortex tube (or vortex tube) is a device enabling producing the hot and cold air when the compressed air flows tangentially into the vortex chamber through the inlet nozzles. This causes the vortex and swirl flow movement inside the

vortex tube. The air in the middle region of the tube has a lower velocity and lower temperature than the inlet air. So the air near the wall tube has higher velocity and higher temperature than the inlet air. The cold air in the core region of the tube flows out through orifice plate opposite way of the cone valve which the hot air near the wall tube flows out through the cone valve as shown in Fig. 1.2(a). The mass flow rate of the hot air and cold air can be controlled by the cone valve.

Generally vortex tube are divided into 2 type; one is the counter flow vortex tube type referred as a standard type. The other is the uni-flow vortex tube type as shown in Fig. 1.2.

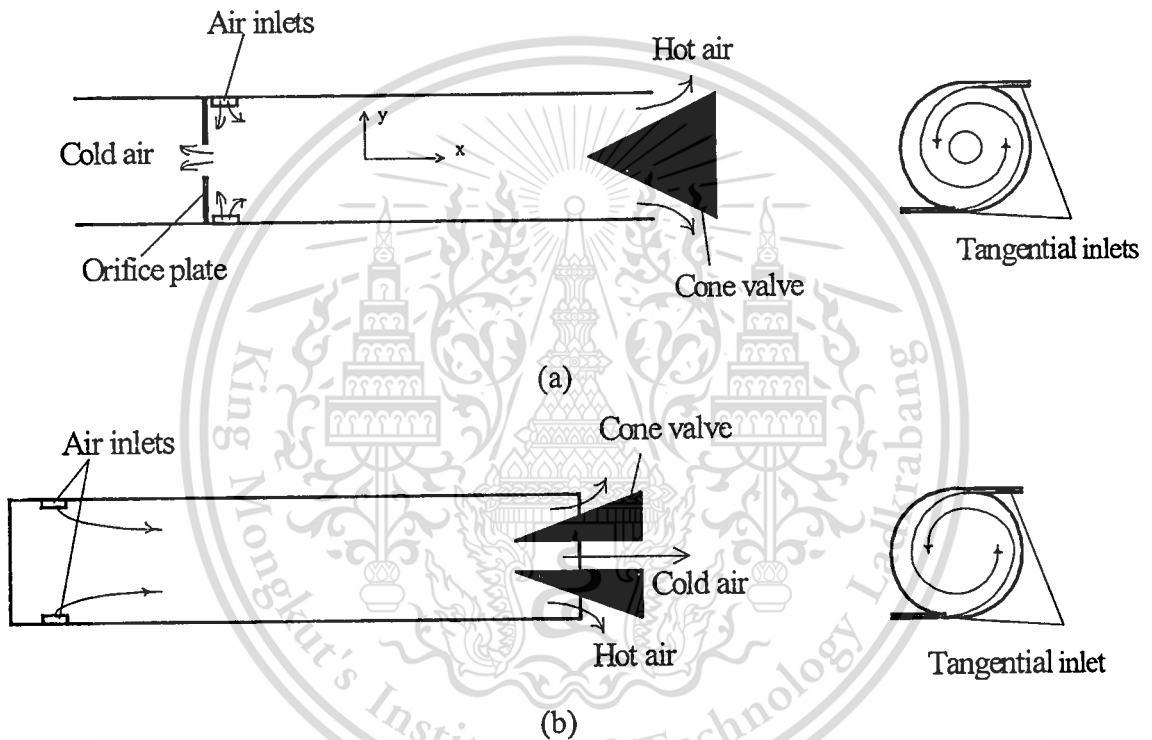


**Figure 1.2** Operation of vortex tube (a) Counter flow vortex, (b) Uni-flow vortex or parallel flow vortex.

### 1.3 Objectives of the Study

- 1.3.1 To evaluate the influence of the orifice plate size ( $d/D$ ) upon the temperature reduction of cooling of counter flow vortex tube type.
- 1.3.2 To evaluate the influence of the numbers of the inlet nozzles ( $N$ ) on the temperature reduction of cooling of counter flow vortex tube type.
- 1.3.3 To evaluate the influence of the number of inlet nozzles on the distribution of wall temperature along the vortex tube.

This material is reserved for educational use only, not allowed for commercial use.

Forbidden to modify the content, and cite the document when use.

- 1.3.4 To evaluate the result of the experimental for the equation for optimizing the working point of vortex tube.

## 1.4 Hypothesis of the Study

- 1.4.1 The fluid flowing through the vortex tube is a compressible fluid.
- 1.4.2 The behavior of flow in the vortex tube is a steady axisymmetrical compressible flow, neglecting body force and any an energy source
- 1.4.3 The changes in temperature inside the vortex tube occur under the condition which the flow undergoes isentropic process.

## 1.5 The Procedure of the Study

- 1.5.1 Changes the geometry shapes and sizes of vortex tube and study their influence on the distribution and the temperature reduction inside the vortex tube.
- 1.5.2 Adjust the cone valve at the end of the hot air tube could help control in the mass flow rate of cold air which led to decreasing the highest temperature inside the vortex tube.

## 1.6 The Scopes of the Research

- 1.6.1 Experimentation in counter flow vortex tube type.
- 1.6.2 Evaluation through selection the size of orifice plates ( $d/D$ ) the ranges were from  $0.4D$  to  $0.9D$ .
- 1.6.3 Evaluation through selecting the number of nozzle ( $N$ ) with the inlet vortex tube equivalent to 1, 2 and 4 nozzles.
- 1.6.4 Experimentation in the inlet pressure ( $P_i$ ) with the results ranges from 2.0 to 3.5 bar (gage).

## 1.7 The Expected Results

Referring to the studied research, the ratio of the vortex tube were found selectable and utilized efficiently for the coldest value in energy working period, thus leading to hypothesis of possible factor avoiding polluting the environmental protection with the most beneficial advantage of application in industries developments.

# CHAPTER 2

## LITERATURE REVIEW

### 2.1 Introduction

Several researchers had put a lot of effort to give the best and clear explanation for the phenomena occurring during the energy separation inside vortex tube ; however, only the inexplicable answer shown. Research studies about these phenomena were formed mainly into 2 groups. The first group performed the experimental research and then through the value of the results to make explanation. The experimentation research method was done into 2 components. The first component studies the size of the parameter, which were differently variable according to the size of the vortex tube. The objectives of this method were to find out the values of performance at the coldest air conditioning. The second component deeply focussed on the systems of the energy separation inside the vortex tube as well as the flow pattern inside the vortex tube available from the pressure, velocity and temperature distribution patterns inside the vortex tube. Accordingly, the results decreased the explanation of the phenomena inside the vortex tube.

The second group performed the study method in the numerical and mathematical model way in order to help in analysis the results through mathematical model application for instance ; the  $k$ -Epsilon model ( $k$ - $\varepsilon$  model), Reynolds stress model (RSM) and Algebraic Reynolds stress model (ASM). The results obtained from the calculation were brought to make comparison with the past results and were explicable for the phenomena of the energy separation inside the vortex tube (Wilcox, 1993; Promvonge,1997).

### 2.2 The Past Research Work

The vortex tube was invented quite by accident in 1928. Ranque, a French physics student, was experimentation with a vortex-tube pump he had developed when he noticed hot air exhausting from one end side, and cold air from other side tube. Ranque soon forgot about his pump and started a small firm to exploit the

commercial potential for his strange device that produced hot and cold air with no moving parts. However, it soon failed.

Interest in the vortex tube has been increasing rapidly in this country since the publication here of the experimental work done in Germany by Hilsch (1947). In this basic work Hilsch determined tube proportions for optimum performance and overall performance data over a wide range of pressures as in Fig. 2.1.

Much earlier, the great nineteenth century physicist, James Clerk Maxwell postulated that since heat involves the movement of moleculars, we might someday be able to get hot and cold air from the same device with the help of a friendly little demon who would sort out and separate the hot and cold molecules of air.

After Hilsch (1947), an experimental study was made by Scheper (1951) who measured the velocity, pressure, and total and static temperature gradients in a Ranque-Hilsch vortex tube, using probes and visualization techniques. He concluded that the axial and radial velocity components were much smaller than the tangential velocity. His measurements indicated that the static temperature decreased in a radially outward direction. This result was contrary to most other observations that were made later. Martynovskii and Alekseev (1956) studied experimentally the effect of various design parameters of vortex tube as in Fig. 2.2. The velocity, temperature and pressure profiles agreed with the hypothesis of Fulton (1950) and supported the suggestion of the conversion of a free vortex into a forced vortex inside the tube. They also carried out measurements with  $CH_4$ ,  $CO_2$  and  $NH_3$  as working fluid and compared the cooling effect with that from air under the same conditions.

Hartnett and Eckert (1956, 1957) measured the velocity, total temperature, and total and static pressure distributions inside a uni.-flow vortex tube. They used the experimental values of static temperature and pressure to estimate the values of density and hence, the mass and energy flow at different cross sections in the tube. The results agreed fairly well with the overall mass and energy flow in the tube. Scheller and Brown (1957) presented measurements of the pressure, temperature, and velocity profiles in a standard vortex tube and observed that the static temperature decreased radially outwards as in the work of Scheper (1951), and hypothesized the energy separation mechanism as heat transfer by forced convection. Lay (1959) used a hot-wire anemometer and probes to measure the pressure, temperature and velocity profiles inside a uni.-flow vortex tube as in Fig. 2.3.

This material is reserved for educational use only, not allowed for commercial use.

Forbidden to modify the content, and cite the document when use.

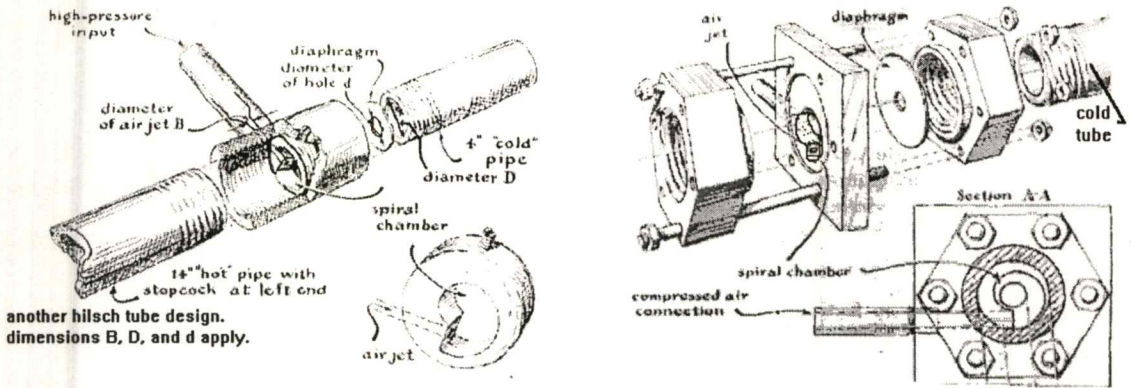


**Figure 2.1** Hilsch vortex tube in 1947

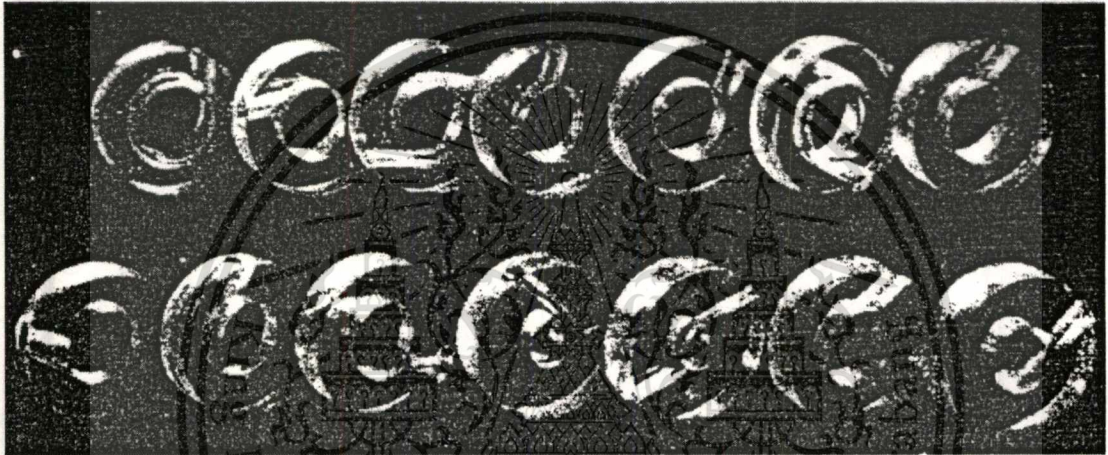
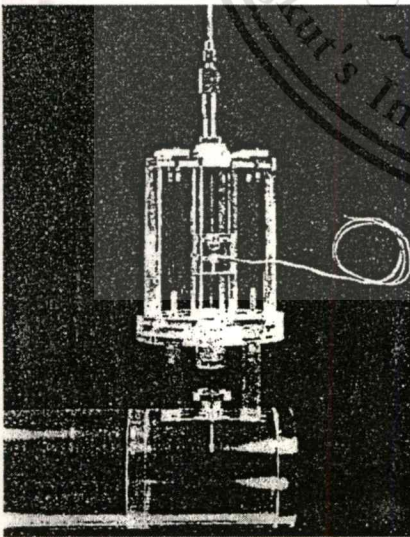
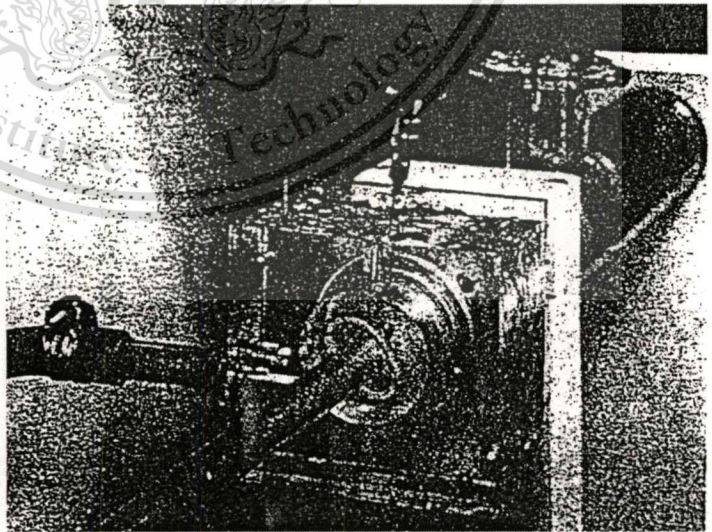


**Figure 2.2** Vortex chamber by Martynovskii and Alekseev (1956)



(a)



(b)

**Figure 2.3** Uni-flow vortex tube type (a) Hot wire anemometer for measurements velocity and temperature (b) Vortex chamber by Lay (1959)

This material is reserved for educational use only, not allowed for commercial use.

Forbidden to modify the content, and cite the document when use.

Blatt and Trusch (1962) investigated experimentally the performance of a uni.-flow vortex tube and improved its performance by adding a radial diffuser to the end of the shortened tube instead of a cone valve. The geometry of the tube was optimised to maximise the temperature difference between the cold and inlet temperatures by changing the various dimensions of the tube such as the gap of the diffuser, tube length, and entrance geometry. Moreover, the effects of inlet pressure and heat fluxes were examined. Erdelyi (1962) postulated that the difference in temperature of the cold and hot air depends only on the type of tube used and the pressure ratio at the inlet and outlet of the vortex tube. Linderstrom-Lang (1964) studied in detail the application of the vortex tube to gas separation, using different gas mixtures and tube geometry and found that the separation effect depended mainly on the ratio of cold and hot gas mass flow rates. The measurements of Takahama (1965) in a counter-flow vortex tube provided data for the design of a standard type vortex tube with a high efficiency of energy separation. He also gave empirical formulae for the profiles of the velocity and temperature of the air flowing through the vortex tube. Takahama and Soga (1966) used the same sets of the vortex tube of Takahama (1965) to study the effect of the tube geometry on the energy separation process and that of the cold air flow rate on the velocity and temperature fields for the optimum proportion ratio of the total area of nozzles to the tube area. They also reported an axisymmetric vortex flow in the tube (Takahama and Kawashima, 1962; Takahama *et al.*, 1971).

Vennos (1968) measured the velocity, total temperature, and total and static pressures inside a standard vortex tube and reported the existence of substantial radial velocity. Bruun (1969) presented the experimental data of pressure, velocity and temperature profiles in a counter-flow vortex tube with a ratio of 0.23 for the cold to total mass flow rate and concluded that radial and axial convective terms in the equations of motion and energy were equally important. Although no measurements of radial velocities were made, his calculation, based on the equation of continuity, showed an outward directed radial velocity near the inlet nozzle and an inward radial velocity in the rest of the tube. He reported that turbulent heat transport accounted for most of the energy separation.

Williams (1971) studied a counter-flow type vortex tube with methane and Algerian natural gas with a high methane content, to study the effects of gas supply temperature and pressure. He reported that the cooling effect decreased with inlet

temperature and was absent at the gas liquefaction point, depending on the pressure expansion ratio across the tube. Soni (1973) tested 170 different standard vortex tube geometries with inlet pressures up to 3 atm to determine the optimal design for each of two criteria, namely the minimum cold temperature and maximum energy separation performance. Only the inlet and cold air flow rates, the inlet air pressure and temperature, and the cold and hot air temperatures were measured and an evolutionary operation technique was used to determine the optimal performance. He presented empirical correlation's for the tube performance and found that the performance of the tube had a significant degree of tolerance to derivation for the optimum design parameters and established, as a result, a relatively simple design procedure based on the pressure drop across the nozzles and the orifice (see also Soni and Thomson, 1975).

Nash (1974) used vortex expansion techniques for high temperature cryogenic cooling, applying for infrared detector applications. A summary of the design parameters of the vortex cooler was reported by Nash (1975), (1991). Marshall (1977) used several different gas mixtures in a variety of sizes of vortex tube and confirmed the effect of the gas separation reported by Linderstrom-Lang (1964). A critical inlet Reynolds number was identified at which the separation was a maximum. Takahama *et al.* (1979) investigated experimentally the energy separation performance of a steam-operated standard vortex tube and reported that the performance worsened with wetness of steam at the nozzle outlet because of the effect of evaporation. Energy separation was absent with the dryness fraction less than around 0.98. The measurements of Collins and Lovelace (1979) with a two-phase, liquid-vapour mixture, propane in a standard counter-flow vortex tube showed that for an inlet pressure of 0.791 MPa, the separation remained significant for a dryness fraction above 80% at the inlet. With a dryness fraction below 80%, the temperature separation became insignificant. But the discharge enthalpies showed considerable differences indicating that the Ranque-Hilsch process is still in effect.

Takahama and Yokosawa (1981) examined the possibility of shortening the chamber length of a standard vortex tube by using divergent tube for the vortex chamber. Earlier researchers such as Parulekar (1961), Otten (1958), and Raiskii and Tunkel (1974) also employed divergent tube for all or part of the vortex chamber in attempts to shorten the chamber and improve energy separation performance, but their emphasis was on the maximum and minimum temperatures in the outflowing streams.

Therefore, Takahama and Yokosawa (1981) compared their results with those from the straight vortex chambers. They found that the uses of a divergent tube with a small angle of divergence led to an improvement in temperature separation and enable the shortening of the chamber. Kurosaka *et al.* (1982) carried out an experiment to study the total temperature separation mechanism in a uni.-flow vortex tube to support their analysis and concluded that the mechanism of energy separation in the tube is due to acoustic streaming induced by the vortex whistle. Schlenz (1982) investigated experimentally the flow field and the energy separation in a uni.-flow vortex tube with an orifice rather than a conical valve to control the flow. The velocity profiles were measured by using laser-doppler velocimetry (LDA), supported by flow visualization.

Experimental studies of a large counter-flow vortex tube with short length by Amitani *et al.* (1983) indicated that the shortened vortex tube of 6 tube diameters length had the same efficiency as a longer and smaller vortex tube when perforated plates are equipped to stop the rotation of the stream in the tube. Stephan *et al.* (1983) measured temperatures in the standard vortex tube with air as a working medium in order to support a similarity relation of the cold gas exit temperature with the cold gas mass ratio, established using dimensional analysis. Kuwattanachai (1985) made the experimentation on a changing in the diameter of the vortex tube and the pressure within various values affecting the cold performance. It was found that the highest temperature decreased at the cold mass fraction of 0.4

Negm *et al.* (1988a, 1988b) studied experimentally the process of energy separation in the standard vortex tube to support their correlation obtained using dimensional analysis and in a double stage vortex tube which found that the performance of the first stage is always higher than that of the second stage tube. Ahlborn *et al.* (1994) carried out measurements in standard vortex tube to support their models for calculating limits of temperature separation.

Cockerill (1995) had made the research study on Doctoral Degree at Sunderland University. Energy separation ,Temperature as shown in Fig. 2.4. The changing of the flow patterns inside the vortex tube both counter flow vortex tube type and uni.-flow vortex tube type were the significant case studies. The study method were done through evaluating velocity, pressure and temperature. Flow visualization techniques were performed comparing with the past result. The calculation by mathematical model from the basic equation : Navier's stroke equation and the semi-empirical model were performance in order to make comparison with the vortex tube

experimental equipment constructed in the style design by the Linder'strom-Lang's : counter flow vortex tube type. While uni.-flow vortex tube type designed by Lay was found that the mathematical model were in accordance with or in similarity with the result of the experimental studies.

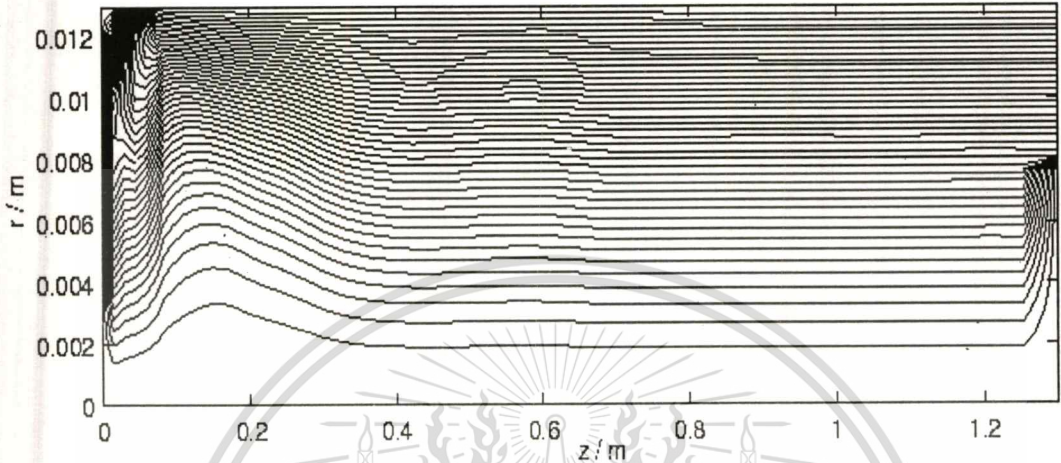


**Figure 2.4** Streamline of uni-flow vortex tube by Cockerill. (1994)

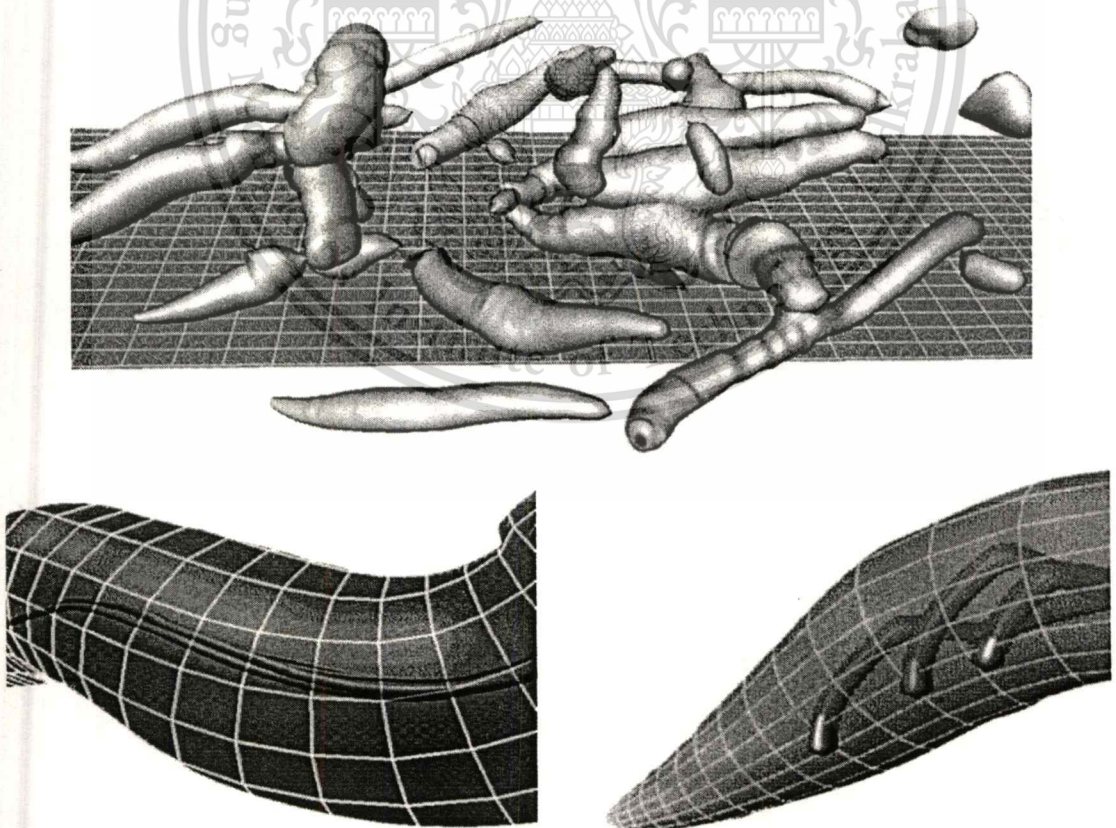


**Figure 2.5** Simulation of 3-Dimension velocity by David and Bart (1995)

This material is reserved for educational use only, not allowed for commercial use.

Forbidden to modify the content, and cite the document when use.

David and Bart (1995) present a new algorithm for identifying vortices in complex flows. The algorithm produces a skeleton line along the center of a vortex by using a two-step predictor-corrector scheme. The vorticity vector field serves as the predictor and the pressure gradient serves as the corrector. We describe an economical depiction of vortex tube's cross-section: a 5-term truncated Fourier series is generally sufficient, and it compresses the representation of the flow by a factor of 4,000 or more. The reconstructed vortex tube are generalized cylinders, providing a polygonal mesh suitable for display on graphics workstation with the Hard disk to 650 GB. He show how to reconstructed geometry of vortex tube can be enhanced to help visualize helical motion in a static image as shown in Fig. 2.5.

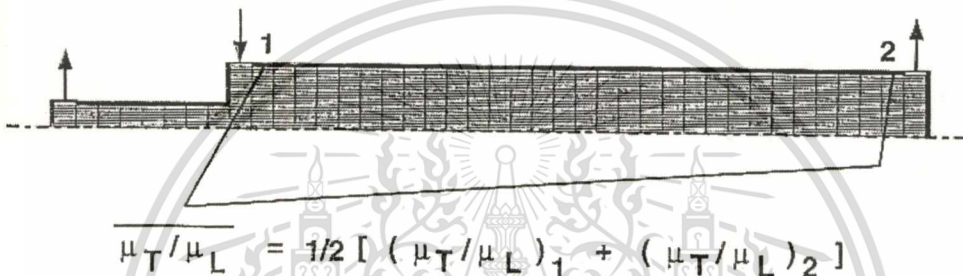


**Figure 2.6** Grid with representation of the arithmetic mean of the relation after the correlation from Keys (Frohlingdorf and Unger, 1999)

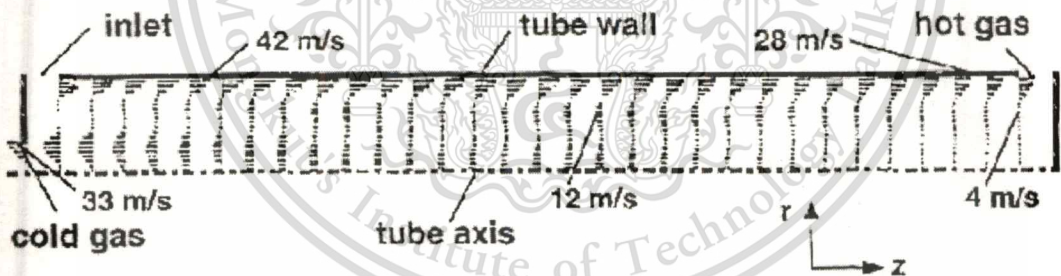


**Figure 2.7** Contour of Velocity of Bruun vortex tube by the CFX code (Frohlingdorf and Unger, 1999)

Frohlingdorf and Unger (1999) study on the depressed flow inside vortex tube (counter flow vortex tube type), the velocity and the phenomena of the energy separation inside the vortex tube were done through Code system CFX and  $k-\varepsilon$  model, the program of finite volume developed by AEA Institute of Technology as shown in Fig. 2.6 and Fig. 2.7. This research study increased the term of Shear-Stress-induced mechanical work. It was found that the results of the calculation velocity and temperature were closed similarity with the past experimental results. (Bruun 1963)

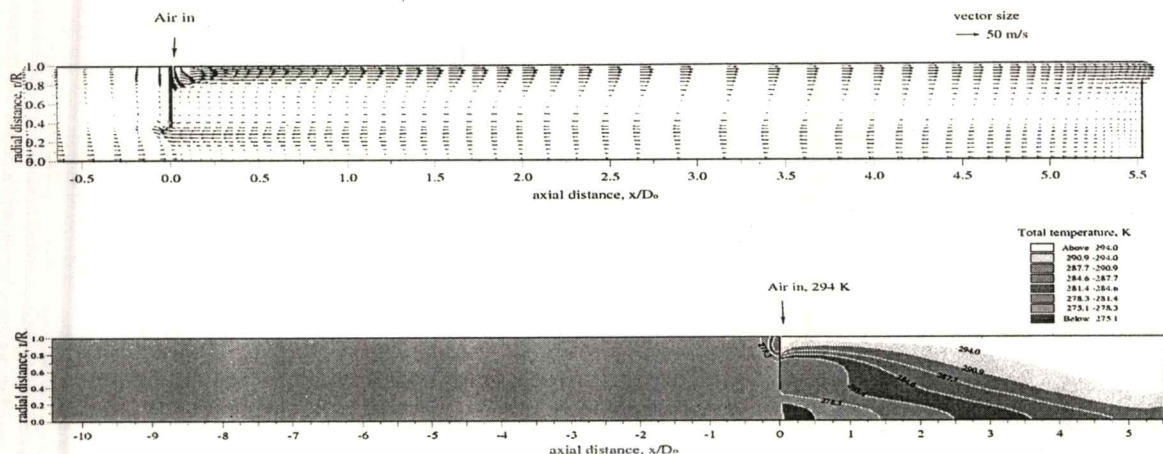


**Figure 2.8** Contour of total temperature and velocity of Eckert and Hartnett vortex tube by the ASM (Promvonge, 1999)

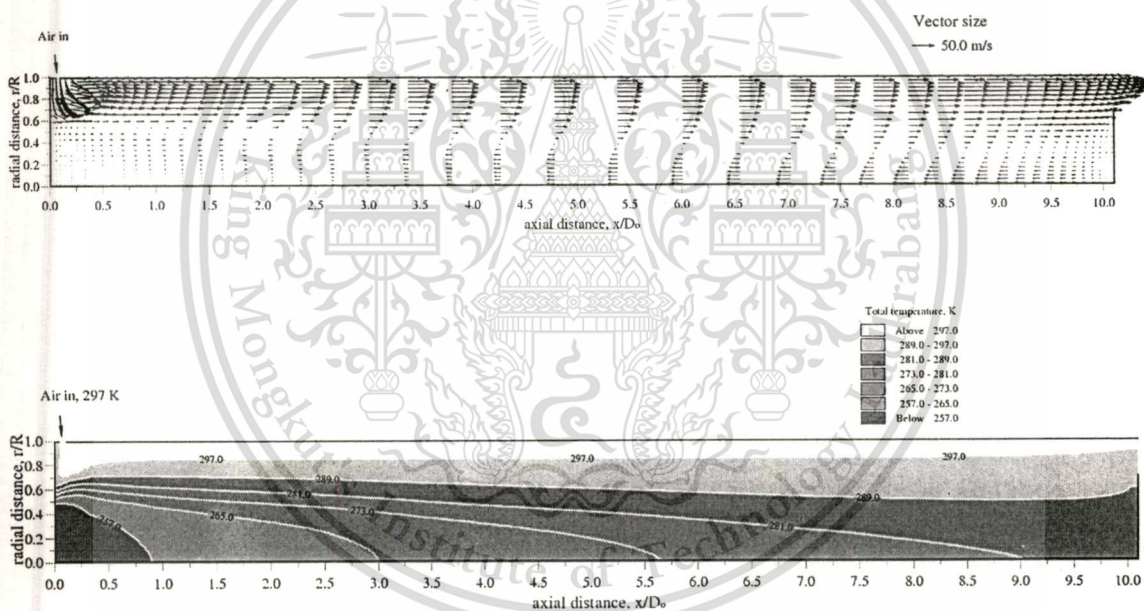


**Figure 2.9** Contour of total temperature and velocity of Bruun vortex tube by the ASM (Promvonge, 1999)

Promvonge (1999) used application of a mathematical model for the simulation of a strongly swirling flow in a vortex tube as shown in Fig. 2.8 and Fig. 2.9. To investigate the effect of numerical diffusion on the predict result. The used of Algebraic Reynolds stress model (ASM) results in more accurate prediction than the  $k-\varepsilon$  model. Besides, influences of the numerical schemes for convection transport are found to be insignificant in this kind of flow.

**Table 2.1** Summary of experimental studies

Year	Studies	Dia.,	$P_i$	Total temperature, °C		$m_c/m_i$
		$D_i$ (mm)	atm (abs.)	$T_h - T_i$	$T_c - T_i$	
1933	Ranque	12	7	38	-32	-
1947	Hilsch	4.6	11	140	-53	0.23
1947	Johnson	4.8	14.6	-	-42.8	0.19
1950	Blaber	9.6	5	68	-40	-
1950	Webster	8.7	-	-	-	-
1951	Scheper	38.1	2	3.9	-11.7	0.26
1956-7	Hartnett and Eckert	76.2	2.4	3.5	-40	-
1956	Martynovskii and Alekseev	4.4/28	12	-	-65	-
1957	Scheller and Brown	25.4	6.1	15.6	-23	0.506
1958	Otten	20	8	40	-50	0.43
1959	Lay	50.8	1.68	9.4	-15.5	0
1960	Suzuki	16	5	54	30	1
1960	Takahama and Kawashima	52.8	-	-	-	-
1962	Sibulkin	44.5	-	-	-	-
1962	Reynolds	76.2	-	-	-	-
1962	Blatt and Trusch	38.1	4	-	-99	0
1965	Takahama	28/78	-	-	-	-
1966	Takahama and Soga	28/78	-	-	-	-
1968	Vennos	41.3	5.76	-1	-13	0.35
1969	Bruun	94	2	6	-20	0.23
1973	Soni	6.4/32	1.5/3	-	-	-

This material is reserved for educational use only, not allowed for commercial use.

Forbidden to modify the content, and cite the document when use.

**Table 2.1** Summary of experimental studies (continued)

1982	Schlenz	50.8	3.36	-	-	-
1983	Stephan <i>et al.</i>	17.6	6	78	-38	0.3
1983	Amitani <i>et al.</i>	800	3.06	15	-19	0.4
1985	Kuwattanachai	9.52	-	-	-29	0.3-0.4
1988	Negm <i>et al.</i>	11/20	6	30	-42	0.38
1994	Ahlborn <i>et al.</i>	18	4	40	-30	-
1995	Cockerill	18	-	-	-35	-

Note:  $P_o$  = inlet pressure before nozzle

**Table 2.2** Summary of computer numerical studies

Year	Studies	Model
1981	Kahlil <i>et al.</i>	$k-\varepsilon$ model
1974	Gosman <i>et al.</i>	$k-\varepsilon$ model
1995	Cockerill	$k-\varepsilon$ model and Semi-empirical model
1999	Frohlingsdorf and Unger	$k-\varepsilon$ model and CFX Code
1997-1999	Promvongse	$k-\varepsilon$ model and ASM model

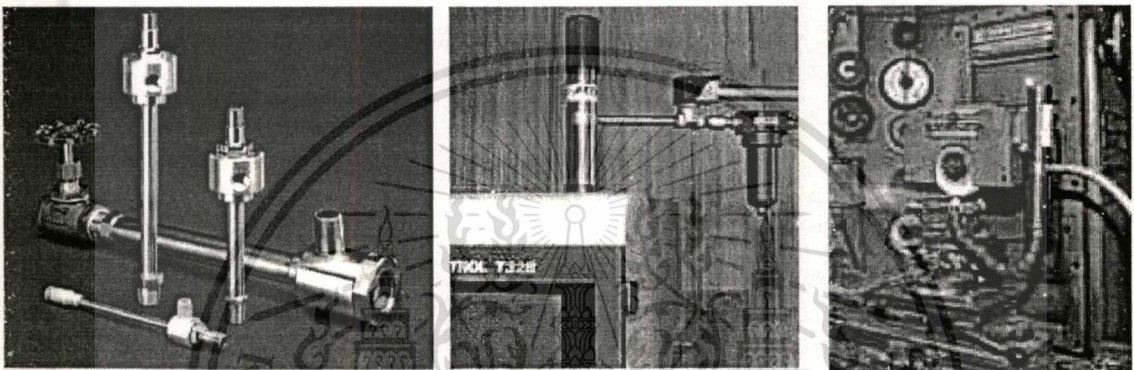
The relevant data from the experimental work are summarized in Table 2.1. It is found that various tube dimensions and operating conditions are used, for example, from diameters as low as 4.6 mm and as high as 800 mm. Table 2.1 presents variations in the maximum temperature difference between the inlet and the hot and cold streams. In this table for the same standard tube type, Scheper (1951) used an inlet pressure of 2.0 atm (abs.) and obtained a temperature difference of about 8°C between the hot and cold streams while Vennos (1968) employed inlet pressure of 5.8 atm (abs.) but obtained only a temperature difference of about 12°C. This means that, at this point, it is nearly impossible to predict how a given tube will perform because the exact nature of flow inside the tube is in doubt. However, it can be achieved if the energy separation mechanisms are understood.

This material is reserved for educational use only, not allowed for commercial use.

Forbidden to modify the content, and cite the document when use.

### 2.3 The Application of Research Study to Industrial Development

Nowadays the property of vortex tube has a great variety of application in industry ; for instance ,Exair Co, Newman Tools Inc (1998). It has been widely used in the cooling industrial fields especially Grilling, Turning and Welding on account of the various advantages of vortex tube such as cooling without moving part, non-electricity consuming, tiny, lightweight and inexpensive working chemical substance inside the vortex tube, uncomplicated cooling point, cleanliness, convenience and non-CFC's free from pollution.



(a)

(b)

(c)

**Figure 2.10** Vortex tube appliance and air conditioning in the work of cooler (Exair Co., 1998)

The two companies made the research study and developed designing vortex tube for the proposed of serving in the work of industrial fields cooling work and different application were absolutely stressed. The vortex tube appliances were developed to be the machines producing cold and hot air efficiently from the data of Exair Co. (1998). It was indicated that the outlet temperature of the cold air had the decreasing value of the highest temperature of  $40^{\circ}\text{C}$  while the outlet temperature of the hot air has the increasing value of the highest temperature. of  $110^{\circ}\text{C}$  and was capable of cooling at the highest of  $20,000 \text{ Btu/hr}$ . The vortex tube used in the industries had the small size made from stainless as Fig. 2.11.

As Fig. 2.11 (a) Vortex tube appliances were applicable in Plastic Cutting work. Plastic was cut in the cutting speed of the highest sharp cut and continually worked while cutting. There had tried suing vortex tube sets in the cooling the blades for decreasing the friction from the plastic friction accumulation and the heat caused at

This material is reserved for educational use only, not allowed for commercial use.

blades and work piece. This enable to help cleaning the blades to prolong the endurance of work with the higher proficiency.

In Fig. 2.11 (b) Vortex tube were used in the brass's screw making which the cold air was used from vortex tube in cooling the piece work and the screw bulb-making instead of water this method was more convenient and cleaner. As in Fig. 2.11 (c), it was found that the turning with the round speed in high cutting made the heat and the accumulated fraction left on the blades ; therefore, vortex tube work was used in the particular point on the blades only.

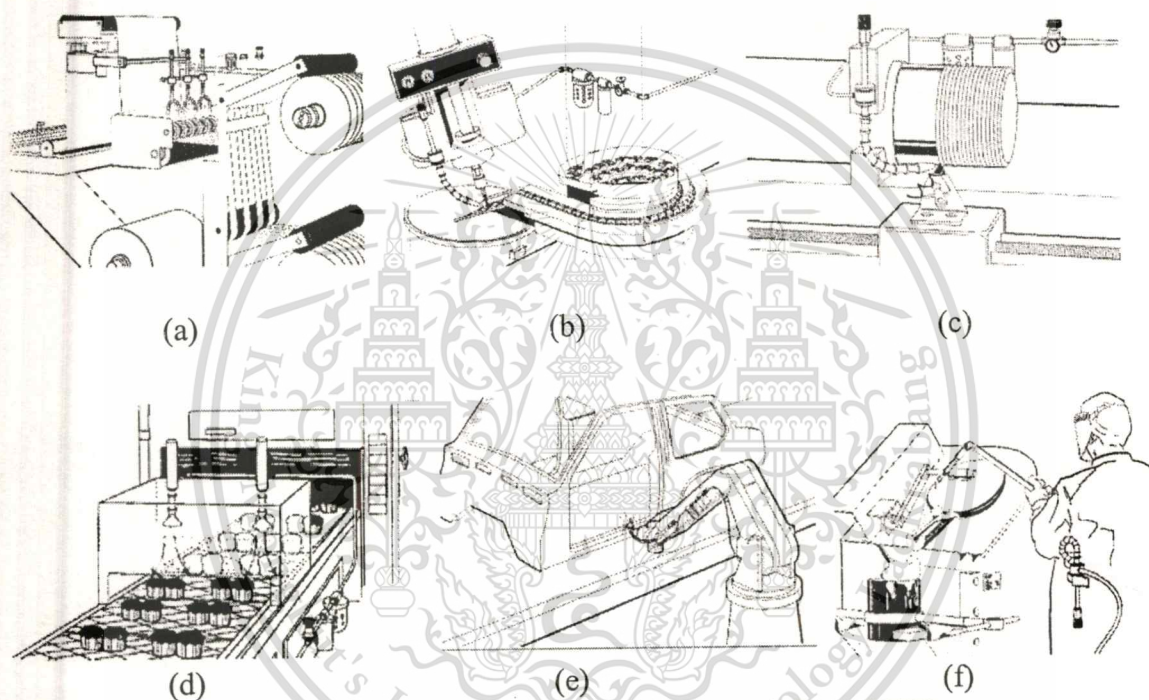


**Figure 2.11** Cooling in different processes (Newman Tools Inc., 1998)

Fig. 2.11 (d) Cleaning and drying the food pack. A set of vortex tube was installed in a set of conveyer which continually working.

Fig. 2.11 (e) Showed the uses of vortex tube in cooling around the work of electricity welding in a specific weld point after finishing welding with a view to facilitating, rapidity and increasing productivity. This method was mostly used in car industry.

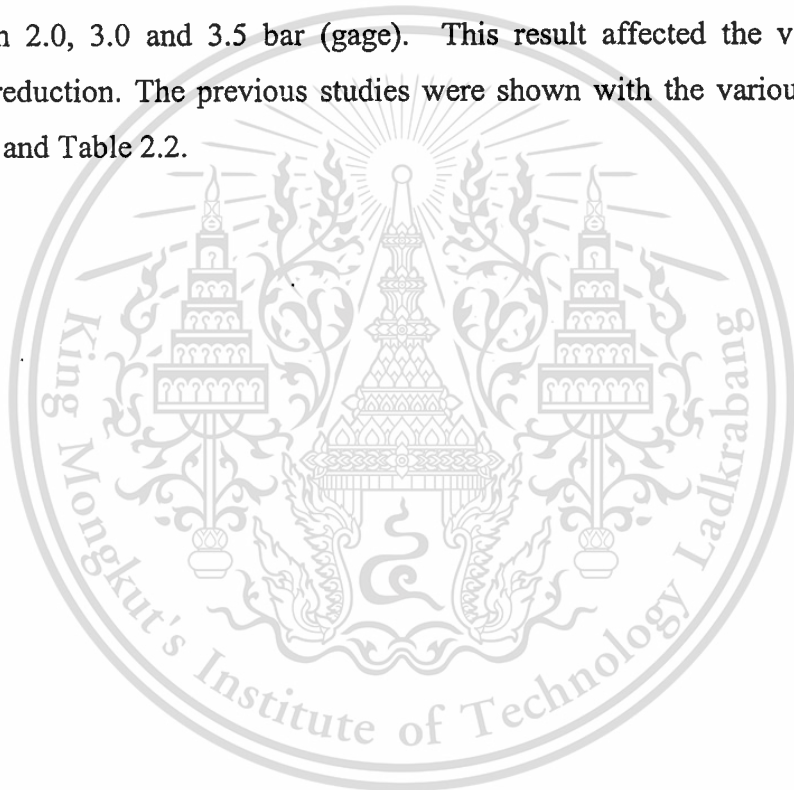
Fig. 2.11 (f) Showed the work process functioning in the molding shop with the great intensity of heat while working. The sets of vortex tube were equipped with the staff's dress. There made them feel cool while working in the high temperature environment.

This material is reserved for educational use only, not allowed for commercial use.

Forbidden to modify the content, and cite the document when use.

At present, it was recognized that the vortex tube became more and more applicable and widely used. Because of a lot of great advantages, vortex tube were used beneficially in many ways; for instance, Air clearance in cooling, applicability of the uses in liquid and gas separation. A lot of companies have been putting a lot of great attempt on proceeding different research studies for the most beneficial advantages of the most developed vortex tube in the industry progress.

From the research report, the increasing changes of the inlet nozzles of 1, 2 and 4 nozzles were made in the experimental studies. Moreover the changes in the ratio size of the orifice plates with the diameter of the vortex tube were indicated the ranges from  $0.4D$ ,  $0.5D$ ,  $0.6D$ ,  $0.7D$ ,  $0.8D$  and  $0.9D$ , insulated and non-insulated and inlet pressure from 2.0, 3.0 and 3.5 bar (gage). This result affected the value of the temperature reduction. The previous studies were shown with the various values in the Table 2.1 and Table 2.2.



# CHAPTER 3

## THEORY AND MECHANISM OF THE RANQUE-HILSCH VORTEX TUBE

### 3.1 Ranque-Hilsch Vortex Tube

In general, vortex tube has been known in different names. The most well known names are: vortex tube, Ranque vortex tube (named after Ranque who discovered the result in the vortex tube in 1928), Hilsch vortex tube or Ranque-Hilsch (named after Hilsch who had studied the sizes and parameters to develop the highest performance of the vortex tube), and Maxwell-Demon vortex tube (derived from the name of Maxwell and Demon group who together studied the molecule of hot air moving within the tube). Through there are various names, “Ranque-Hilsch vortex tube” and “vortex tube” will be used in this thesis.

### 3.2 Types of Vortex Tubes

As determined by flow patterns within the vortex tube, the vortex tube is divided into two types which are the counter flow and uni-flow vortex tubes.

#### 3.2.1 Counter Flow Vortex Tube

Fig. 3.1 shows the counter flow pattern within the tube. The compressed air flows through inlet nozzles which sometimes can be done through 1-2-4 nozzles as Fig. 3.2. When the air flows in the tube, it will swirl in tangential line as Fig. 3.6 which causes two flows of air: cold and hot. To separate the air, orifice plate is installed by the nozzle's entry. The hot air flows out through the hot tube a controlled by cone valve while the cold air leaves through the orifice plate.

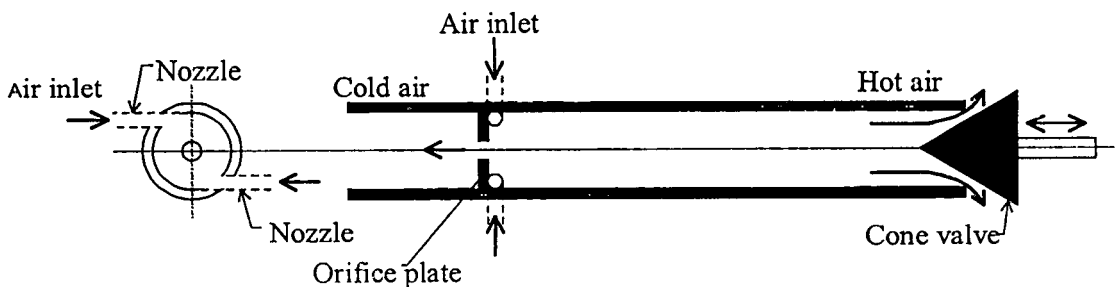


**Figure 3.1** Counter flow vortex tube type

For this counter flow vortex tube type, the cone valve located by the exit of the hot air helps prevent the combination of cold and hot air and control the mass's flow-out quantity in the cold and hot air tube. Both functions effectively produce the highest decreasing rate of cold temperature.

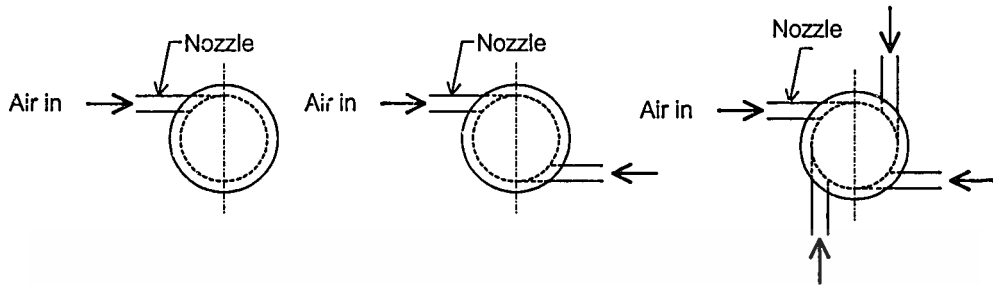


Figure 3.2 Vortex tube with 1, 2 and 4 inlet nozzles.

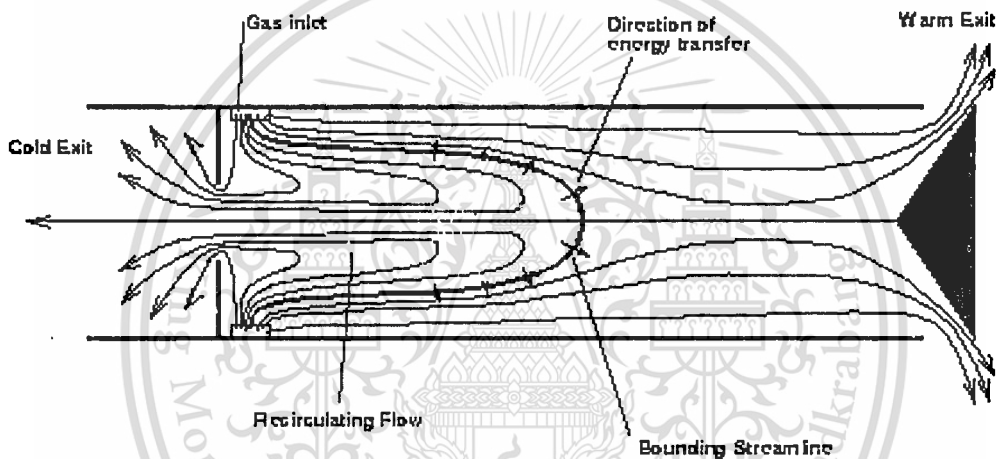


Figure 3.3 Flow pattern in a counter flow vortex tube type.

A possible flow pattern of the counter flow vortex tube type, proposed by Fulton (1950) and Van Deemter (1952) and Stephan (1983), is shown in Fig. 3.3. The solid line presents the stream surface of revolutions. The radial arrows indicate the resulting net outward of energy. During the energy separation process there exists a stagnation point on the axis of the vortex tube, and a stream surface through this point divides the future cold air from the future hot air. As indicated by Fulton and Deemter, slightly downstream toward the hot air exit of this stagnation point, the air has a radial temperature distribution ranging from a low value at the axis to a very high one at the wall. Furthermore Fulton stated that the tube wall in that region is hotter than the final mixed air, and hotter than the tube wall either at the inlet or at the far end of the tube. For a high hot air flow rate or a small value of  $\mu_c$  the highest temperature of the tube wall is located near the far end of the tube.

This material is reserved for educational use only, not allowed for commercial use.

Forbidden to modify the content, and cite the document when use.

### 3.2.2 Uni-Flow Vortex Tube

The other type of the flow is uni-flow or parallel flow demonstrated in Fig. 3.4 and 3.5. The Fig. 3.1 is similar to those of the counter flow vortex tube type. The difference is that in uni-flow vortex tube type, one end of the tube, opposite the cone valve, is closed or has no orifice plate. The closure causes both air to flow out in the same direction to the cone valve. Many experts experimental the flow research recommend that this tube is low cooling performance than the counter flow type and the energy efficiency is ineffective comparing to those of the counter flow vortex tube type.

Fig. 3.4 and 3.5 are alike. The difference is that the cone valve in Fig. 3.4 has a inlet nozzle in the middle of the valve while the cone valve in Fig. 3.5 has none.

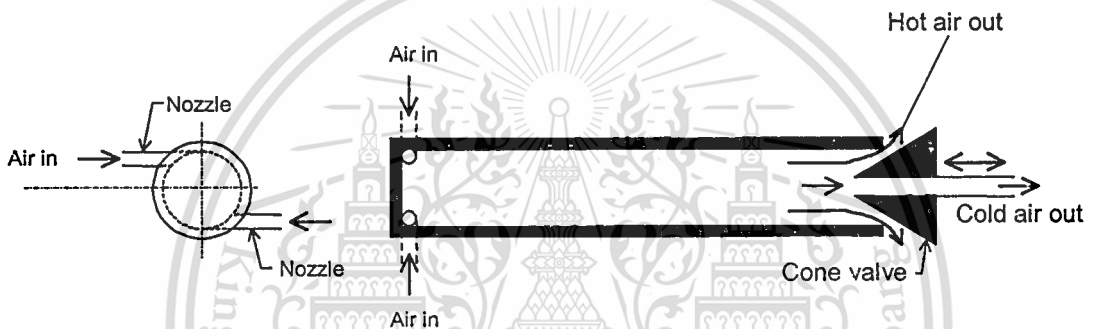


**Figure 3.4** Uni-flow vortex tube type or parallel flow vortex tube type

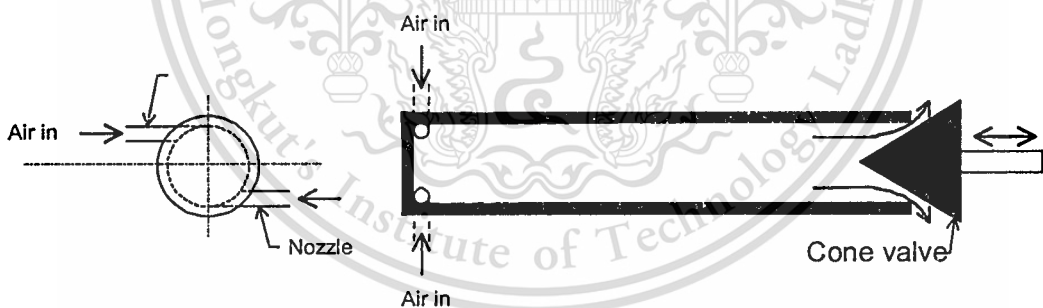


**Figure 3.5** Uni-flow vortex tube type or parallel flow vortex tube type

### 3.3 Hypothesis on the Mechanism of the Vortex Separation Effect

Several hypotheses have been advanced to explain the mechanism of the vortex effect (Webster, 1950; Fulton, 1950; Scheper, 1951; Martynovskii and Alekseev, 1956). The most correct of those seems to us to that Fulton and Hilsch, which in essence is the following. The air current leaving the tube inlet to the nozzle with high velocity and decreased static temperature develops a free vortex which, due to the rotary current motion toward the throttle, is transformed by friction into a force

This material is reserved for educational use only, not allowed for commercial use.

vortex. While the vortex is so transformed, there arises a kinetic energy current outward, so that the angular velocity of the inner air layers decreases at the greater rate than that of the outer ones. Simultaneously, there is an inward heat current, caused by difference in the static temperature of the outer and inner air layers. These two radial energy currents in the vortex are not equal; the kinetic energy current is greater than the heat current. The outer air layers thus receive more kinetic energy than they give away heat, and they thus attain a lower stagnation temperature whose magnitude is close to that of the static temperature acquired by the air on leaving the nozzles. This cold current leaves the tube through the cone valve opening.

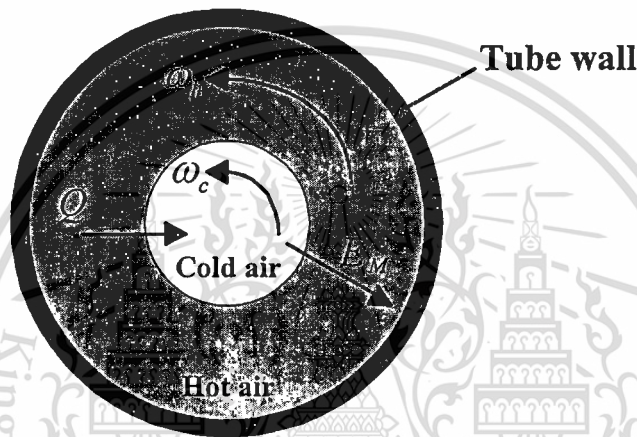


**Figure 3.6** Temperature distribution in the vortex tube.

### 3.4 Thermodynamics: The First and Second Laws in Vortex tube

At first sight, the vortex tube may appear to represent an impossible phenomenon, violating some fundamental laws of thermodynamics. The reader should rest assured, however that fabric of Physics remains intact.

#### 3.4.1 First Law Analysis

The vortex tube satisfies the First Law of Thermodynamics. Energy is conserved. Indeed, we can write:

$$(h)_{inlet} = \mu_c (h)_{cold} + (1 - \mu_c)(h)_{hot} \quad (3.1)$$

Where  $\mu_c = \frac{\dot{m}_c}{\dot{m}_i}$  is the fraction of the inlet mass flow leaving through the cold

exit, and  $h$  represents the stagnation enthalpy. In many cases, especially with long

This material is reserved for educational use only, not allowed for commercial use.

vortex tube, the flow velocities at the exits to the tube are small and their influence on the stagnation enthalpy may be neglected. For an ideal gas, the conservation equation may now be written:

$$c_p T_i = \mu_c c_p T_c + (1 - \mu_c) c_p T_h \quad (3.2)$$

Where  $T_i$  represents the stagnation temperature of the inlet gas,  $T_c$  the static temperature of the cold stream and  $T_h$  the static temperature of the hot stream. When rearranged  $\mu_c$  the subject, equation (3.2) gives a convenient means of estimating the cold mass flow fraction from temperature readings alone.

For a perfect gas,  $c_p$  with a specific heat capacity independent of thermodynamic state, equation (3.2) may be simplified by canceling the from each term. With a real gas, account must be taken of the dependence of enthalpy on pressure, that is the Joule Thomson effect, and then equation (3.2) is invalid. A revised relationship might be written

$$T_i = \mu_c (T_c - T_{jt}) + (1 - \mu_c) (T_h - T_{jt}) \quad (3.3)$$

Where  $T_{jt}$  represents the influence of the Joule Thomson effects. Over the range of pressure changes encountered in this thesis, generally less than 670 kPa, Joule Thomson cooling in air is relatively small at less than 2 K. Since much of the discussion deals with air, the Joule Thomson effect will be ignored except where noted explicitly. Moreover, gases will in general be treated as perfect throughout this word and thence immune to Joule Thomson cooling.

### 3.4.2 Second Law Analysis

#### *The Clausius Statement of the Second Law Thermodynamics reads*

It is impossible to construct a system, which will operate in a cycle and transfer heat from a cooler body to a hotter body without work being done on the system by the surroundings.

To reconcile the vortex tube with the Second Law, we have to broaden our outlook and recognize that the closed system we should consider a system consisting

This material is reserved for educational use only, not allowed for commercial use.

of a compressor and a vortex tube, as shown in Fig. 3.7. The arrangement pictured is quasi-cyclic in as much as the outlet air has been returned to its inlet pressure, specifically, atmospheric pressure. If the two outlet streams were mixed, the resultant gas would have a uniform enthalpy equal to that of the inlet gas, assuming that the heat transfer from the compressor was sufficient to cool the newly compressed gas back to ambient temperature. Note that we assume the working gas is perfect here. Thus the open system pictured in bold could be simply converted to closed cycle operation with no effect on its performance by addition of the equipment drawn lightly. The outlet gas is mixed, passed through a heat exchanger if necessary and returned to the compressor.

With such a scheme, the Second Law is obviously satisfied. Work is done to cause the transfer of heat from the cold gas stream to the hot stream (Cockerill, 1995)

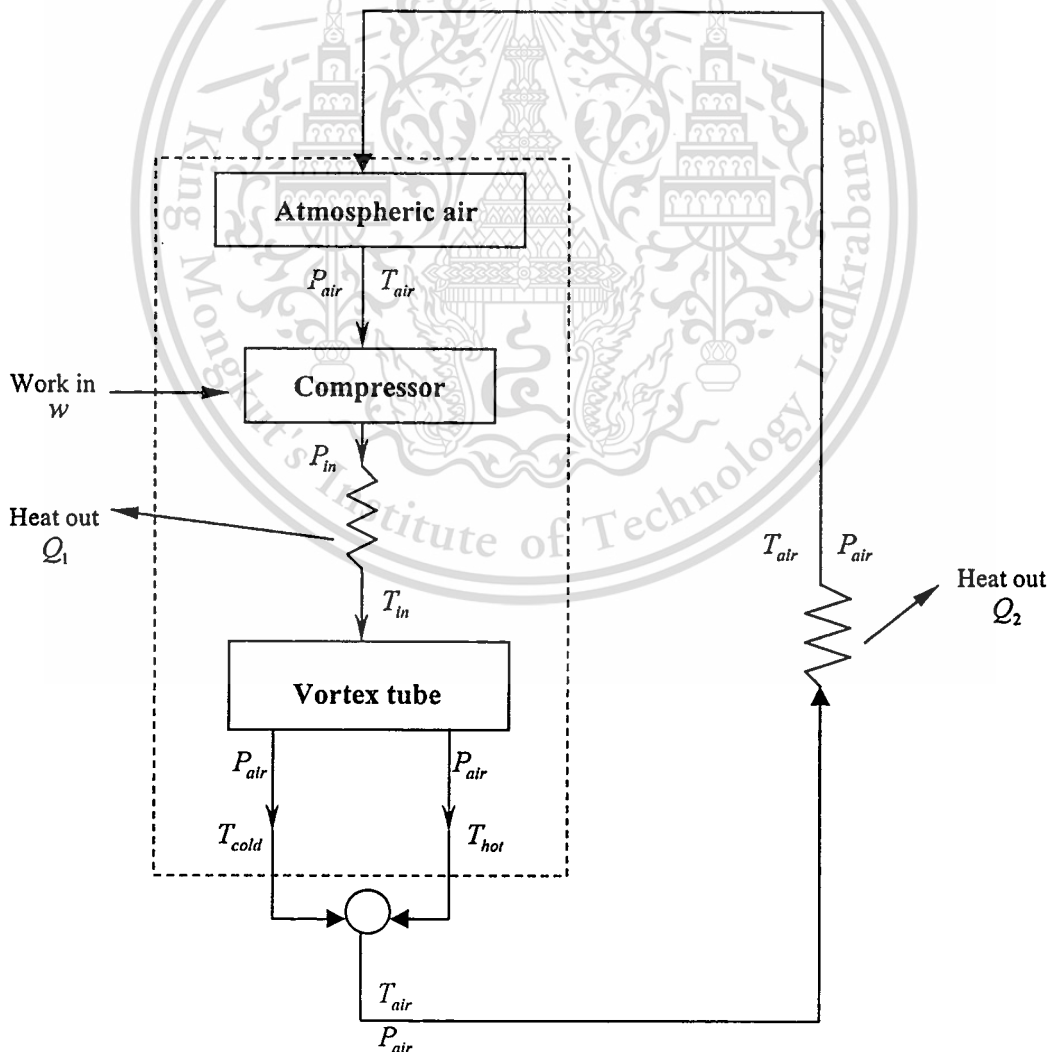


**Figure. 3.7** Diagram of thermodynamic in the vortex tube

This material is reserved for educational use only, not allowed for commercial use.

Forbidden to modify the content, and cite the document when use.

### 3.5 Parameter Indicating Vortex Tube Performance

The most important parameter indicating vortex tube's performance is the cold mass fraction. It is a ratio between a mass flow rate in the cold section per a mass flow rate by the air entry (Kuwattanachai, 1985). This is shown in Fig. 3.8. It may be written;

$$\mu_c = \frac{m_c}{m_i} \quad (3.4)$$

Whereas the temperature reduction of cold air is

$$(\Delta T)_c = T_i - T_c \quad (3.5)$$

And, the temperature increasing is

$$(\Delta T)_h = T_h - T_i \quad (3.6)$$

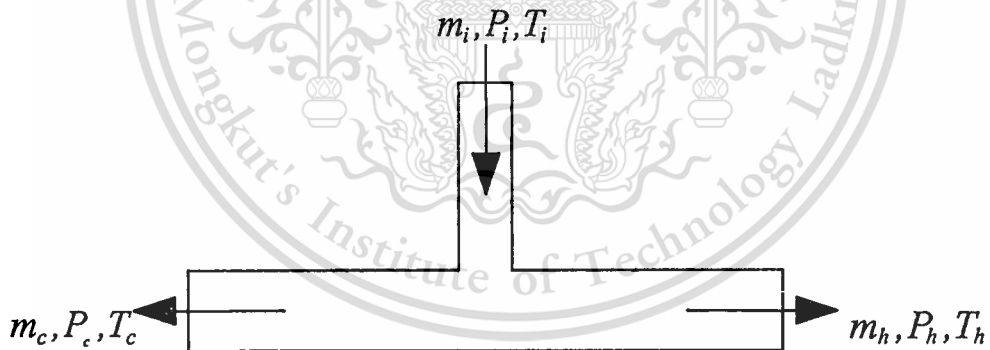


**Figure 3.8** Mass, pressure and temperature at the inlet and exit of the hot and cold section within the vortex tube.

#### 3.5.1 Cooling Air Ratio per unit of Air Inlet in the Vortex Tube

$Q_T$  is cooling air ratio derived from the vortex tube. The equation may be written as follow:

$$Q_T = m_c c_p (T_i - T_c) \quad (3.7)$$

This material is reserved for educational use only, not allowed for commercial use.

Forbidden to modify the content, and cite the document when use.

Where as  $c_p$  is specific heat at pressure constant and  $Q_c$  can be found from equation (3.8)

$$Q_c = \frac{Q_T}{m_i} \quad (3.8)$$

$$Q_c = \frac{m_c c_p (T_i - T_c)}{m_i} \quad (3.9)$$

Equation (3.9) can be replaced by equation (3.4), which gives

$$Q_c = \mu_c c_p (\Delta T)_c \quad (3.10)$$

### 3.5.2 Cooling Efficiency in Thermodynamics of the Vortex Tube

To calculate the cooling efficiency of the vortex tube, the principle of adiabatic expansion of ideal gas will be used. As the air flows into the vortex tube, the expansion in isentropic process occurs. This can be written

$$(\Delta T)_c = \eta_c (\Delta T)_{isen} \quad (3.11)$$

When;  $\eta_c$  is cooling efficiency,  $(\Delta T)_c$  is the difference of temperature reduction and  $(\Delta T)_{isen}$  is the difference of decreasing temperature in isentropic process.

In the case that air expands from pressure  $P_i$  to pressure  $P_c$  by using isentropic process as shown in Fig. 3.9, the expansion rate of temperature from  $T_i$  to  $T_1$  can be written

$$PV^\gamma = \text{constant} \quad (3.12)$$

The relation between temperature and pressure is

$$\frac{T_i}{T_1} = \left( \frac{P_i}{P_c} \right)^{\left( \frac{\gamma-1}{\gamma} \right)} \quad (3.13)$$

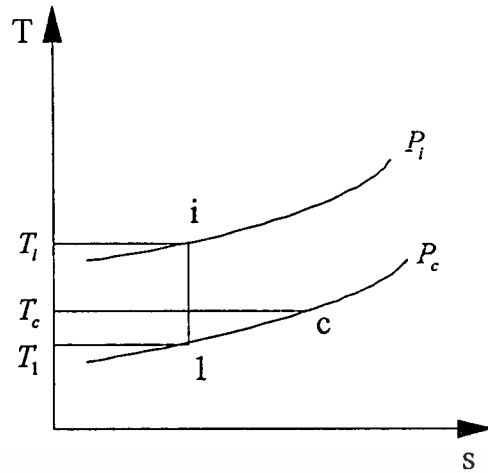


**Figure 3.9** T-s isentropic process diagram

The temperature at point 1 can be obtained from equation (3.13).

$$T_1 = \frac{T_i}{\left(\frac{P_i}{P_c}\right)^{\left(\frac{\gamma-1}{\gamma}\right)}} \quad (3.14)$$

The temperature reduction in isentropic process is

$$(\Delta T)_{isen} = T_i - T_1 \quad (3.15)$$

Substitute equation (3.14) and derive

$$(\Delta T)_{isen} = T_i - \frac{T_i}{\left(\frac{P_i}{P_c}\right)^{\left(\frac{\gamma-1}{\gamma}\right)}} = T_i \left(1 - \left(\frac{P_c}{P_i}\right)^{\left(\frac{\gamma-1}{\gamma}\right)}\right) \quad (3.16)$$

The temperature reduction after flowing into the vortex tube is

$$(\Delta T)_c = \eta_c T_i \left(1 - \left(\frac{P_c}{P_i}\right)^{\left(\frac{\gamma-1}{\gamma}\right)}\right) \quad (3.17)$$

This material is reserved for educational use only, not allowed for commercial use.

Forbidden to modify the content, and cite the document when use.

Cooling efficiency is received from

$$\eta_c = \frac{T_i - T_c}{T_i \left( 1 - \left( \frac{P_c}{P_i} \right)^{\frac{\gamma-1}{\gamma}} \right)} \quad (3.18)$$

### 3.5.3 Coefficient of Performance

To find coefficient performance (*C.O.P*), the same principle of isentropic expansion of ideal gas will be used. When *C.O.P* is ratio between cooling rate and energy used in cooling, the equation is

$$C.O.P = \frac{Q_c}{w} \quad (3.19)$$

When; *C.O.P* is coefficient of performance,  $Q_c$  is cooling rate per unit of air inlet in the vortex tube,  $w$  is mechanical energy used in cooling per unit of air inlet the tube and  $w$  is found from

$$W = m_i c_p T_i \left[ \left( \frac{P_i}{P_c} \right)^{\frac{\gamma-1}{\gamma}} - 1 \right] \quad (3.20)$$

Mechanical energy derived from gas expansion from pressure  $P_i$  to pressure  $P_c$  in isentropic process may be written

$$w = \frac{W}{m_i} \quad (3.21)$$

Combine equation (3.2) and (3.21) and obtain

$$w = \frac{\gamma}{\gamma-1} RT_i \left[ \left( \frac{P_i}{P_c} \right)^{\frac{\gamma-1}{\gamma}} - 1 \right] \quad (3.23)$$

Substitute equation (3.19) with equation (3.9) and (3.23) and derive

$$C.O.P = \frac{\mu_c c_p (T_i - T_c)}{\frac{\gamma}{\gamma - 1} R T_i \left[ \left( \frac{P_i}{P_c} \right)^{\frac{\gamma - 1}{\gamma}} - 1 \right]} \quad (3.24)$$

In equation (3.14), *C.O.P.* is found. The equation demonstrates the use of mechanical energy in isentropic process per mass. But isentropic process is an ideal process that does not really occur. Thus, the mechanical energy practically used must be higher.



# CHAPTER 4

## EXPERIMENTAL APPARATUS AND PROCEDURE

### 4.1 Experimental Set-Up

Vortex cooling Device or generally called vortex tube is a particular device designed to enable to operate the cooling function producing the hot and the cold air simultaneously without any moving parts in the counter flow vortex tube type. The device was designed to mainly consist of : vortex chamber, the hot tube, the cold tube, the number and diameter of inlet nozzles, the pressure inlet to the vortex tube, cone valve, orifice meter and orifice plate equipped between the hot and the cold tube as shown in Fig. 4.1. All of this packaging equipment immensely influenced over cooling and temperature reduction inside the vortex tube.

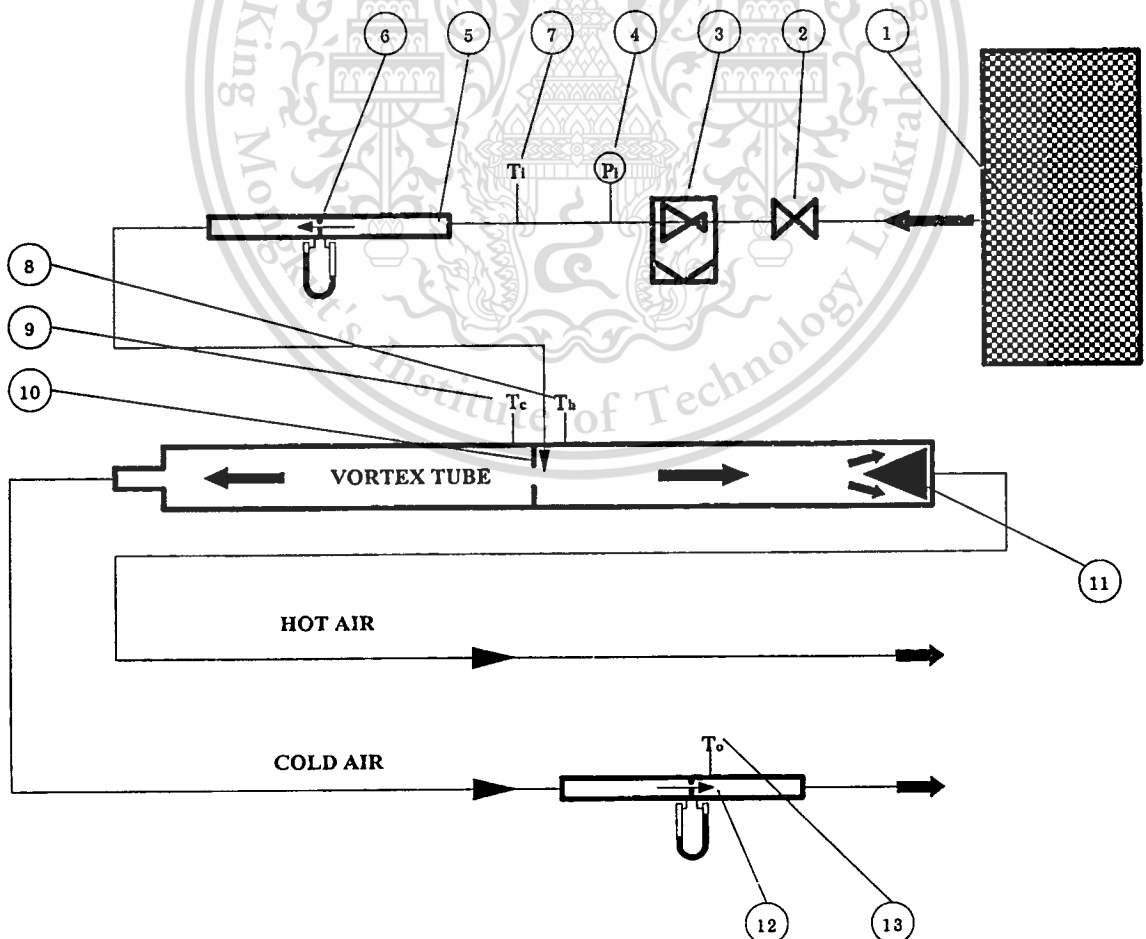


**Figure 4.1** The working system of the Ranque-Hilsch vortex tube.

This material is reserved for educational use only, not allowed for commercial use.

Forbidden to modify the content, and cite the document when use.

In figure 4.1 as shown; (1) Compressor air pump, (2) Ball valve, (3) Air dry filter, (4) Pressure gauge, (5,12) Orifice meter, (6,10) Orifice plate, (7,8,9,13) Thermocouple and (11) Cone valve.

In the past, there were researches trying to evaluate the geometry of the vortex tube size for the sake of producing the temperature reduction at highest value. This thesis was made the presentation by the analyzing the applicability of contain piece size of equipment designed by Hilsch in 1947 to the new proportion. The applicable design was proportional to the ability of increasing the inlet nozzle numbers through vortex chamber from 1, 2 and 4 inlet nozzles and the applicability of the ratio of orifice plate holes sizes ( $d/D$ ) from  $0.4D$  to  $0.9D$  for the purpose of studying the temperature distribution at the wall of the vortex tube and the decreasing of the highest temperature at the cold tube. The thesis presentation was profusely emphasized on the different proportional value of vortex tube to analyze the proportional value of tube enabling the coldest with the design equipment as detailed description shown in the Fig. 4.2

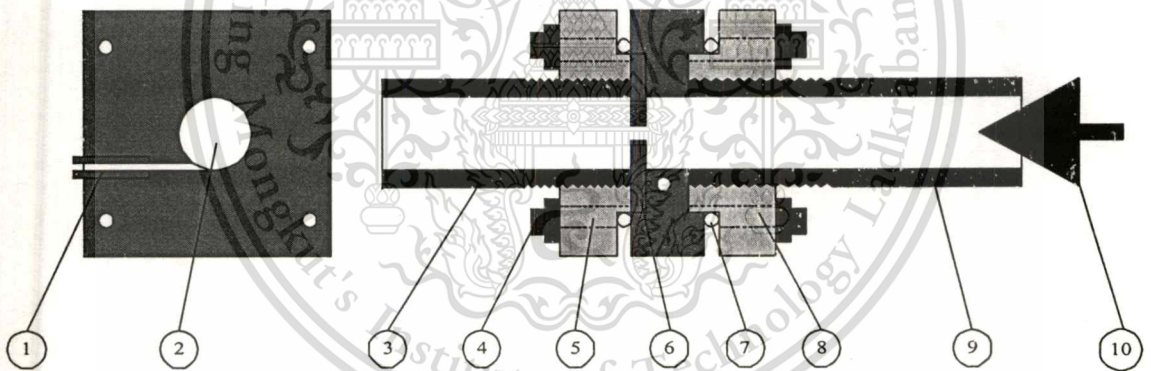


**Figure 4.2** The Ranque–Hilsch vortex tube

In figure 4.2 as shown; (1) Cold tube, (2) Orifice plate, (3) Nut and Bolt, (4) Hot tube, (5) Cone valve, (6) Cold flange, (7) Hot flange and (8) Inlet nozzles.

## 4.2 Equipment and Measurement Device

### 4.2.1 The Hot and the Cold of the Vortex Tube

The results of the vortex tube's length concerning the hot and the cold tube greatly affected the increasing of the temperature inside vortex tube. Regarding to Hilsch's research, it was suggested that the proper length of the hot air tube should be

This material is reserved for educational use only, not allowed for commercial use.

32 times of the diameter of the vortex tube ( $32D$ ); while the proper length of the cold air tube should be 10 times of the diameter of the vortex tube ( $10D$ ). Vortex tube was indicated to be selective of the size of the diameter ( $D$ )  $16\text{ mm}$  which obtained the tube length of the hot air equivalent to  $512\text{ mm}$ ; while the cold air equivalent to  $160\text{ mm}$ . The vortex tube should be made from acrylic with the smooth surface in order to reduce potential friction between the air and the tube surface.

All of the vortex tubes were absolutely insulated. The evaluating nozzles were drilled for temperature distribution at the hot air tube altogether 15 points. And the points were placed at  $(x/D)$  intervals equivalent to 0.5 as shown in Fig. 4.3.

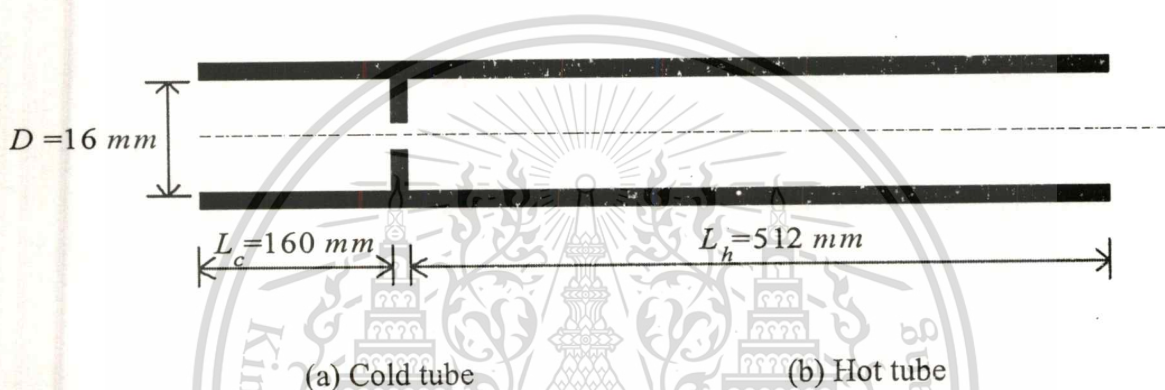


**Figure 4.3** Hot tube and the cold tube.

#### 4.2.2 Nozzles at the Inlet of the Vortex Chamber

Different sizes of the inlet nozzles were made on experimental studies. And it was found that the bigger the sizes of the diameter inlet nozzles were, the lower the temperature values were; whereas in fact, the exaggeratedly big inlet nozzles were unable to drive the swirl flow inside the vortex tube. It was indicated that much lower decline of the temperature depended on the proportionally higher compressed air pump; therefore, the sizes of the inlet nozzles were selected in proportion to the sizes of the diameter of vortex tube which were equivalent to  $(D/9)$  according to the result of Hilsch's suggestion. The numbers of nozzles were increased to 2 and 4 inlet nozzles and the sizes of diameter of inlet nozzles were equivalent to  $2\text{ mm}$ . The nozzles of the vortex chamber were drilled through the areas of the inlet nozzles where to meet the tangential line of vortex tube rightfully as shown in Fig. 4.4. The vortex chamber, which had the thickness dimension of  $20\text{ mm}$ , was made from acrylic. Being compatible with the hot air tube as well as the cold air tube, the vortex

This material is reserved for educational use only, not allowed for commercial use.

chamber was operated with the 4 points of nut lock with the o-ring placed in the middle of the tube to seal the air within the tube.

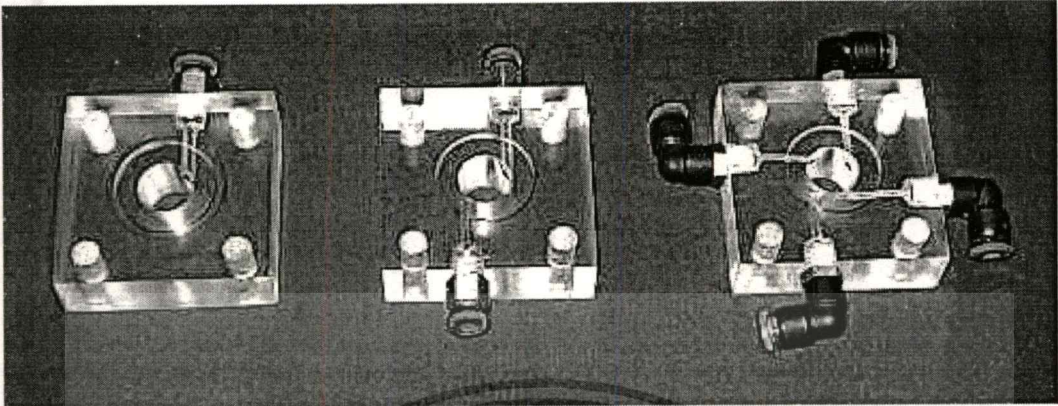


**Figure 4.4** The vortex chamber with 1, 2 and 4 inlet nozzles

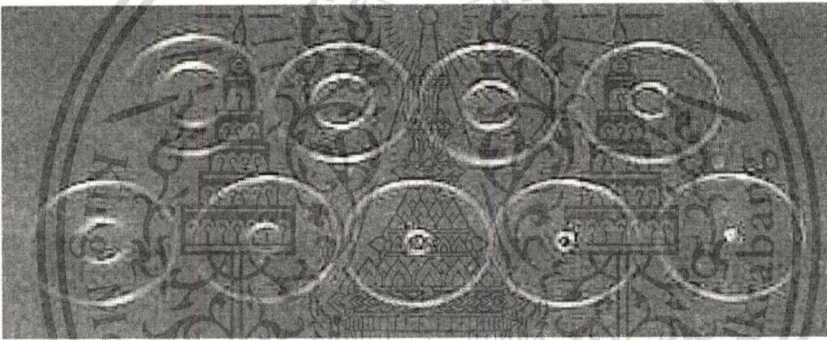


**Figure 4.5** The orifice plates with the ratio ( $d/D$ ) equivalent to  $0.4D$  to  $0.9D$ .

#### 4.2.3 Orifice Plates

The ratio sizes of the orifice plates immensely and efficiently affected to the temperature reduction at the cold tube. The too much bigger the diameter of the orifice plates were, the more the mass of the hot air flowing mixing with the mass of the cold air increased. This influenced on the higher temperature out of the orifice plates. Meanwhile, the too much smaller the orifice plates were, the more the mass of the cold air flowing out decreased the values. This influence on the outcome temperature with the inability of the producing the value of the highest temperature reduction. In this experimentation, it was indicated to select the ratio of the diameter of the orifice plate to the diameter of the vortex tube ( $d/D$ ) from  $0.4D$ ,  $0.5D$ ,  $0.6D$ ,  $0.7D$ ,  $0.8D$  and  $0.9D$  with the  $2\text{ mm}$  thickness orifice plate. The orifice plate was made from acrylic. The orifice plates were specifically designed to the place the

This material is reserved for educational use only, not allowed for commercial use.

Forbidden to modify the content, and cite the document when use.

position installation around the vortex chamber near the position of the nozzle at the distance of 2 mm from the nozzle as shown in Fig. 4.5.

#### 4.2.4 Cone Valve

The air flowing out of the nozzles came out through 2 outlets ; the hot tube outlets and the cold tube outlets. To control the flow of the hot air and the cold air, the cone valves were installed at the end of the hot tube, equipped with the set of the hot tube connection with the ability of moving in and out to make the applicable mass flow rate. Cone valve has the cone shape with the angle 30 degree for the purpose of keeping flowing in the perfect symmetry of the flow and avoiding the mixing between the cold and the hot air in the tube. The cone valve was equipped with the set of the hot tube connection as shown in Fig. 4.6.

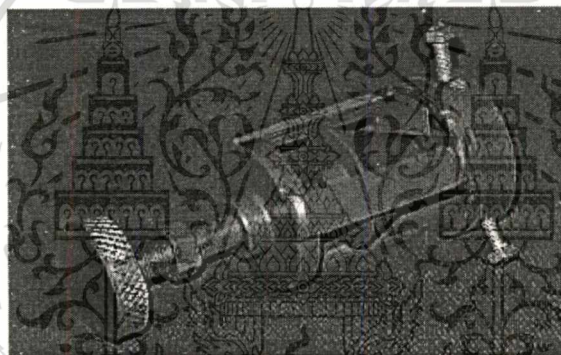


**Figure 4.6** The cone valve controlling the flow was equipped with the hot tube connection.

#### 4.2.5 Air Compression

For air compressor or air pump, it is advisable that the piston type should be more usefully applicable with the size of 10 HP and the mass flow rate of  $4.5 \times 10^3 \text{ m}^3/\text{s}$  the air volumn limited with the flow passing the nozzle with the diameter value 1 and the variable pressure between 2.0, 3.0 and 3.5 bar (gage).

The pressure on function from the air compressor was at constant at the pass of 4 bar with the temperature inside the tank around  $29^\circ\text{C}$ . The air from the air compressor flow through the air dry filter and pressure gauge at the inlets of the vortex tube and all of the data of counter flow vortex tube type were shown at Table 4.1.

This material is reserved for educational use only, not allowed for commercial use.

Forbidden to modify the content, and cite the document when use.

**Table 4.1** Summary of the data of the Ranque –Hilsch vortex tube

<b>Tube characteristic</b>	<b>Dimension</b>
Hot tube length, $L_h$ (mm)	512
Cold tube length, $L_c$ (mm)	160
Diameter of the vortex tube, $D$ (mm)	16
Number of the inlet nozzles, $N$	1, 2 and 4
Diameter of the inlet nozzles, $\delta$ (mm)	2
Thickness of the vortex chamber, $T$ (mm)	20
<b>Cone valve characteristic</b>	
Angle of control valve, (degree)	30
Ratio of orifice plate, ( $d / D$ )	0.4 to 0.9
Thickness of orifice plate, $t$ (mm)	2
<b>Inlet properties</b>	
Fluid inlet	Air
Temperature at the inlet of vortex tube, $T_i$ ( $^{\circ}\text{C}$ )	29
Pressure at the inlet of vortex tube, $P_i$ (bar)	2.0, 3.0 and 3.5

#### 4.2.6 Measurement Devices

##### 4.2.6.1 The Flow Measuring Devices

To evaluate the flow rate at the inlets and the outlets of vortex tube, it was essential that the measurement should be done through the orifice meter as shown in Fig. 4.7. The orifice meter was preferably created in accordance with the indication of the Japanese industrial standard (JIS Z 8762-1988). The complex construction of the device consisted of the ratio of orifice plates ( $d / D$ ) with the ratio size equivalent to 0.5, the diameter of the vortex tube equivalent to 16 mm and the products of the aqualic plate of 2 mm thickness. This measuring device evaluated the result values of the pressure drop through the U-tube Manometer (Dwyer Co.), which was able to evaluate the pressure drop on the wide range of 0-500 mm of water. By means of this method, the mass flow rate was enabled to be found out from the following equation:

$$\dot{m} = (2.5017 \times 10^{-4}) \epsilon c \sqrt{2\Delta P \rho_i} \quad (4.1)$$

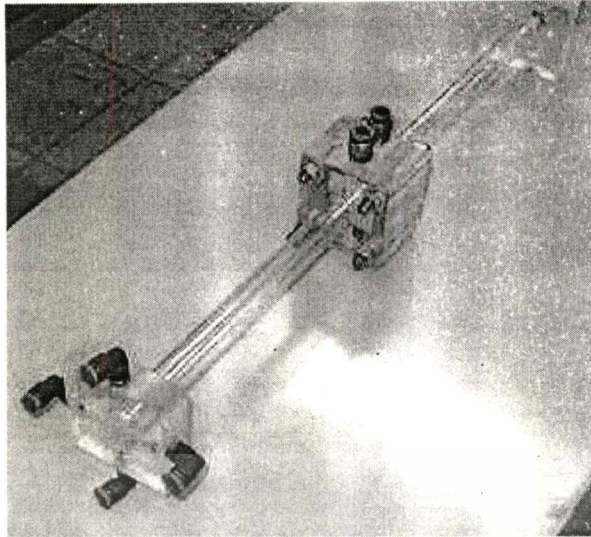


**Figure 4.7** The orifice meter

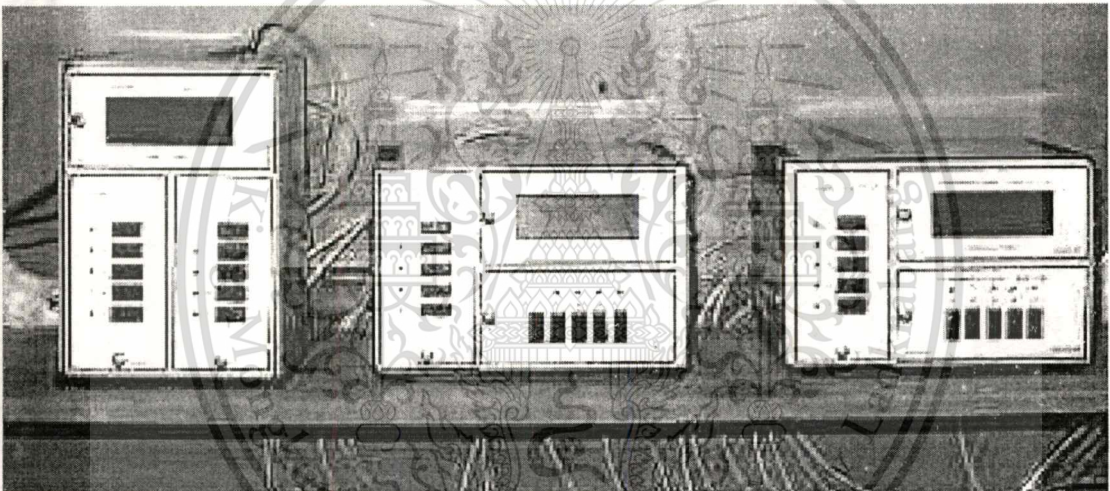


**Figure 4.8** Thermocouple type K

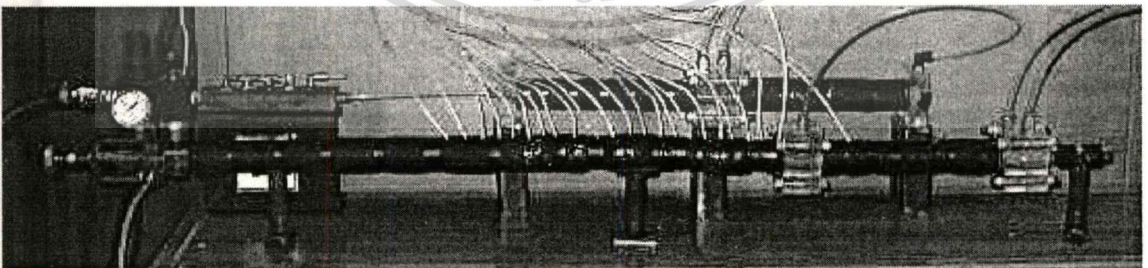


**Figure 4.9** The insulated at the Ranque –Hilsch vortex tube.

#### **4.2.6.2 Temperature Measuring Devices**

To measure temperature inside the vortex tube was specifically performed both in the hot tube and the cold tube as in Fig. 4.9, both of the temperature at entry and temperature at the orifice meter.

All were performed through Thermocouple type K and the range of measurement is  $-10^{\circ}\text{C}$ - $150^{\circ}\text{C}$ . There were 3 sets of Thermocouples (from Sang-chai meter Co.). And each set was capable of making measurement altogether 8 points and all of the tube were insulated on the temperature distribution as shown in Fig. 4.8-4.9.

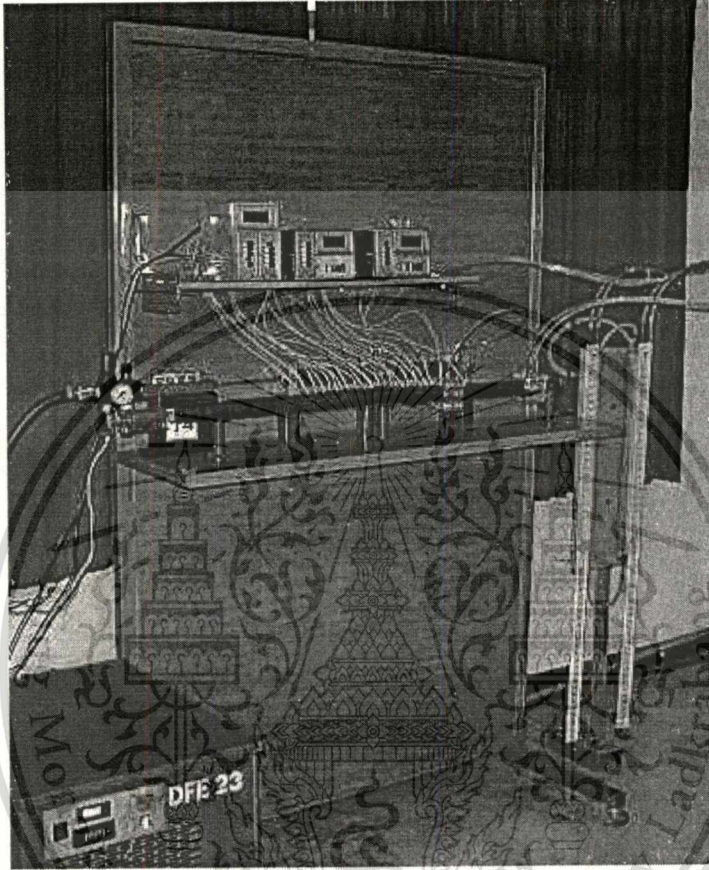


**Figure 4.10** The set of Ranque-Hilsch vortex tube apparatus.

### 4.3 Procedure of Experimentation

The experimental device for the potentiality of the vortex tube as shown in Fig. 4.1,4.9 and 4.10. The experimentation was started when the air was compressed from the air pump (1) and flow past through the ball valve (2), and the pressure gauge (4) and then filtered at the air dry filter (3) before entering the vortex tube (5) and finally flow into the set of orifice meter (6). The air mass flow rate values was evaluated before entering the vortex tube ; in addition, the air would flow pass the nozzles to the vortex chamber at the inlet pressure 2.0 bar air constant; consequently, the swirl flow of the air occurred in the vortex flow inside the tube. Inside the vortex tube, the air

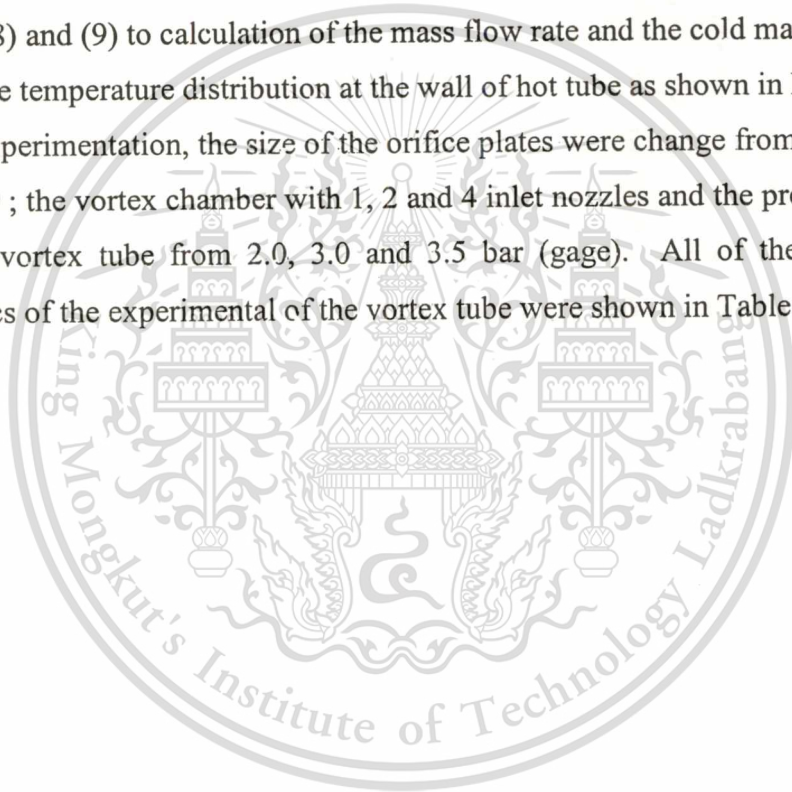
were expanded; according, the air separation occurred into 2 stream: the hot and the cold air.

The cold air would flow out from the orifice plates installed next to the inlet of the nozzles, which the hot air would flow to the end of another tube equipped with the control valve. The flow rate value of the cold air out of the vortex tube at the cold air side was evaluate through adapting the mass flow rate by the cone valve.

The mass flow rate value at the inlet side, the cold air and temperature at the wall tube would be evaluate in this following methods:

- (1)By the pressure drop at the orifice plates readable from the U-tube manometer.
- (2)By measuring the temperature at the inlet and the cold tube after steady flow (7), (8) and (9) to calculation of the mass flow rate and the cold mass fraction.
- (3)By the temperature distribution at the wall of hot tube as shown in Fig. 4.9.

In the experimentation, the size of the orifice plates were change from the ratio of  $0.4D$  to  $0.9D$  ; the vortex chamber with 1, 2 and 4 inlet nozzles and the pressure at the inlet of the vortex tube from 2.0, 3.0 and 3.5 bar (gage). All of the significant characteristics of the experimental of the vortex tube were shown in Table 4.1.



## CHAPTER 5

# EXPERIMENTAL RESULTS AND DISCUSSION

The thesis studies and analyses several tube parameters affecting the decrease in temperature in the cold tube of the vortex tube. The tube parameters to be considered in the present study are (1) insulated and non-insulated vortex tubes, (2) cold orifice plate diameter and (3) number of the inlet nozzles including inlet conditions (supply pressure). There are no critical dimensions of these parameters that would result in a unique value of maximum temperature separation. Thus, the experiments of a vortex tube with different tube parameters are needed to obtain the highest temperature difference from these runs. The dimensional analysis and similarity geometry is used to find the optimal performance in a design of the vortex tube.

### 5.1 Insulated and Non-Insulated Vortex Tubes

In the experiment, measurements of the vortex tube are made without and with insulation at both the hot and cold tubes as shown in Fig. 4.9. The size of orifice plate is 0.5 of the tube diameter ( $D$ ) and the number of 1, 2 and 4 inlet nozzles is used, at inlet temperature of  $29^{\circ}\text{C}$  and inlet pressure of 3.5 bar (gage).

Fig. 5.1 shows that the insulated tube has higher temperature reduction in the cold air tube than the non-insulated one. At the cold mass fraction ( $\mu_c$ ) of 0.328, the orifice size of  $0.5D$ , and number of 4 inlet nozzles, the highest temperature reductions of the insulated and non-insulated vortex tubes are  $-30^{\circ}\text{C}$  and  $-27^{\circ}\text{C}$  respectively. Moreover, in the hot tube the maximum temperature differences of the insulated and non-insulated tubes are  $78^{\circ}\text{C}$  and  $68^{\circ}\text{C}$ , respectively, at the cold mass fraction ( $\mu_c$ ) of 0.829.

The trends of the temperature reduction in the cold air tube and the temperature increase in the hot tube are similar to the non-insulated tube for all the inlet nozzles. The average temperature differences of the insulated and non-insulated tubes are between 2 to  $4^{\circ}\text{C}$  at the cold tube and between 2 to  $12^{\circ}\text{C}$  at the hot tube. It is

because the insulated tube has less energy transferred to surrounding than the non-insulated one, which then causes the higher change of temperature within the tube. For the cold mass fraction ( $\mu_c$ ) in a range between 0.1 and 0.4, the temperature reduction in the cold tube for all nozzles is rather higher than that for the cold mass fraction ( $\mu_c$ ) above 0.4. For the hot tube, when the cold mass fraction ( $\mu_c$ ) is in a range of 0.1 to 0.8, the temperature proportionally increases but then decrease rapidly for the cold mass fraction ( $\mu_c$ ) above 0.8.

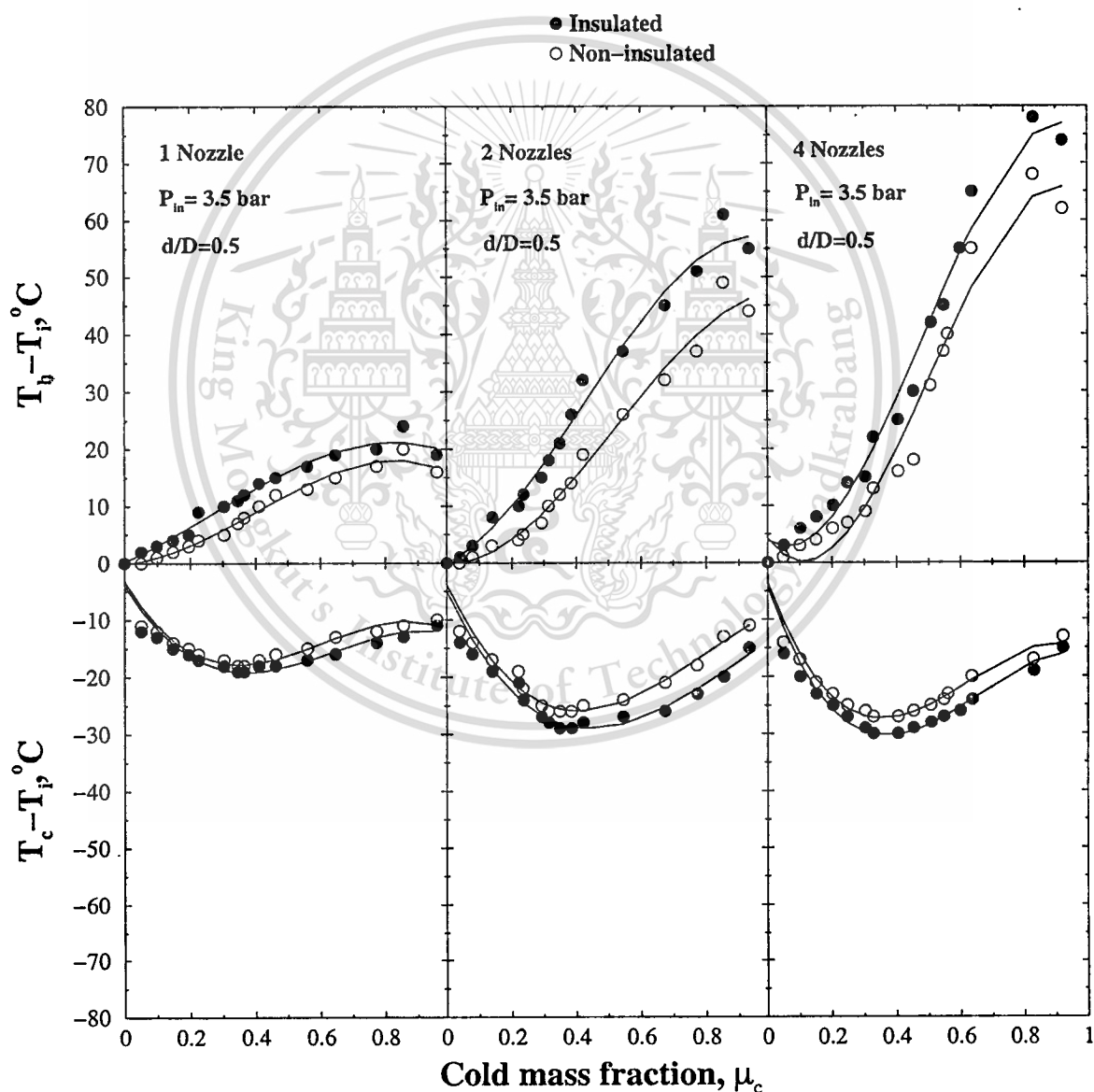


**Figure 5.1** Temperature differences at various cold mass fractions between insulated

This material is intended for personal use only and is not to be used for commercial use.

Forbidden to modify the content, and cite the document when use.

## 5.2 Inlet Pressure of Insulated Vortex Tube

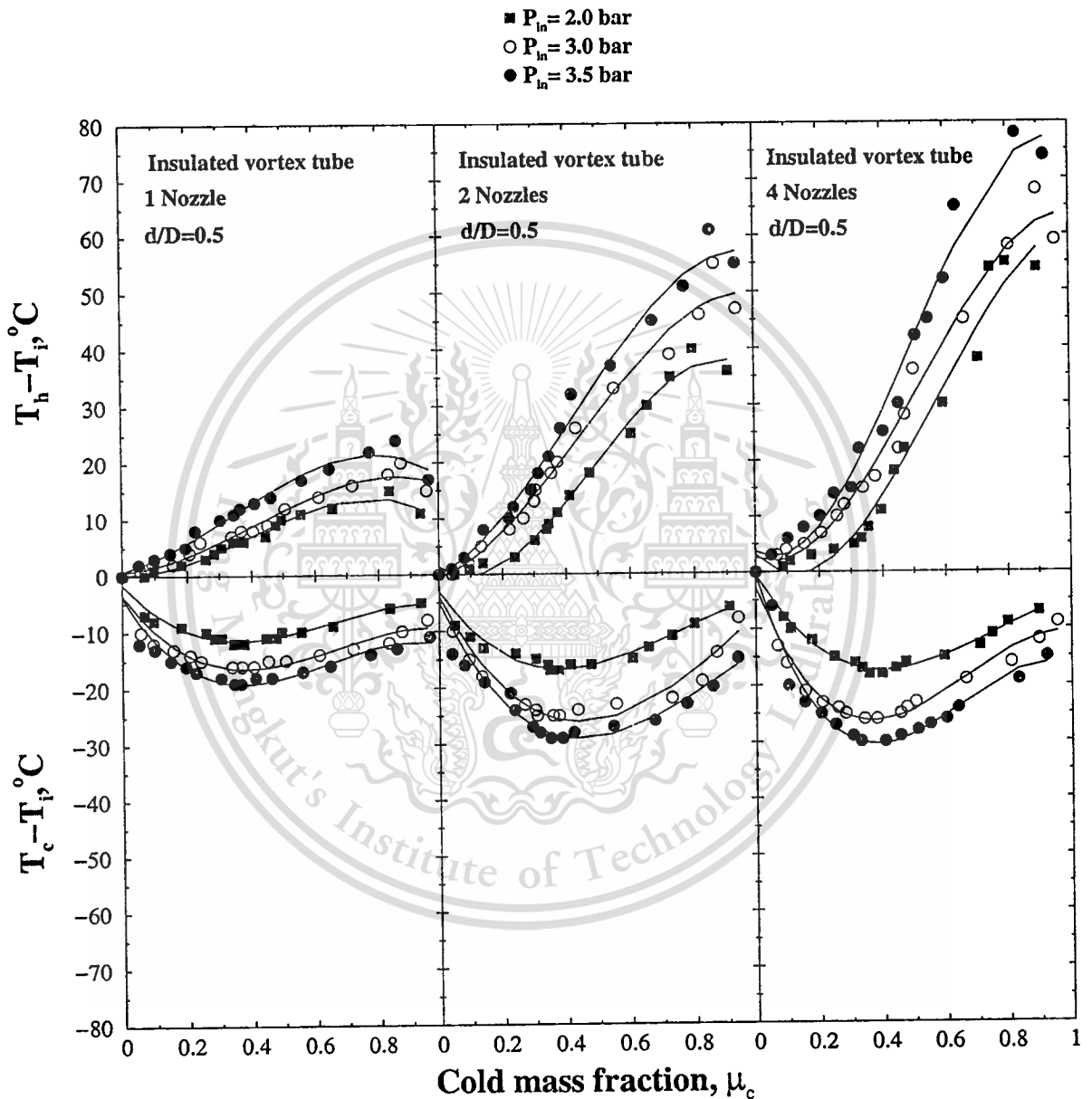
The insulated vortex tube with 16-mm diameter,  $0.5D$  orifice diameter and multiple inlet nozzles was selected and tested. The tests were run for three different inlet pressures; 2.0-3.0 and 3.5 bars, and each run was at constant inlet temperature of  $29^{\circ}\text{C}$ . From experimental results, it indicates that temperature difference in the hot and the cold tubes is a function of the cold mass fraction. In addition, the potential of decreasing and increasing temperatures in the cold and the hot tube respectively is similar to the case in section 5.1.

Fig. 5.2 demonstrates that for the cold mass fraction ( $\mu_c$ ) in a range of 0.1 to 0.4, there is distinctively a potential of higher rate of temperature reduction in the cold tube but lower rate of temperature reduction for the range beyond 0.4. Because the hot air in the hot tube mixes with the cold air in the core region which flows out more through the orifice plate. For the cold mass fraction ( $\mu_c$ ) in a range between 0.3 and 0.4, there is the highest rate of temperature reduction in the cold tube for all inlet pressures supplied. When inlet pressures are at 2.0, 3.0 and 3.5 bars, the highest rate of decreasing temperature in the cold tube are  $18^{\circ}\text{C}$ ,  $26^{\circ}\text{C}$  and  $30^{\circ}\text{C}$ , respectively, for 4 inlet nozzles. Moreover at a pressure of 3.5 bar, the highest rate of decreasing temperature for 1, 2 and 4 inlet nozzles is  $19^{\circ}\text{C}$ ,  $29^{\circ}\text{C}$  and  $30^{\circ}\text{C}$  respectively.

The higher the inlet pressure, the more decreasing temperature for each cold mass fraction used. Since the air enters the vortex tube tangentially with a higher pressure, it causes the higher tangential velocity and air mass flow rate within the tube. This leads to an acceleration of velocity and temperature layer within the tube. Furthermore, there is a higher momentum transfer from the central region of the tube to the tube wall in terms of thermal energy which causes higher temperature at the tube's surface and reduces temperature in the core region of the tube.

In hot tube, there is a potential of higher rate of increasing temperature for the cold mass fraction ( $\mu_c$ ) from 0.1 to 0.8, but a rapid potential of lower rate of increasing temperature for the cold mass fraction near unity. The maximum temperature differences in the hot tube are  $24^{\circ}\text{C}$ ,  $61^{\circ}\text{C}$ ,  $78^{\circ}\text{C}$ , respectively, with 2.5, 3.0 and 3.5 bar (gage), at 4 inlet nozzles for the cold mass fraction of 0.835, 0.854 and 0.829. The same result is found in the cold tube. When pressure at the inlet is higher and the increasing temperature at the hot tube is higher as well. The higher the

pressure, the more the mass flow rate into vortex tube and the momentum transfer of hot and cold air within the tube is further higher. Thus, the temperature of the hot air increases while that of cold air decreases.



**Figure 5.2** Effect of inlet pressures on the increasing temperature at the hot tube and the temperature reduction at the cold tube.

### 5.3 Wall Temperature Distribution along the Insulated Vortex Tube

In experiment, the 16-mm diameter, insulated vortex tube with 0.5D orifice diameter and multiple-inlet nozzles was employed and investigated. Each run was at 29°C. Wall temperatures of the tube were measured at 15 axial stations equally spaced along the axial length from the orifice. The distance between stations is 0.5D and details of locations of temperature to be measured are shown in Fig. 5.3.

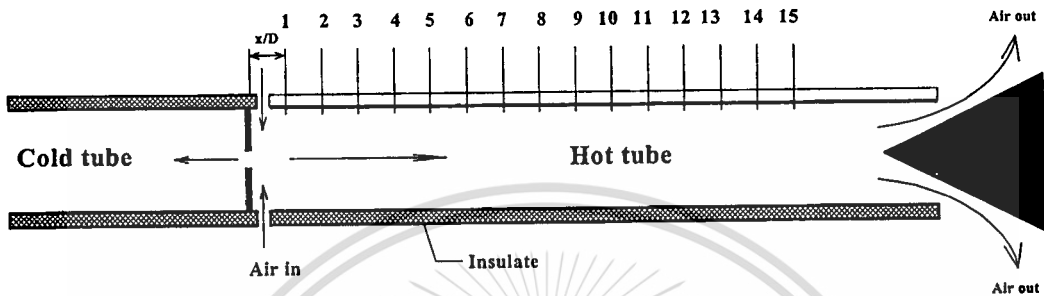


Figure 5.3 Location of temperature to be measured in the insulated vortex tube.

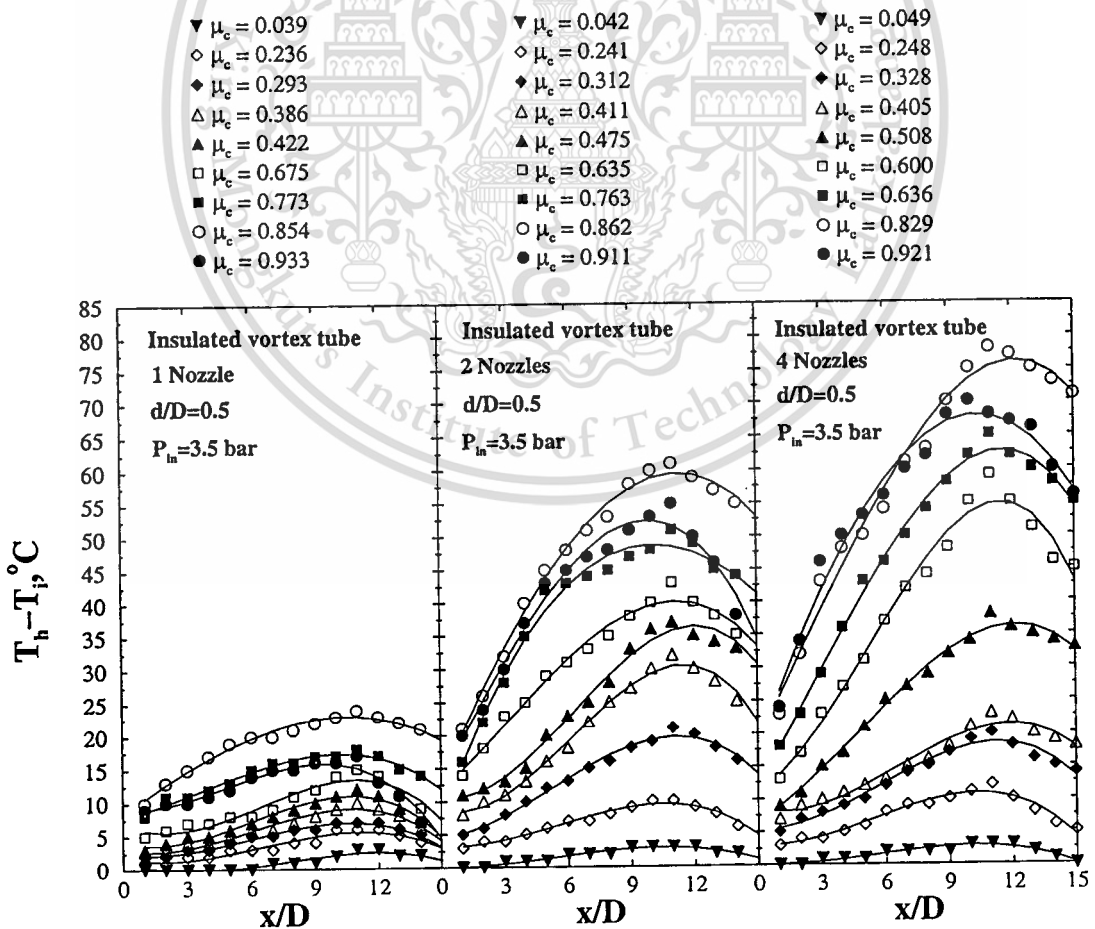


Figure 5.4 Axial wall temperature distribution

This material is reserved for educational use only, not allowed for commercial use.

Forbidden to modify the content, and cite the document when use.

Fig. 5.4 displays the wall temperature distribution in terms of temperature difference between the wall and inlet temperatures against the cold mass fraction. It is found that in a range from  $x/D=1$  to  $x/D=11$ , the difference of temperature distribution has a trend to increase gradually and maximum at  $x/D=11$ . After  $x/D=11$ , the difference of temperature distribution tends to decrease because the hot air and the cold air are mixed together at the beginning of the tube. The temperature of the tube wall increases proportionally with the cold mass fraction, except for the cold mass fraction approaching to 1. At  $x/D=11$ , the temperature differences at the tube wall with 1, 2 and 4 inlet nozzles are  $24^{\circ}\text{C}$ ,  $61^{\circ}\text{C}$  and  $78^{\circ}\text{C}$  respectively, for the cold mass fractions ( $\mu_c$ ) of 0.854, 0.852 and 0.829.

## 5.4 Parametric Study of the Insulated Vortex Tube

### 5.4.1 Influence of the Orifice Plate Sizes

To consider the influence of orifice plate sizes on the temperature difference of the tube, several orifice plate sizes ranging from  $0.4D$  to  $0.9D$  were employed with different inlet nozzles. An compressed air at 3.5 bar (gage) and  $29^{\circ}\text{C}$  was used as a working fluid throughout the experiments. The experimental result of temperature differences between the inlet and cold temperature for various the cold mass fraction is depicted in Fig. 5.5. A closer look reveals that the highest temperature reduction is achieved for all orifice plates when the cold mass fraction ( $\mu_c$ ) is in a range of 0.3 to 0.4. This means that the maximum temperature difference occurs if the cone valve is adjusted to let the cold mass flow rate leave the tube at 30 - 40% of the inlet air.

From Fig. 5.5, The orifice plate size of  $0.5D$  yields the maximum temperature reduction. The highest temperature differences for using 1, 2 and 4 nozzles are  $19^{\circ}\text{C}$ ,  $29^{\circ}\text{C}$  and  $30^{\circ}\text{C}$  respectively. Moreover, the decrease in temperature at the cold tube is found to be  $29^{\circ}\text{C}$ ,  $30^{\circ}\text{C}$ ,  $27^{\circ}\text{C}$ ,  $23^{\circ}\text{C}$ ,  $19^{\circ}\text{C}$ , and  $16^{\circ}\text{C}$  for orifice plate of  $0.4D$ ,  $0.5D$ ,  $0.6D$ ,  $0.7D$ ,  $0.8D$  and  $0.9D$ , respectively, at the cold mass fraction ( $\mu_c$ ) of 0.329 and the number of 4 inlet nozzles.

In addition, the orifice plate of  $0.5D$  has the highest potential of temperature reduction at the cold tube than the rest of orifice plates. Because the orifice plate sizes ranging from  $0.6D$  to  $0.9D$  have the bigger diameters than the  $0.5D$  one, this allows some hot air near the wall to exit the tube with the cold air. Both the hot air

This material is reserved for educational use only, not allowed for commercial use.

Forbidden to modify the content, and cite the document when use.

and cold air while flowing out mix together which further affects the cold air to have higher temperature or be warmer. In the other hand, for a small orifice plate of  $0.4D$ , it has a higher pressure drop and makes the temperature reduction at the cold tube lower.

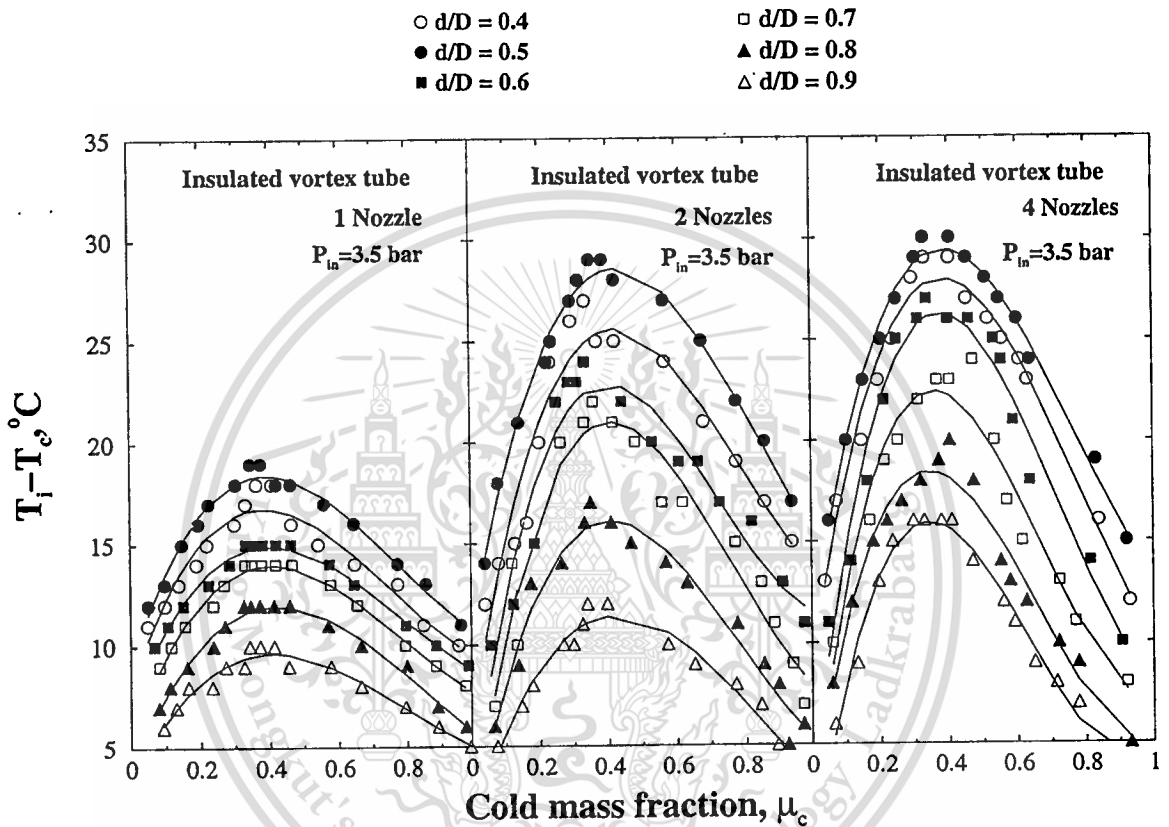


**Figure 5.5** Influence of the orifice plates size on temperature reduction.

#### 5.4.2 Influence of the Number of Inlet Nozzles

Effects of a number of inlet nozzles on temperature reduction in the vortex tube are experimentally investigated. A compressed air at 3.5 bar (gage) and  $29^{\circ}C$  also was used as a working fluid. Measurements were made with three sets of inlet nozzles, namely, 1, 2 and 4 nozzles, and three different orifice plate sizes ;  $d = 0.4D$ ,  $0.5D$  and  $0.6D$ . A set of multi-nozzles is equally spaced around the circumference of the tube. The experimental results of temperature reduction against the cold mass fractions for different orifice sizes and nozzles are depicted in Fig 5.6. It is seen that the maximum decrease in temperature in comparison with the inlet temperature is at the cold mass fraction in a range of 0.3 to 0.4. A closer examination reveals that the

This material is reserved for educational use only, not allowed for commercial use.

increase in number of inlet nozzles of the tube leads to substantial temperature difference.

From Fig 5.6, the use of 4 inlet nozzles results in a higher decreasing temperature at the cold tube than those of single and two nozzles for all orifice plates. Besides, the highest temperature differences are found to be  $19^{\circ}\text{C}$ ,  $29^{\circ}\text{C}$  and  $30^{\circ}\text{C}$  for using 1, 2 and 4 inlet nozzles, respectively. The maximum reduction mostly occurs at the cold mass fraction ( $\mu_c$ ) in a range of 0.375. This indicates that the cone valve should be adjusted to let the cold air at about 37.5% of total inlet air leave the tube.

Adjusting the number of the inlet nozzles to be 1, 2 and 4 nozzles, for all orifice plates, would speed up the flow and increases the air mass flow rate into the vortex tube. Furthermore, it causes higher friction between the boundary of the flows and a higher momentum transfer from the core region to the wall one. This finally reduces temperature in the core region but increases temperature in the tube wall area.

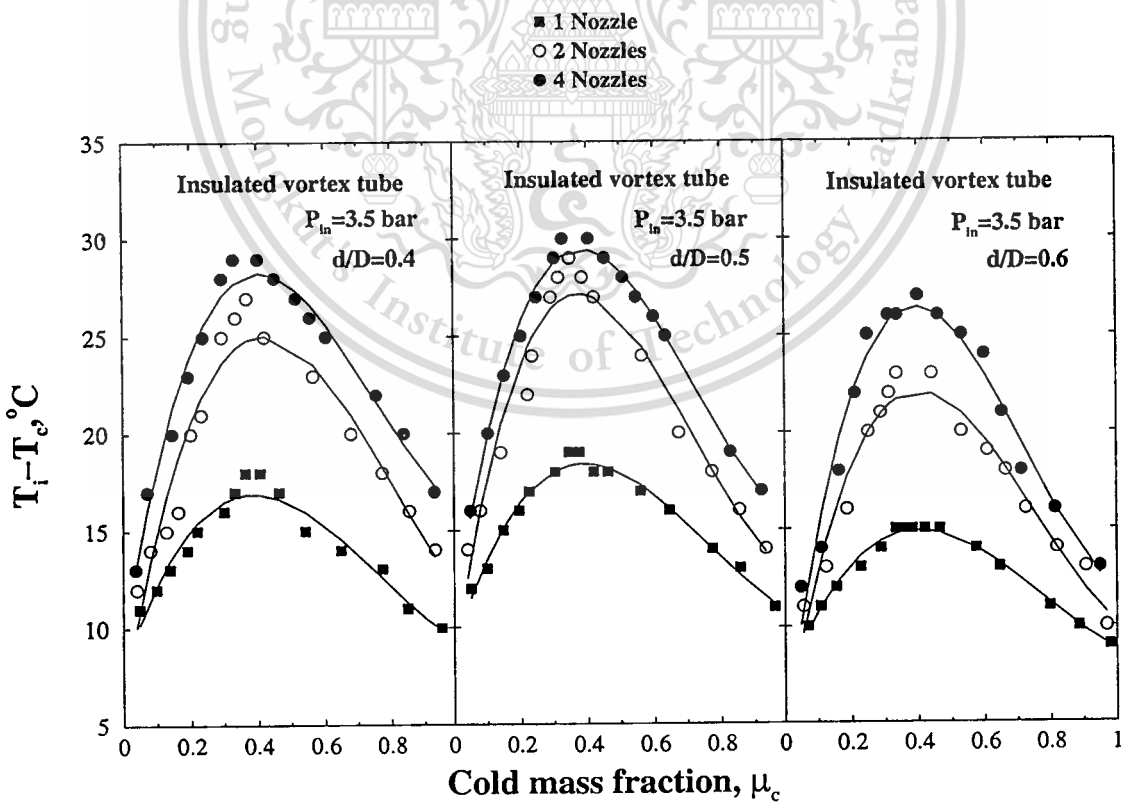


**Figure 5.6** Influence of the number of the inlet nozzles on temperature reduction.

This material is reserved for educational use only, not allowed for commercial use.

Forbidden to modify the content, and cite the document when use.

## 5.5 Comparison with Previous Work

The present experiment work was brought in comparison with those in Hilsch's work in 1947. With reference to Hilsch's sizes of vortex tubes, the present vortex tubes were partially designed; moreover, the results of the present work also are compared with those of Stephan's work in 1983. The sizes and working conditions of the various vortex tubes are shown in Table 5.1 below.

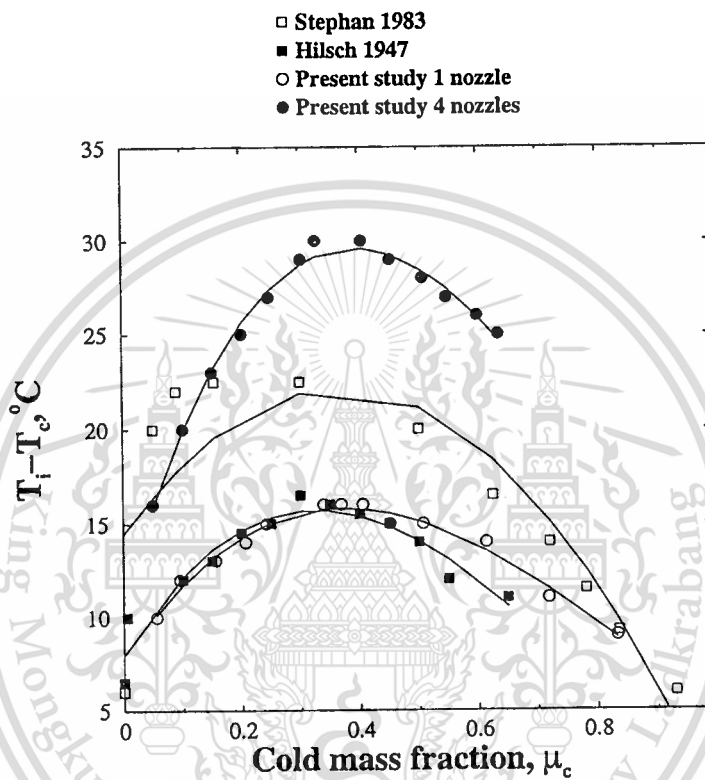


**Figure 5.7** Comparison of temperature reduction in the cold tube among the present work, Hilsch work (1947) and Staephan work (1983).

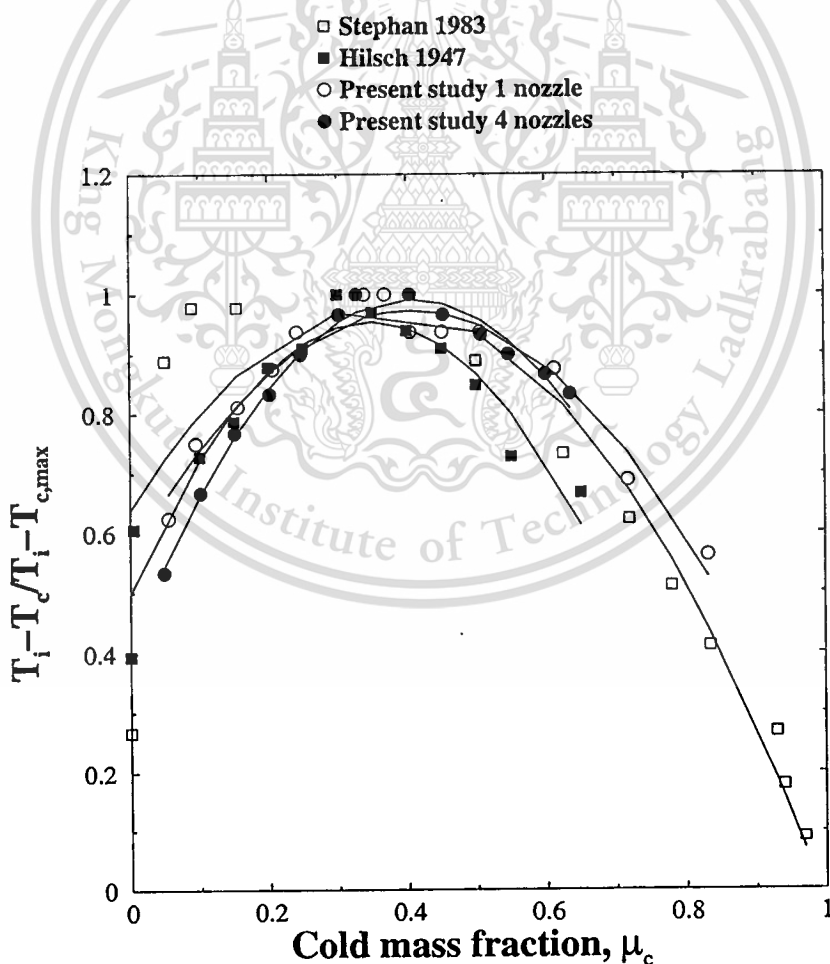
Fig. 5.7 shows the temperature reduction in the cold tube against the cold mass fraction for the present tube, Hilsch's tube and Stephan's tube. It is worth noting that the trend of temperature reduction for all tubes is similar despite different tube and conditions. All tubes yield a maximum temperature difference at the cold mass fraction ( $\mu_c$ ) value between 0.3 to 0.4 except for Stephan's tube that gives a slightly small value. A closer look reveals that for a single nozzle, the temperature difference profile of the present tube is very close to that of Hilsch's tube as can be seen in Fig 5.7, and has a maximum value at about 16°C for both tubes. While Stephan's tube gives the highest value at about 25°C for the cold mass fraction ( $\mu_c$ ) of 0.3.

This material is reserved for educational use only, not allowed for commercial use.

Forbidden to modify the content, and cite the document when use.

**Table 5.1** Comparison of the present tube with Hilsch's tube and Stephan's tube

Vortex tube characteristic	This Study	Stephan (1983)	Hilsch (1947)
Pressure at the inlet, $P_i$ (bar)	3.0	2.5	3
Hot tube length, $L_h$ (mm)	512 (32D)	-	300 (32D)
Cold tube length, $L_c$ (mm)	160(10D)	352(20D)	90 (10D)
Diameter of the vortex tube, $D$ (mm)	16	17.6	9.2
Diameter of nozzles, $\delta$ (mm)	2 ( $D/9$ )	4 ( $D/4.2$ )	1.1 ( $D/9$ )
Number of inlet nozzles, $N$	1 and 4	1	1
Ratio of orifice plate, ( $d/D$ )	0.5	0.4	-

**Figure 5.8** Comparison of the non-dimensional temperature reduction among the present work, Hilsch's and Stephan's work.

This material is reserved for educational use only, not allowed for commercial use.

Forbidden to modify the content, and cite the document when use.

However, when the number of inlet nozzles was replaced from 1 to be 4 nozzles, the temperature difference in the cold tube decreases significantly and is found to be  $30^{\circ}\text{C}$ .

The non-dimensional temperature reduction in the cold tube is depicted in Fig. 5.8 for various cold mass fraction ( $\mu_c$ ) values. It is obvious that all the profiles in Fig. 5.7 can be dropped to be a single profile when all are in a dimensional form. Closer examination reveals that maximum temperature reduction is at a cold mass fraction ( $\mu_c$ ) value ranging from 0.3 to 0.4.

## 5.6 Empirical Relationship of the Insulated Vortex Tube

In dimensional analysis and similarity geometry, we consider a steady axisymmetrical compressible flow in a vortex tube according to Fig. 5.9 with neglecting body force and any energy source. The vortex is well insulated to avoid heat leakage to surroundings. The air flowing through the vortex tube is considered to be an ideal gas. For the process of energy separation of the vortex tube, the temperature of the cold tube is an important variable, which remains to determine. To predict the cold tube temperature, the method of dimensional analysis is used. The independent parameters, which are involved in the energy separation process, can be listed as shown in Table 5.1 and 5.2.

For the prediction of temperature ( $T_c$ ) of the cold tube, the following functional relationship can be written;

$$f(T_c, T_i, P_i, \rho_i, w_i, P_{\infty}, k, c_p, c_v, \mu, \beta, \dot{m}_c, L, D, \delta, d_c, d_h) = 0 \quad (5.1)$$

Then, equation (5.1) can be expressed in a non-dimensional form as follows;

$$\theta_c = F(Ma, Re, Pr, Eu, \gamma, C^*, \beta^*, \rho^*, L^*, \Delta, D_c, D_h, \mu_c) \quad (5.2)$$

As a first approximation, equation (5.2) can be represented by the following equation for a variation of the inlet pressure;

$$\begin{aligned} \theta_c = & f_1(Ma) f_2(Re) f_3(Pr) f_4(Eu) f_5(\gamma) f_6(C^*) f_7(\beta^*) \\ & \times f_8(\rho^*) f_9(L^*) f_{10}(\Delta) f_{11}(D_c) f_{12}(D_h) f_{13}(\mu_c) \end{aligned} \quad (5.3)$$

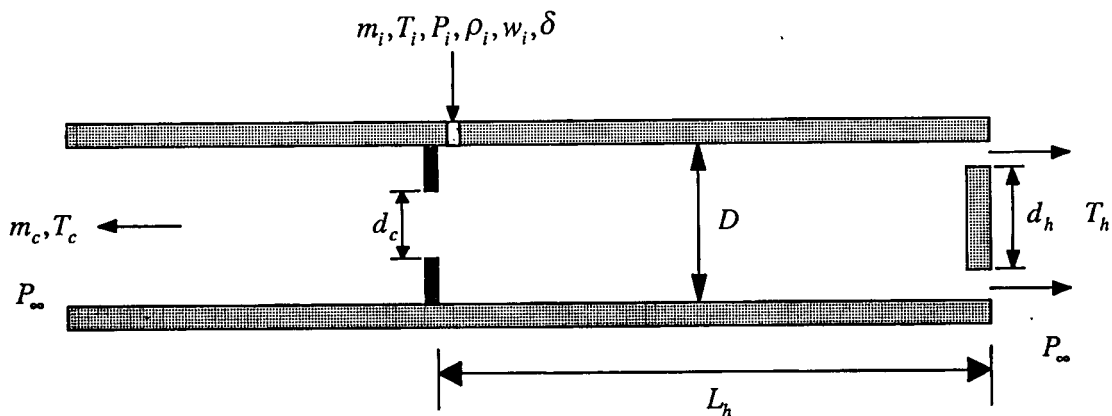


Figure 5.9 Dimension of the vortex tube.

Table 5.2 Summary of different independent parameter equations (Cockerill, 1995).

Independent parameters		
$\gamma = \frac{c_p}{c_v}$	$Ma = \frac{w_i}{(\gamma P_i / \rho_i)^{1/2}}$	$Re = c_p \mu / k$
$Eu = \frac{P_\infty}{(\rho_i w_i^2)}$	$C^* = \frac{c_p}{(P_i / \rho_i T_i)}$	$\beta^* = \beta T_i$
$\theta_c = \frac{(T_i - T_c)}{T_i}$	$L^* = L / D$	$\Delta = \delta / D$
$D_c = d_c / D$	$D_h = d_h / D$	$\mu_c = \dot{m}_c / \dot{m}_i$

Table 5.3 Summary of independent variables (Cockerill, 1995).

Independent variable	Non-dimension	Remark
Ratio of temperature reduction at the cold tube	$(\Delta T_c / T_i)$	$(T_c - T_i) / T_i$
Ratio of temperature increase at the hot tube	$(\Delta T_h / T_i)$	$(T_h - T_i) / T_i$
Velocity ratio	$u / v_i, v / v_i, w / v_i$	
Pressure ratio	$P / \rho_i v_i^2$	
Density ratio	$\rho / \rho_i$	
Temperature ratio	$T / T_i$	

Experimental results indicate that, when the cold mass fraction ( $\mu_c$ ) varies from 0.0 to 1.0 and other parameters are kept constant, possesses a maximum value, which can be, determined from the equation (5.3) as follows;

$$\begin{aligned} \theta_{c,max} &= f_1(Ma)f_2(Re)f_3(Pr)f_4(Eu)f_5(\gamma)f_6(C^*)f_7(\beta^*) \\ &\times f_8(\rho^*)f_9(L^*)f_{10}(\Delta)f_{11}(D_c)f_{12}(D_h)f_{13}(\mu_{c,max}) \end{aligned} \quad (5.4)$$

Dividing equation (5.3) by equation (5.4), we obtain

$$\frac{\theta_c}{\theta_{c,max}} = \frac{f_{13}(\mu_c)}{f_{13}(\mu_{c,max})} = g(\mu_c) \quad (5.5)$$

Substituting the definition for  $\theta_c = \frac{(T_i - T_c)}{T_i}$  in equation (5.5) and letting,

$$\Delta T_c = T_i - T_c \quad (5.6)$$

and

$$\Delta T_{c,max} = T_i - T_{c,max} \quad (5.7)$$

We obtain

$$\frac{\Delta T_c}{\Delta T_{c,max}} = g(\mu_c) \quad (5.8)$$

Equation (5.8) shows the relation of the similarity for the change of temperature at the cold tube. The function of the cold mass fraction ( $\mu_c$ ) depends on each the vortex tube with similar shapes, each of which has the inlet nozzles from a range of 1, 2 and 4 nozzles and the size of the orifice plate ( $d/D$ ) is in a range of  $0.4D$  to  $0.9D$  as shown in Fig. 5.5 and 5.6. Through using the relation of the similarity in equation (5.8), the experimental results are obtained from Fig. 5.6.

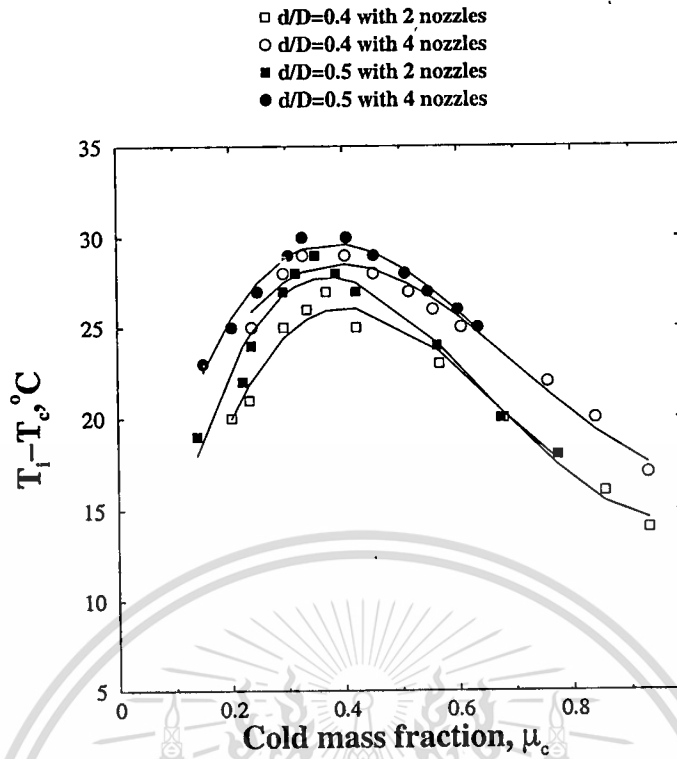


**Figure 5.10** Temperature reduction at various orifice plates of  $0.4D$  to  $0.5D$  and for 2 and 4 inlet nozzles.

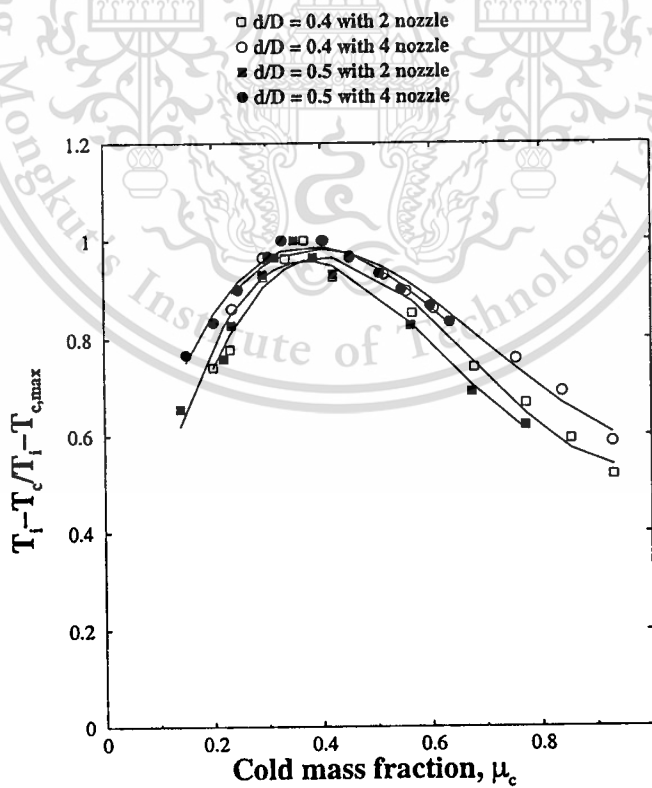


**Figure 5.11** Non-dimensional temperature reduction at various orifice plates of  $0.4D$  to  $0.5D$  and for 2 and 4 inlet nozzles.

This material is reserved for educational use only, not allowed for commercial use.

Forbidden to modify the content, and cite the document when use.

In experimental optimization, the data at 3.5 bar of the tubes with two sizes of the orifice plates (0.4D and 0.5D) and two numbers of inlet nozzles (2 and 4 nozzles) are selected for comparison. This is because their working intervals give the maximum decrease in temperature in the tube. Then, all data required of the selected tubes are plotted and shown in Fig. 5.10. Fig. 5.11 shows the same plot as in Fig. 5.10 but in the non-dimensional form of temperature reduction, which is divided by its maximum cooling.

From Fig. 5.10 and 5.11, It is found that use of an 0.5D orifice plate and 4 inlet nozzles lead to a maximum temperature reduction. Thus, the conditions of the vortex tube as mentioned earlier are employed and the result obtained is brought to plot, as show in Fig. 5.12. Fig. 5.12 illustrates the non-dimensional decrease in temperature for various inlet pressures, which can be dropped to a single curve.

Using equation (5.8) and the optimizing technique, the single curve can be expressed as:

$$\frac{\Delta T_c}{\Delta T_{c,\max}} = 3.79\mu_c^3 - 8.3\mu_c^2 + 4.65\mu_c + 0.21 \quad (5.9)$$

Equation (5.9) helps design the ranges of highest temperature reduction or cooling which is used to predict the decreasing temperature at the cold tube for the vortex tube having the orifice plate of 0.5D and 4 inlet nozzles. Following Stephan (1983), and a cubic fitting yields, (5.10)

$$\frac{\Delta T_c}{\Delta T_{c,\max}} = 3.23\mu_c^3 - 7.97\mu_c^2 + 3.97\mu_c + 0.39 \quad (5.10)$$

Following Cockerill (1995), and a cubic fitting yields, (5.11)

$$\frac{\Delta T_c}{\Delta T_{c,\max}} = 3.34\mu_c^3 - 6.97\mu_c^2 + 3.07\mu_c + 0.57 \quad (5.11)$$

Equation (5.10) and (5.11) are experimental results used in making equation that shows ranges of highest temperature of the vortex tube. They are experimental results

of Stephan's in 1983 and Cockerill's in 1995. Both researchers experimented by using the tube that has diameter of 18 mm and nozzle diameter of 5 mm for Stephan's and 7.5 mm for Cockerill's. When compared with equation (5.9) that is already experimented, it is found that the equation (5.9) is very similar to equation (5.10) and (5.11).

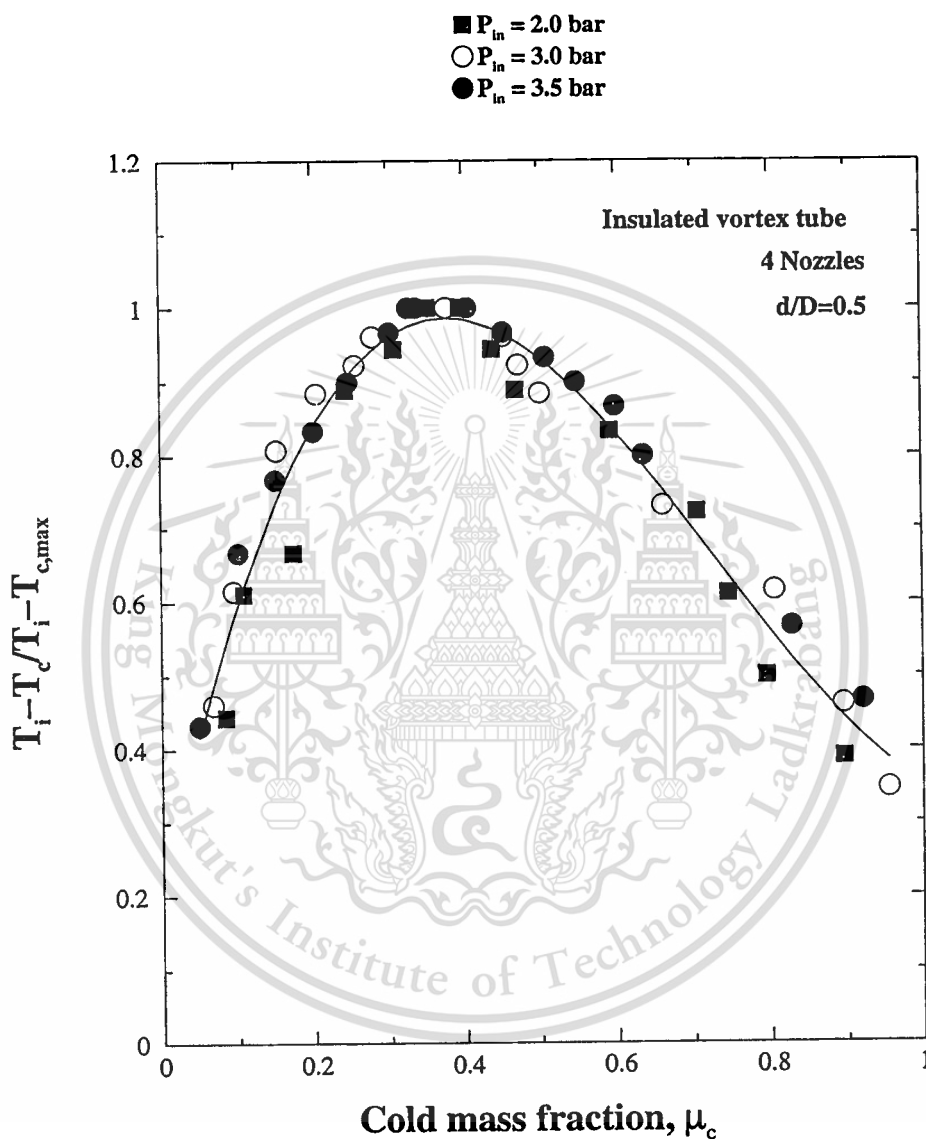


**Figure 5.12** The temperature reduction in the cold tube with the inlet pressure at 2.0, 3.0 and 3.5 bars

### 5.7 Rate of Cooling and Coefficient of Performance

As a result of the experiment, the vortex tube gives highest rate of cooling and coefficient of performance (*C.O.P*) of 99,881 *J/kg* and 0.11, when the ratio of orifice plate is  $0.5D$  ; 4 inlet nozzles and the cold mass fraction ( $\mu_c$ ) of 0.328.

This material is reserved for educational use only, not allowed for commercial use.

Forbidden to modify the content, and cite the document when use.

The rate is considered to be very low value because it is already hypothesized the phenomenon in the vortex tube to be in isentropic process which is ideal state. In fact, ideal state can not actually occurs, which then causes the deriving value to be less than the reality.

Hilsch doing research in 1947 found that cooling equipment as the vortex tube is inappropriate to be used in air condition. Since vortex device has low efficiency of cooling. Lately, many companies apply it to the industry that demands it in small area, which becomes more popular nowadays.



## CHAPTER 6

# CONCLUSION AND RECOMMENDATION

### 6.1 Research Summary

The research studies and analyzes the result of the insulation in the vortex tube, the pressure adjustment at the vortex tube's inlet, the change of numbers of nozzles, and the change of orifice plate ratio. Various parameters and sizes affects cooling rate and decreasing of temperature at cool air section as following.

6.1.1 Although an experimental set-up can merely provide adiabatic condition, it is reasonable to conclude that insulation around the vortex tube helps lessen the loss energy to external environment. Insulated vortex tube has higher rate of temperature reduction at the cool air section than non-insulated does. The difference of decreasing temperature in both tubes is 2 to 12°C. Moreover, the insulated one has higher rate of increasing of temperature at the hot air section than the non-insulated one does which is 10 to 20°C higher at diameter of vortex tube of 16 mm, 1, 2 and 4 inlet nozzles and the size of the orifice plate is 0.5D.

6.1.2 Increasing in the inlet pressure at the vortex tube's and the number of inlet nozzles at the entry of vortex chamber will influence the higher rate of temperature reduction. It is a result of more air mass flowing into the tube, which then increases momentum transfer within the vortex tube. The more momentum transfer, the more the difference of temperature at the tube's wall and that at the middle of the tube becomes which means lower temperature in the middle of the tube.

6.1.3 In adjusting the ratio of orifice plate to permit cool air to flow out to cold tube, it is found that the bigger the inlet nozzles are, the more hot mass from hot tube flowing out and mixing with cold air is. In addition, if the inlet nozzles are too small, the air flowing out will mix with the air in the cold section which then doesn't allow the highest rate of decreasing of temperature or coolest air to occur. Thus, it is necessary to choose sizes of the orifice plate that appropriately let the airflow out through the plate.

6.1.4 The result of experiment using dimensionless parameters and similarity geometry (which provides equations to calculate optimization coolness) presents the

similarity to those of Hilsch and Stephan having done in 1947 and 1983 respectively under similar experimental conditions.

6.1.5 In distribution the temperature at the vortex tube's wall, it is found that by the tube's head the temperature distribution is high. Then it gradually decreases when moved close to the cone valve. In other words, when  $\mu_c$  increases, the temperature distribution will increase as well (except when  $\mu_c$  is close to 1 because it is a position to close the cone valve that the air flows out to the cold section and mix with the other air more).

6.1.6 The vortex tube can decrease temperature down to  $30^\circ\text{C}$  or  $-5^\circ\text{C}$ . It enables cooling up to  $99,881 \text{ J/kg}$  and coefficient of performance (*C.O.P*) of 0.11. This result occurs when pressure at the inlet of the vortex tube is 3.5 bar; numbers of nozzles are 4 inlet nozzles; size of orifice plate is  $0.5D$  and cold mass fraction ( $\mu_c$ ) is 0.328 at diameter of vortex tube of 16 mm.

6.1.7 Adjusting cone valve helps control the flow from the hot and cold tube and decreases the mixing of hot and cold air within the vortex tube. The decreasing of temperature is optimized when adjusting cone valve to have cold mass fraction ( $\mu_c$ ) at 0.3-0.4 or to let the airflow out at 30-40% of all air.

## 6.2 Recommendations

Moisture in the external environment considerably affect the cooling of the vortex tube since moisture air when entering into the tube condenses into water which sucks the energy in the form of heat. This makes lower rate of the decreasing of temperature within the tube. It is suggested to use air dry filter to lessen the moisture in the air. If there is a need to adjust pressure at the inlet of the tube to be higher, it is essential to use air dry filter having higher quality in filtering the air because higher pressure at the inlet means higher chance of the air to be condensed within the vortex tube.

# BIBLIOGRAPHY

- Ahlborn, B. *et al.* 1994. "Limits of Temperature Separation in a Vortex Tube." **Journal of Physics D: Applied Physics.** 27 : 480-488.
- Amitani, T. *et al.* 1983. "A Study on Temperature Separation in a Large Vortex Tube." **Transaction of JSME.** 49 : 877-884.
- Arkharov, A. M. *et al.* October 1983: "Vortex pipe for gas separation has sound radiator at the inlet nozzle connection zone to separation chamber." **USSR Patent na. SU-1048254. WPI Acc No: 84-169119/27.**
- Blaber, M.P. 1950. "A Simply Constructed Vortex Tube for Producing Hot and Cold Air Streams." **Journal of Scientific Instruments.** 27 : 168-169.
- Blatt, T.A. and Trusch, R.B. November 1962. "An Experimental Investigation of an Improved Vortex Cooling Device." **American Society of Mechanical Engineers.** Winter Annual Meeting : 25-30.
- Bruno, T.J. 1992. "Applications of the Vortex Tube in Chemical Analysis." **Process Control and quality 3, Elsevier Science Publishers B.V., Amsterdam.** : 195-207.
- Bruno, T.J. 1993. "Applications of the Vortex Tube in Chemical Analysis Part 1: Introductory Principle." **American Laboratory.** 25 : 15-20.
- Bruun, H.H. 1969. "Experimental investigation of the energy separation in vortex tubes." **Journal of Mechanical Engineering Science.** 11(6) : 367-382.
- Cockerill, T. 1995. "Ranque-Hilsch Vortex Tubes." Ph.D. Thesis, University of Sunderland.
- Collins, R.L. and Lovelace, R.B. 1979. "Experimental study of two-phase propane expanded through the Ranque-Hilsch tube." **Transaction of the ASME: Journal of Heat Transfer.** 101 : 300-305.
- David, C. Banks and Bart, A. Singer 1995. "Vortex Tubes in Turbulent Flows: Identification, Representation, Reconstruction." **National Aeronautics and space Administration under NASA contract No.NAS1-19480.**
- Deissier, R.G. and Pertmutter, M. 1960. "Analysis of the flow and energy separation in a vortex tube." **International Journal of Heat Mass Transfer.** 1 : 173-191.
- Erdelyi, J. 1962. "Wirkung des Zentrifugalfeldes auf Warmezustand der Gase Erklarung der Ranque Erschemung, Forsch." **Forsch. Ing.Wes.** 28 : 181-186.

This material is reserved for educational use only, not allowed for commercial use.

Forbidden to modify the content, and cite the document when use.

- EXAIR Corporation. 1998. **Vortex Tube**. [Online]. Available :  
[http://www.exair.com/vortex tube/frmain.htm](http://www.exair.com/vortex_tube/frmain.htm).
- Frohlingsdorf, W. and Unger, H. 1999. "Numerical investigations of the compressible flow and the energy separation in the Ranque-Hilsch vortex tube." **International Journal of Heat and Mass Transfer**. 42 : 415-422.
- Fulton, C.D. 1950. "Ranque's tube." **ASRE Refrigeration Engineering**. 5 : 473-479.
- Gosman, A.D. and Pun, W.M. 1974. "Calculation of recirculating flows." **Technical Report HTS/74/2, Mechanical Engineering Department**. Imperial Collage.
- Gupta, A.K., *et.al.* 1984. "Swirl Flows." Abacus Press, Turnbridge Wells, England.
- Hartnett, J.P. and Eckert, E.R.G. 1956. "Experimental study of the velocity and temperature distribution in a high-velocity vortex-type flow." **Technical report, Heat Transfer and Fluid Mechanics Institute**.
- Hartnett, J.P., and Eckert, E.R.G. 1957. "Experimental study of the velocity and temperature distribution in a high-velocity vortex-type flow." **Transaction of the ASME, Series C, Journal of Heat Transfer**. 79 : 751-758.
- Hilsch, R. 1947. "The Use of the Expansion of Gases in a Centrifugal Field as Cooling Process." **The review of scientific instruments**. 18(2) : 108-113.
- James Clerk Maxwell. 1891. "*Theory of Heat Longman*." tenth edition. : 338-339.
- Japanese Industrial Standard, 1988. "*Measurement of Fluid Flow by Means of Orifice Plates, Nozzles and Venturi Tubes. JIS Z 8762-1988*." Translated by Japanese Standards Association, Japan
- Johnson, A.F. 1947. "Quantitative Study of the Hilsch Heat separator." **Canadian Journal Research**. 25 : 299.
- Khalil, F.F. and Assaf, H.M.W. 1981. "Computer modeling of turbulent recirculation flow in engineering applications." **In Proceeding of the Second International Conference on Numerical Methods in Laminar and Turbulent Flow Venice**.
- Kurosaka, M. 1982. "Acoustic Streaming in Swirling Flow and the Ranque-Hilsch (Vortex Tube) Effect." **Journal of Fluid Mechanics**. 124 : 139-172.
- Kuwattanachai, N. June 1985. "Vortex tube." **Proceeding of the 3<sup>rd</sup> Conference of Mechanical Engineering Network Thailand**.

- Lay, J.E. August 1959. "An experimental and analytical studies of vortex-flow temperature separation by superposition of spiral and axial flow part 1." **Transaction of the ASME.** : 202-212.
- Lay, J.E. August 1959. "An experimental and analytical studies of vortex-flow temperature separation by superposition of spiral and axial flow part 2." **Transaction of the ASME.** : 213-222.
- Lewellen, W.S. 1962. "A solution for three dimensional vortex flows with strong circulation." **Journal of Fluid Mechanics.** 14(1) : 420ff
- Linderstrom-Lang, C.U. 1964. "Gas separation in the Ranque-Hilsch vortex tube." **International Journal of Heat Mass Transfer.** 7 : 1200-1206.
- Linderstrom-Lang, C.U. 1971. "The three-dimensional distributions of tangential velocity and total-temperature in vortex tubes." **Journal of Fluid Mechanics.** 45 (1) : 161-187.
- Newman Tools Inc. 1998 **Vortex Tubes.** [Online]. Available : <http://www.newmantools.com/vortex.htm>.
- Nash, J.M. October 1974. "Vortex Heat Exchanger Cooling for Infrared Detectors." **Annual Meeting of the Optical Society of America.** : 15-18.
- Nash, J.M. April 1975. "Design of the Vortex Cooler, American Society of Mechanical Engineers." **Annual Design Engineering Conference.** New York, : 21-24.
- Nash, J.M. August 1991. "Vortex Expansion Devices for High Temperature Cryogenics." **Proceedings of the Intersociety Energy Conversion Engineering Conference, IECEC'91.** 4(4-9) : 521-525.
- Negm, M.I.M, *et al.* 1988a. "Performance Characteristics of Energy Separation in Double Stage Vortex Tubes." **Modeling, Simulation & Control B: Mechanical & Thermal Engineering, Materials & Resources, Chemistry.** 14 : 21-32.
- Negm, M.I.M, *et al.* 1988b. "Generalized Correlation's for the Process of Energy Separation in Vortex Tubes." **Modeling, Simulation & Control B: Mechanical & Thermal Engineering, Materials & Resources, Chemistry.** 14 : 47-64.
- Marshall, J. 1977. "Effect of operating conditions Physical size and fluid characteristic on the gas separation performance of a Linderstrom-Lang vortex tube." **International Journal of Heat and Mass Transfer.** 20 : 227-231.
- Martynovskii and Alekseev. 1957. "Investigation of the vortex thermal separation effect of gases and vapor." **Soviet Phys.tech.Phys.** 1 : 233.

- Otten, E.H. 1958. "Production of Cold Air." **Engineering, London.** 154.
- Parulekar, B.B. 1961. "The Short Vortex Tube." **Journal of Refrigeration.** 4 : 74-80.
- Promvong, P. 1997. "A Numerical Study of Vortex Tubes with an Algebraic Reynolds Stress Model." Ph.D. Thesis, University of London.
- Promvong, P. 1999. "Numerical Simulation of Turbulent Compressible Vortex-Tubes Flow." 3<sup>rd</sup> **Joint of ASME/JSME Fluid Engineering**, Sanfrancisco
- Raiskii, Yu. D. and Tankel, L.E. 1974. "Influence of Vortex-Tube Saturation and Length on the Process of Energetic Gas Separation." **Journal Engineering Physics.** 27(6) : 1578-1581.
- Reynolds, A.J. 1961a. "Energy Flows in a Vortex Tube." **Journal Applied Math Physics,** 12 : 343.
- Reynolds, A.J. 1961b. "Studies of Rotating Fluids: I. Plane Axisymmetric Flow. II. The Ranque-Hilsch Vortex Tube." Ph.D. Thesis, University of London, U.K.
- Reynolds, A.J. 1962. "A Note on Vortex-Tube Flows." **Journal of Fluid Mechanic,** 14 : 18.
- Ranque, G.J. 1933. "Experiments on Expansion in a Vortex with Simultaneous Exhaust of Hot Air and Cold Air." **Le Journal de Physique et le Radium (Paris).** 4 : 112-114, S-115, June. Also translated as General Electric Co., Schenectady Works Library, T.F. 3294 (1947).
- Ranque, G.J. March 27 1934. "Method and Apparatus for obtaining from a Fluid Under Pressure Two Current of Fluid at Different Temperature." **U.S. Patent office.** 1 : 952,281.
- Scheller, W.A. and Brown, G.M. 1957. "The Ranque-Hilsch Vortex Tube." **Journal Industrial & Engineering Chemistry.** 49(6) : 1013-16.
- Scheper, G.W. 1951. "The Vortex Tube; Internal Flow Data and a Heat Transfer Theory." **Journal of ASRE, Refrigerating Engineering.** 59 : 985-989.
- Schultz-Grunow, F. 1951. "Turbulenter Warmedurchgang im Zentrifugalfeld." **Forsch. Ing.Wes.** 17(3) : 66-76.
- Schlenz, D. 1982. "Kompressible Strahlgetriebene Drallströmung in Rotationssymmetrischen Kanälen." Ph.D. Thesis, Technische Fakultät Universität, Erlangen-Nürnberg.

- Sibulkin, M. 1962. "Unsteady, Viscous, Circular Flow, Part 3." **Application to the Ranque-Hilsch Vortex Tube**, *J. Fluid Mechanics*. 12 : 269-293.
- Soni, Y. 1973. "A Parametric Study of the Ranque-Hilsch Tube." Ph.D. Thesis, Chemical Engineering Dept., University of Idaho, USA.
- Stephan, K. *et al.* 1983. "A similarity relation for energy separation and vortex tube." **International Journal of Heat Mass Transfer**. 27(6) : 911-920.
- Suzuki, M. 1960. "Theoretical and Experimental Studies on the Vortex-Tube." **Scientific Papers of the Institute of Physical and Chemical Research (Japan)**. 54(1) : 43-87.
- Takahama, H. and Kawashima, K.I. 1960. "An Experimental Study of Vortex tubes." **Mem. Faculty of Engineering**. Nagoya University, 12-2 : 227-245.
- Takayama, H. 1965. "Studies on vortex tubes." **Bulletin of the JSME**. 8(31) : 443-440.
- Takahama, H. and Soga, N. 1966. "Studies on vortex tubes (second report)." **Bulletin of JSME**. 9(33) : 121-130.
- Takahama, H. *et al.* 1971. "Performance characteristics of energy separation in a stream-operation vortex tube." **International Journal of Engineering Science**. 17 : 369-375.
- Takahama, H., *et al.* 1979. "Performance Characteristics of Energy Separation in a Steam Operated Vortex Tube." **International of Journal Engineering Science**. 17 : 735-44.
- Takahama, H and Yokosawa, H. 1981. "Energy separation in vortex tubes with a divergent chamber." **Transactions of the ASME: Journal of Heat Transfer**. 103 : 196-203.
- Van Deemter, J.J. 1952. "On the Theory of the Ranque-Hilsch Cooling Effect." **Applied Scientific Research Netherlands**. 3 (Section A, No.3) : 174-196.
- Vennos, S.L.N. 1968. "An Experimental Investigation of the Gaseous Vortex." Ph.D. Thesis, Rensselaer Polytechnic Institute, Troy, New York, USA
- Webster, D.S. 1950. "An Analysis of the Hilsch Vortex Tube." **Journal of ASRE.Refrigerating Engineering**. 58 : 163-170.
- Wilcox, C.D. 1993. "*Turbulent Modeling for CFD*." California : D CW Industries Inc.
- Williams, A. 1971. "The cooling of methane with vortex tubes." **Journal of Mechanical Engineering Science**. 13(6) : 365-375.

# APPENDICES



This material is reserved for educational use only, not allowed for commercial use.

Forbidden to modify the content, and cite the document when use.

# APPENDIX A

## EXAMPLE OF CALCULATIONS OF THE COLD MASS FRACTION

In calculation to find out the cold mass fraction ( $\mu_c$ ), it was essential that both of the mass flow rate at the inlet and also the mass flow rate at the cold tubes, were to be evaluated. On evaluation of the mass flow rates at both sides through the orifice meter designed by the references from the Japanese industrial standard (JIS Z 8762 - 1988). Thus, the fixed values will be standardized as the followings:

### Givens:

Gravitational acceleration ( $g$ )	= 9.81 $m/s^2$
Density of water ( $\rho_w$ )	= 1000 $kg/m^3$
Pressure at atmosphere ( $P_a$ )	= 101.325 $kPa$
Viscosity ( $\mu_a$ )	= 1.71 $\times 10^{-5}$ $kg/m.s$
The ratio of the orifice plate ( $d/D = \beta$ )	= 0.5 $D$
Pressure drop at the inlet of the vortex tube ( $\Delta h_i$ )	= 830 $mm$
Pressure drop at the cold tube ( $\Delta h_c$ )	= 126 $mm$
The temperature of the inlet air ( $T_i$ )	= 29 $^{\circ}C$
The temperatures of the air through the orifice	= 25 $^{\circ}C$

### To Find

#### 1. The Pressure Loss Inside the Vortex Tube

From the Japanese industrial standard, we could find the loss inside the tubes that:

$$\Delta \bar{w} = \frac{1 - \alpha \beta^2}{1 + \alpha \beta^2} \cdot \Delta P \quad (1)$$

This material is reserved for educational use only, not allowed for commercial use.

Forbidden to modify the content, and cite the document when use.

$$= 0.73\Delta P \quad (2)$$

The pressure loss inside the vortex tube at the inlet vortex tube found from equation (2): Computing equation :

$$\begin{aligned} \Delta \bar{w}_i &= 0.73 \times \rho_w g \Delta h_i = (0.73)(1000 \text{ kg/m}^3)(9.81 \text{ m/s}^2)(0.83 \text{ m}) \\ &= 5,943 \text{ N/m}^2 \end{aligned}$$

And for the pressure loss inside the vortex tube at the cold air tubes capably found from the equation (2): Computing equation:

$$\begin{aligned} \Delta \bar{w}_c &= 0.73 \times \rho_w g \Delta h_c = (0.73)(1000 \text{ kg/m}^3)(9.81 \text{ m/s}^2)(0.126 \text{ m}) \\ &= 902 \text{ N/m}^2 \end{aligned}$$

## 2. The Pressure at the inlet of the Orifice Plates

In experimentation, the values of the pressure at the pre inlets to the orifice plates both the air at the inlet side and the cold air sides for the purpose of evaluating the values of the expandability factor.

Therefore, computing equation

$$P_i = P_a + \Delta P + \Delta \bar{w} \quad (3)$$

The pressure in front of the orifice plates at the inlets to the vortex tube

$$\begin{aligned} P_{i,i} &= P_{a,i} + \Delta P_i + \Delta \bar{w}_i = 101,325 + 8,142 + 5,943 \\ &= 115,411 \text{ N/m}^2 \end{aligned}$$

The pressure in front of the orifice plates at the exits of the cold air

$$\begin{aligned} P_{i,c} &= P_{a,c} + \Delta P_c + \Delta \bar{w}_c = 101,325 + 1,236 + 902 \\ &= 103,463 \text{ N/m}^2 \end{aligned}$$

### 3. Evaluation of Expandability Factor ( $\epsilon$ )

For the flow of the air inside the vortex tube, this enables the compressed compression. It was necessary that finding the constant values ( $\epsilon$ ) should do for the purpose of obtaining the flow rate much more accurately. Computing equation :

$$\epsilon = -0.45157355 + 2.62740835 \left( \frac{P_2}{P_1} \right) - 1.18259361 \left( \frac{P_2}{P_1} \right)^2 \quad (4)$$

The values of expandability factor ( $\epsilon$ ) at the inlet of the vortex tube.

$$\begin{aligned} \epsilon_i &= -0.45157355 + 2.62740835 \left( \frac{107,269}{115,411} \right) - 1.18259361 \left( \frac{107,269}{115,411} \right)^2 \\ &= 0.94 \end{aligned}$$

The value of expandability factor ( $\epsilon$ ) at the cold tube.

$$\begin{aligned} \epsilon_c &= -0.45157355 + 2.62740835 \left( \frac{102,227}{103,463} \right) - 1.18259361 \left( \frac{102,227}{103,463} \right)^2 \\ &= 0.98 \end{aligned}$$

### 4. Evaluation the Mass Flow Rate and Discharge of Coefficient

The mass flow rate was enabled to write out the computing equation which had the increased discharge coefficient values for the purpose of the increase of accretion.

$$\dot{m} = \dot{m}_o C \quad (5)$$

By

$$\dot{m}_o = (2.5017 \times 10^{-4}) \epsilon \sqrt{2\Delta P_o \rho_1} \quad (6)$$

and

This material is reserved for educational use only, not allowed for commercial use.

Forbidden to modify the content, and cite the document when use.

$$\rho_1 = \frac{P_1}{RT_1} \quad (7)$$

The mass flow rate of  $m_{o,i}$  was enabled to find at the inlets through pre-evaluation of the density values.

Thus :

$$\begin{aligned} \rho_{1,i} &= \frac{115,411}{287(273 + 25)} \\ &= 1.35 \text{ kg / m}^3 \end{aligned}$$

And the mass flow rate at the inlets were :

$$\dot{m}_{o,i} = (2.5017 \times 10^{-4})(0.94)\sqrt{(2 \times 8,142 \times 1.35)} = 0.035 \text{ kg / s}$$

Therefore, the values of mass flow rate of  $m_{o,c}$  at the exits of cold air tube were enabled to evaluate through

$$\begin{aligned} \rho_{1,c} &= \frac{103,463}{287(273 + 25)} \\ &= 1.35 \text{ kg / m}^3 \end{aligned}$$

And the mass flow rate at the vortex tube were :

$$\dot{m}_{o,c} = (2.5017 \times 10^{-4})(0.98)\sqrt{(2 \times 1,236 \times 1.35)} = 0.01422 \text{ kg / s}$$

The discharge coefficient obtained from the evaluation the standard formula of JIS result in the discharge coefficient combining of different values of parameter.

Thus, the computing equation were ;

$$\begin{aligned} C &= 0.5959 + 0.0312 \beta^{2.1} - 0.1840 \beta^8 + 0.0029 \beta^{2.5} \left( \frac{10^6}{Re} \right)^{0.75} \\ &\quad + 0.0900 L_1 \beta^4 (1 - \beta^4)^{-1} - 0.0337 L_2 \beta^3 \end{aligned} \quad (8)$$

This material is reserved for educational use only, not allowed for commercial use.

Forbidden to modify the content, and cite the document when use.

And equation (8) could be written :

$$C = 0.5959 + 0.07278 - 0.00071875 + 0.00051265 \left( \frac{10^6}{Re} \right)^{0.75} \\ + 0.0005952 - 0.00041788$$

In evaluation the coefficient of discharge, it was essential that the value of the Reynolds number should be known before. Then we could write as the following ;

$$Re = \frac{\rho V D}{\mu_{air}} = \frac{\dot{m} D}{A \mu_{air}}$$

Sine the area of the cutting section of the vortex tube came were  $A = 2.016 \times 10^{-4} m^2$ , the solution was accordingly rewritten;

$$Re = \frac{\dot{m}(0.016)}{(2.016 \times 10^{-4})(1.71 \times 10^{-5})} = 4.6537 \times 10^6 \dot{m}$$

Therefore ;

The values of Reynolds number at the inlet of vortex tube :

$$Re_i = (4.6537 \times 10^6)(0.035) = 162,832$$

The values of Reynolds number at the cold tube :

$$Re_c = (4.6537 \times 10^6)(0.014) = 66,175$$

Solution of Reynolds number were evaluated to find the values of  $C_i$  and  $C_c$  and the results were :

$$C_i = 0.5959 + 0.07278 - 0.00071875 + 0.00051265 \left( \frac{10^6}{162832.963} \right)^{0.75} \\ + 0.000595 - 0.00041788 \\ = 0.67014$$

And

$$\begin{aligned}
 C_c &= 0.5959 + 0.07278 - 0.00071875 + 0.00051265 \left( \frac{10^6}{66175.614} \right)^{0.75} \\
 &\quad + 0.000595 - 0.00041788 \\
 &= 0.67207
 \end{aligned}$$

## 5. Cold Mass Fraction ( $\mu_c$ )

The ratio of the cold mass fraction ( $\mu_c$ ) obtainable from the formula of : (3.1)

And the mass flow rate at the inlet of the vortex tube and the cold tube were obtained from equation (5) and multiple with coefficient of discharge values. Thus, the results were:

Mass flow rate at the inlet of the vortex tube.

$$\begin{aligned}
 \dot{m}_i &= C_i \dot{m}_{o,i} = 0.67014 \times 0.035 \\
 &= 0.02345 \text{ kg / s}
 \end{aligned}$$

Mass flow rate at the cold tube were :

$$\begin{aligned}
 \dot{m}_c &= C_c \dot{m}_{o,c} = 0.67207 \times 0.01422 \\
 &= 0.00956 \text{ kg / s}
 \end{aligned}$$

Mass flow rate leading to evaluate the values of cold mass fraction. Therefore

$$\begin{aligned}
 \mu_c &= \frac{\dot{m}_c}{\dot{m}_i} = \frac{0.00956}{0.02345} \\
 &= 0.4077
 \end{aligned}$$

In the experimental study, the cone valve were adjusted for the purpose of using to evaluate the values of the mass flow rate at the vortex tube. It was accordingly necessary that the evaluation of the values of the cold mass fraction should be done in every process.

This material is reserved for educational use only, not allowed for commercial use.

Forbidden to modify the content, and cite the document when use.

## APPENDIX B

# TABLE OF EXPERIMENTAL RESULTS

**Table A 1. The influence of the insulated vortex tubes on the temperature reduction and increasing of vortex tube.**

**Given ;**

- Orifice plates ( $d / D$ ) = 0.5D
- Number of nozzles ( $N$ ) = 1 inlet nozzles
- Pressure at the inlet of the vortex tube ( $P_i$ ) = 3.5 bar (gage)
- Temperature at the inlet of the vortex tube ( $T_i$ ) = 29°C
- Temperature reduction at the cold tube ( $\Delta T_c = T_i - T_c$ )
- Temperature increase at the hot tube ( $\Delta T_h = T_h - T_i$ )
- Cold mass fraction ( $\mu_c$ )

Insulated			Non-insulated		
$\mu_c$	$\Delta T_h$ (°C)	$\Delta T_c$ (°C)	$\mu_c$	$\Delta T_h$ (°C)	$\Delta T_c$ (°C)
0.051	2	12	0.051	0	11
0.147	4	15	0.147	2	14
0.196	5	16	0.196	3	15
0.225	9	17	0.225	4	16
0.303	10	18	0.303	5	17
0.345	11	19	0.345	7	18
0.365	12	19	0.365	8	18
0.411	14	18	0.411	10	17
0.463	15	18	0.463	12	16
0.559	17	17	0.559	13	15
0.647	19	16	0.647	15	13
0.774	20	14	0.774	17	12
0.857	24	13	0.857	20	11
0.959	19	11	0.959	16	10

**Table A 2. The influence of the insulated vortex tubes on the temperature reduction and increasing of vortex tube.**

Given ;

Orifice plates ( $d/D$ )	=	0.5D
Number of nozzles ( $N$ )	=	2 inlet nozzles
Pressure at the inlet of the vortex tube ( $P_i$ )	=	3.5 bar (gage)
Temperature at the inlet of the vortex tube ( $T_i$ )	=	29°C
Temperature reduction at the cold tube ( $\Delta T_c = T_i - T_c$ )		
Temperature increase at the hot tube ( $\Delta T_h = T_h - T_i$ )		
Cold mass fraction ( $\mu_c$ )		

Insulated			Non-insulated		
$\mu_c$	$\Delta T_h$ (°C)	$\Delta T_c$ (°C)	$\mu_c$	$\Delta T_h$ (°C)	$\Delta T_c$ (°C)
0.039	1	14	0.038	0	12
0.079	3	16	0.078	1	14
0.140	8	19	0.139	3	17
0.221	10	21	0.220	4	19
0.236	12	24	0.235	5	22
0.293	15	27	0.292	7	25
0.315	18	28	0.314	10	26
0.350	21	29	0.349	12	26
0.386	26	29	0.385	14	26
0.422	32	28	0.421	19	25
0.546	37	27	0.545	26	24
0.675	45	26	0.674	32	21
0.773	51	23	0.772	37	18
0.854	61	20	0.853	49	13
0.933	55	15	0.932	44	11

**Table A 3. The influence of the insulated vortex tubes on the temperature reduction and increasing of vortex tube.**

**Given ;**

- Orifice plates ( $d / D$ ) = 0.5D  
 Number of nozzles ( $N$ ) = 4 inlet nozzles  
 Pressure at the inlet of the vortex tube ( $P_i$ ) = 3.5 bar (gage)  
 Temperature at the inlet of the vortex tube ( $T_i$ ) = 29°C  
 Temperature reduction at the cold tube ( $\Delta T_c = T_i - T_c$ )  
 Temperature increase at the hot tube ( $\Delta T_h = T_h - T_i$ )  
 Cold mass fraction ( $\mu_c$ )

Insulated			Non-insulated		
$\mu_c$	$\Delta T_h$ (°C)	$\Delta T_c$ (°C)	$\mu_c$	$\Delta T_h$ (°C)	$\Delta T_c$ (°C)
0.049	3	16	0.048	1	14
0.101	6	20	0.100	3	17
0.151	8	23	0.150	4	21
0.202	10	25	0.201	6	23
0.248	14	27	0.247	7	25
0.303	15	29	0.302	9	26
0.328	22	30	0.327	13	27
0.405	25	30	0.404	16	27
0.453	30	29	0.452	18	26
0.508	42	28	0.507	31	25
0.548	45	27	0.547	37	24
0.600	55	26	0.559	40	23
0.636	65	24	0.635	55	20
0.829	78	19	0.828	68	17
0.921	74	15	0.920	62	13

**Table B 1. The influence of the inlet pressure on the temperature reduction and increasing of the vortex tube.**

Given ;

- Orifice plates ( $d / D$ ) = 0.5D  
 Number of nozzles ( $N$ ) = 1 inlet nozzles  
 Pressure at the inlet of the vortex tube ( $P_i$ ) = 2.0, 3.0 and 3.5 bar (gage)  
 Temperature at the inlet of the vortex tube ( $T_i$ ) = 29°C  
 Temperature reduction at the cold tube ( $\Delta T_c = T_i - T_c$ )  
 Temperature increase at the hot tube ( $\Delta T_h = T_h - T_i$ )

$P_{in} = 2.0 \text{ bar}$			$P_{in} = 3.0 \text{ bar}$			$P_{in} = 3.5 \text{ bar}$		
$\mu_c$	$\Delta T_h$ (°C)	$\Delta T_c$ (°C)	$\mu_c$	$\Delta T_h$ (°C)	$\Delta T_c$ (°C)	$\mu_c$	$\Delta T_h$ (°C)	$\Delta T_c$ (°C)
0.068	0	7	0.055	1	10	0.051	2	12
0.096	1	8	0.095	2	12	0.098	3	13
0.181	2	9	0.156	2	13	0.147	4	15
0.257	3	10	0.207	4	14	0.196	5	16
0.283	4	11	0.242	6	15	0.225	8	17
0.307	5	11	0.339	7	16	0.303	10	18
0.344	6	12	0.369	8	16	0.345	11	19
0.376	6	12	0.405	8	16	0.365	12	19
0.445	7	11	0.451	9	15	0.411	13	18
0.476	9	11	0.507	12	15	0.463	14	18
0.494	10	10	0.613	14	14	0.559	17	17
0.556	11	10	0.718	16	13	0.647	19	16
0.655	12	9	0.832	18	12	0.774	22	14
0.835	15	6	0.872	20	10	0.857	24	13
0.933	11	5	0.952	15	8	0.959	17	11

**Table B 2. The influence of the inlet pressure on the temperature reduction and increasing of the vortex tube.**

**Given ;**

- Orifice plates ( $d/D$ ) = 0.5D  
 Number of nozzles ( $N$ ) = 2 inlet nozzles  
 Pressure at the inlet of the vortex tube ( $P_i$ ) = 2.0, 3.0 and 3.5 bar (gage)  
 Temperature at the inlet of the vortex tube ( $T_i$ ) = 29°C  
 Temperature reduction at the cold tube ( $\Delta T_c = T_i - T_c$ )  
 Temperature increase at the hot tube ( $\Delta T_h = T_h - T_i$ )

$P_{in} = 2.0$ bar			$P_{in} = 3.0$ bar			$P_{in} = 3.5$ bar		
$\mu_c$	$\Delta T_h$ (°C)	$\Delta T_c$ (°C)	$\mu_c$	$\Delta T_h$ (°C)	$\Delta T_c$ (°C)	$\mu_c$	$\Delta T_h$ (°C)	$\Delta T_c$ (°C)
0.048	0	9	0.042	0	10	0.039	1	14
0.097	1	11	0.093	2	15	0.079	3	16
0.138	2	13	0.133	5	18	0.140	8	19
0.240	3	14	0.224	8	21	0.221	10	21
0.303	6	15	0.268	10	23	0.236	12	24
0.341	8	16	0.301	13	24	0.293	15	27
0.348	9	17	0.307	15	25	0.315	18	28
0.376	11	17	0.356	18	25	0.350	21	29
0.412	14	16	0.376	20	25	0.386	26	29
0.477	18	16	0.434	26	24	0.422	32	28
0.606	25	15	0.554	33	23	0.546	37	27
0.657	30	13	0.728	39	22	0.675	45	26
0.730	35	11	0.822	46	19	0.773	51	23
0.799	40	9	0.867	55	14	0.854	61	20
0.907	36	6	0.935	47	8	0.933	55	15

**Table B 3. The influence of the inlet pressure on the temperature reduction and increasing of the vortex tube.**

Given ;

Orifice plates ( $d/D$ )	=	0.5D
Number of nozzles ( $N$ )	=	4 inlet nozzles
Pressure at the inlet of the vortex tube ( $P_i$ )	=	2.0, 3.0 and 3.5 bar (gage)
Temperature at the inlet of the vortex tube ( $T_i$ )	=	29°C
Temperature reduction at the cold tube ( $\Delta T_c = T_i - T_c$ )		
Temperature increase at the hot tube ( $\Delta T_h = T_h - T_i$ )		

$P_{in} = 2.0 \text{ bar}$			$P_{in} = 3.0 \text{ bar}$			$P_{in} = 3.5 \text{ bar}$		
$\mu_c$	$\Delta T_h$ (°C)	$\Delta T_c$ (°C)	$\mu_c$	$\Delta T_h$ (°C)	$\Delta T_c$ (°C)	$\mu_c$	$\Delta T_h$ (°C)	$\Delta T_c$ (°C)
0.084	1	8	0.067	3	13	0.049	3	6
0.108	2	10	0.095	4	16	0.101	6	20
0.175	3	12	0.153	5	21	0.151	8	23
0.245	4	15	0.206	7	23	0.202	10	25
0.309	5	16	0.257	10	24	0.248	14	27
0.333	6	17	0.28	12	25	0.303	15	29
0.354	8	18	0.338	15	26	0.328	22	30
0.396	11	18	0.378	17	26	0.405	25	30
0.439	18	17	0.453	22	25	0.453	30	29
0.47	22	16	0.473	28	24	0.508	42	28
0.593	30	15	0.501	36	23	0.548	45	27
0.706	38	13	0.661	45	19	0.6	52	26
0.746	54	11	0.806	58	16	0.636	65	24
0.795	55	9	0.895	68	12	0.829	78	19
0.896	54	7	0.955	59	9	0.921	74	15

**Table C 1. The influence of the number of inlet nozzles on the temperature distribution at the wall of hot tube.**

**Given ;**

Orifice plates ( $d/D$ )	=	0.5D
Number of nozzles ( $N$ )	=	1 inlet nozzles
Pressure at the inlet of the vortex tube ( $P_i$ )	=	3.5 bar (gage)
Temperature at the inlet of the vortex tube ( $T_i$ )	=	29°C
Temperature increase at the hot tube ( $\Delta T_h = T_h - T_i$ )		
Cold mass fraction ( $\mu_c$ )		

Position	$\Delta T_h$ (°C)									
	( $\mu_c$ ) 0.039	( $\mu_c$ ) 0.140	( $\mu_c$ ) 0.236	( $\mu_c$ ) 0.293	( $\mu_c$ ) 0.386	( $\mu_c$ ) 0.422	( $\mu_c$ ) 0.675	( $\mu_c$ ) 0.773	( $\mu_c$ ) 0.854	( $\mu_c$ ) 0.933
1	0	0	1	2	2	3	5	8	10	9
2	0	0	1	2	3	4	6	11	13	10
3	0	0	2	3	4	5	7	11	15	10
4	0	1	2	3	4	5	7	12	17	11
5	0	1	3	4	5	6	8	13	19	12
6	0	1	3	5	6	7	8	15	20	14
7	1	2	3	5	6	8	9	16	20	15
8	1	2	4	6	7	9	11	16	21	15
9	1	2	4	6	8	10	12	17	22	16
10	2	3	5	7	9	11	14	17	23	16
11	2	3	5	7	10	12	15	18	24	17
12	2	3	4	7	9	11	14	15	23	13
13	1	2	4	6	8	9	11	13	22	11
14	1	1	3	5	6	7	9	11	21	7
15	0	0	2	3	4	5	8	10	19	6

**Table C 2. The influence of the number of inlet nozzles on the temperature distribution at the wall of hot tube.**

Given ;

Orifice plates ( $d/D$ )	=	0.5D
Number of nozzles ( $N$ )	=	2 inlet nozzles
Pressure at the inlet of the vortex tube ( $P_i$ )	=	3.5 bar (gage)
Temperature at the inlet of the vortex tube ( $T_i$ )	=	29°C
Temperature increase at the hot tube ( $\Delta T_h = T_h - T_i$ )		
Cold mass fraction ( $\mu_c$ )		

Position	$\Delta T_h$ (°C)									
	( $\mu_c$ ) 0.039	( $\mu_c$ ) 0.140	( $\mu_c$ ) 0.236	( $\mu_c$ ) 0.293	( $\mu_c$ ) 0.386	( $\mu_c$ ) 0.422	( $\mu_c$ ) 0.675	( $\mu_c$ ) 0.773	( $\mu_c$ ) 0.854	( $\mu_c$ ) 0.933
1	0	1	3	5	8	11	14	16	21	20
2	0	1	4	6	10	12	18	22	26	24
3	1	2	4	8	11	13	23	28	32	30
4	1	2	5	10	13	15	25	35	40	37
5	1	3	6	12	16	20	29	42	45	43
6	2	3	7	13	18	23	31	43	48	45
7	2	4	7	15	22	25	33	44	51	47
8	2	5	8	16	25	28	35	45	53	48
9	3	5	9	18	27	33	38	47	58	51
10	3	6	10	19	30	36	40	48	60	53
11	3	6	10	21	32	37	43	51	61	55
12	2	5	9	20	30	35	40	49	59	50
13	2	4	8	18	28	34	38	45	57	46
14	1	3	6	16	25	33	35	44	55	38
15	0	1	5	14	23	32	34	41	54	36

**Table C 3. The influence of the number of inlet nozzles on the temperature distribution at the wall of hot tube.**

**Given ;**

Orifice plates ( $d / D$ )	=	$0.5D$
Number of nozzles ( $N$ )	=	4 inlet nozzles
Pressure at the inlet of the vortex tube ( $P_i$ )	=	3.5 bar (gage)
Temperature at the inlet of the vortex tube ( $T_i$ )	=	$29^\circ C$
Temperature increase at the hot tube ( $\Delta T_h = T_h - T_i$ )		
Cold mass fraction ( $\mu_c$ )		

Position	$\Delta T_h (^\circ C)$									
	$(\mu_c)$ 0.049	$(\mu_c)$ 0.151	$(\mu_c)$ 0.248	$(\mu_c)$ 0.328	$(\mu_c)$ 0.405	$(\mu_c)$ 0.508	$(\mu_c)$ 0.600	$(\mu_c)$ 0.636	$(\mu_c)$ 0.829	$(\mu_c)$ 0.921
1	0	1	3	5	7	9	13	18	23	24
2	0	2	4	7	9	11	17	23	32	34
3	1	2	4	8	10	15	23	29	43	46
4	1	3	5	9	11	17	27	36	48	50
5	1	3	6	10	12	21	31	43	50	53
6	2	4	8	12	13	25	37	46	54	56
7	2	4	9	14	15	27	42	50	61	60
8	2	5	9	15	16	29	44	54	63	62
9	2	5	10	17	18	32	48	58	70	68
10	3	5	11	19	21	34	55	62	75	71
11	3	6	12	20	23	38	59	65	78	74
12	3	5	10	18	22	36	55	62	77	70
13	2	3	8	16	20	35	51	60	75	66
14	1	2	6	15	19	34	46	58	73	62
15	0	2	5	14	18	33	45	55	71	58

**Table D 1. The influence of the numbers of inlet nozzles on the temperature reduction of the cold tube.**

**Given ;**

Orifice plates ( $d/D$ )	=	$0.4D$
Number of nozzles ( $N$ )	=	1, 2 and 4inlet nozzles
Pressure at the inlet of the vortex tube ( $P_i$ )	=	3.5 bar (gage)
Temperature at the inlet of the vortex tube ( $T_i$ )	=	$29^\circ\text{C}$
Temperature reduction at the cold tube ( $\Delta T_c = T_i - T_c$ )		
Cold mass fraction ( $\mu_c$ )		

$N=1$		$N=2$		$N=4$	
$\mu_c$	$\Delta T_c$ ( $^\circ\text{C}$ )	$\mu_c$	$\Delta T_c$ ( $^\circ\text{C}$ )	$\mu_c$	$\Delta T_c$ ( $^\circ\text{C}$ )
0.049	11	0.040	12	0.036	13
0.098	12	0.081	14	0.072	17
0.139	13	0.129	15	0.146	20
0.190	14	0.164	16	0.193	23
0.220	15	0.201	20	0.237	25
0.300	16	0.233	21	0.294	28
0.332	17	0.294	25	0.329	29
0.364	18	0.335	26	0.402	29
0.408	18	0.369	27	0.452	28
0.464	17	0.422	25	0.515	27
0.541	15	0.567	23	0.557	26
0.648	14	0.680	20	0.606	25
0.773	13	0.774	18	0.756	22
0.850	11	0.855	16	0.839	20
0.952	10	0.932	14	0.930	17

**Table D 2. The influence of the numbers of inlet nozzles on the temperature reduction of the cold tube.**

Given ;

Orifice plates ( $d/D$ ) = 0.5D

Number of nozzles ( $N$ ) = 1, 2 and 4 inlet nozzles

Pressure at the inlet of the vortex tube ( $P_i$ ) = 3.5 bar (gage)

Temperature at the inlet of the vortex tube ( $T_i$ ) = 29°C

Temperature reduction at the cold tube ( $\Delta T_c = T_i - T_c$ )

Cold mass fraction ( $\mu_c$ )

N = 1		N = 2		N = 4	
$\mu_c$	$\Delta T_c$ (°C)	$\mu_c$	$\Delta T_c$ (°C)	$\mu_c$	$\Delta T_c$ (°C)
0.051	12	0.039	14	0.049	16
0.098	13	0.079	16	0.101	20
0.147	15	0.140	19	0.151	23
0.196	16	0.221	22	0.202	25
0.225	17	0.236	24	0.248	27
0.303	18	0.293	27	0.303	29
0.345	19	0.315	28	0.328	30
0.375	19	0.350	29	0.405	30
0.420	18	0.386	28	0.453	29
0.463	18	0.422	27	0.508	28
0.559	17	0.564	24	0.548	27
0.647	16	0.675	20	0.600	26
0.774	14	0.773	18	0.636	25
0.857	13	0.854	16	0.829	19
0.959	11	0.933	14	0.921	17

**Table D 3. The influence of the numbers of inlet nozzles on the temperature reduction of the cold tube.**

Given ;

Orifice plates ( $d/D$ ) = 0.6D

Number of nozzles ( $N$ ) = 1, 2 and 4 inlet nozzles

Pressure at the inlet of the vortex tube ( $P_i$ ) = 3.5 bar (gage)

Temperature at the inlet of the vortex tube ( $T_i$ ) = 29°C

Temperature reduction at the cold tube ( $\Delta T_c = T_i - T_c$ )

Cold mass fraction ( $\mu_c$ )

$N=1$		$N=2$		$N=4$	
$\mu_c$	$\Delta T_c$ (°C)	$\mu_c$	$\Delta T_c$ (°C)	$\mu_c$	$\Delta T_c$ (°C)
0.068	10	0.055	11	0.048	12
0.107	11	0.123	13	0.108	14
0.152	12	0.185	16	0.162	18
0.226	13	0.250	20	0.210	22
0.286	14	0.286	21	0.247	25
0.332	15	0.311	22	0.309	26
0.349	15	0.334	23	0.336	26
0.381	15	0.441	23	0.399	27
0.419	15	0.530	20	0.459	26
0.463	15	0.608	19	0.532	25
0.575	14	0.663	18	0.600	24
0.646	13	0.725	16	0.653	21
0.797	11	0.818	14	0.712	18
0.884	10	0.906	13	0.814	16
0.980	9	0.968	10	0.950	13

**Table E 1. The influence the sizes of the orifice plates on the temperature reduction of the cold tube.**

**Given ;**

Orifice plates ( $d/D$ ) = 0.4  $D$  to 0.9 $D$

Number of nozzles ( $N$ ) = 1 inlet nozzles

Pressure at the inlet of the vortex tube ( $P_i$ ) = 3.5 bar (gage)

Temperature at the inlet of the vortex tube ( $T_i$ ) = 29°C

Temperature reduction at the cold tube ( $\Delta T_c = T_i - T_c$ )

Cold mass fraction ( $\mu_c$ )

$d/D = 0.4$		$d/D = 0.5$		$d/D = 0.6$		$d/D = 0.7$		$d/D = 0.8$		$d/D = 0.9$	
$\mu_c$	$\Delta T_c$ (°C)	$\mu_c$	$\Delta T_c$ (°C)	$\mu_c$	$\Delta T_c$ (°C)	$\mu_c$	$\Delta T_c$ (°C)	$\mu_c$	$\Delta T_c$ (°C)	$\mu_c$	$\Delta T_c$ (°C)
0.049	11	0.051	12	0.068	10	0.082	9	0.080	7	0.092	6
0.098	12	0.098	13	0.107	11	0.116	10	0.112	8	0.130	7
0.139	13	0.147	15	0.152	12	0.157	11	0.161	9	0.166	8
0.190	14	0.196	16	0.226	13	0.237	12	0.237	10	0.235	8
0.220	15	0.225	17	0.286	14	0.269	13	0.271	11	0.273	9
0.300	16	0.303	18	0.332	15	0.330	14	0.326	12	0.326	9
0.332	17	0.345	19	0.349	15	0.350	14	0.346	12	0.342	10
0.364	18	0.375	19	0.381	15	0.378	14	0.373	12	0.372	10
0.408	18	0.420	18	0.419	15	0.418	14	0.412	12	0.412	10
0.464	16	0.463	18	0.463	15	0.465	14	0.459	12	0.456	9
0.541	15	0.559	17	0.575	14	0.577	13	0.570	11	0.578	9
0.648	14	0.647	16	0.646	13	0.655	12	0.665	10	0.665	8
0.773	13	0.774	14	0.797	11	0.795	10	0.800	9	0.794	7
0.850	11	0.857	13	0.884	10	0.884	9	0.890	7	0.892	6
0.952	10	0.959	11	0.980	9	0.972	8	0.973	6	0.985	5

**Table E 2. The influence the sizes of the orifice plates on the temperature reduction of the cold tube.**

**Given ;**

Orifice plates ( $d/D$ ) = 0.4  $D$  to 0.9 $D$

Number of nozzles ( $N$ ) = 2 inlet nozzles

Pressure at the inlet of the vortex tube ( $P_i$ ) = 3.5 bar (gage)

Temperature at the inlet of the vortex tube ( $T_i$ ) = 29°C

Temperature reduction at the cold tube ( $\Delta T_c = T_i - T_c$ )

Cold mass fraction ( $\mu_c$ )

$d/D = 0.4$		$d/D = 0.5$		$d/D = 0.6$		$d/D = 0.7$		$d/D = 0.8$		$d/D = 0.9$	
$\mu_c$	$\Delta T_c$ (°C)	$\mu_c$	$\Delta T_c$ (°C)	$\mu_c$	$\Delta T_c$ (°C)	$\mu_c$	$\Delta T_c$ (°C)	$\mu_c$	$\Delta T_c$ (°C)	$\mu_c$	$\Delta T_c$ (°C)
0.040	12	0.039	14	0.055	10	0.066	7	0.067	6	0.074	5
0.081	14	0.079	18	0.123	12	0.133	10	0.137	9	0.146	7
0.129	15	0.140	21	0.185	15	0.119	14	0.175	13	0.177	8
0.164	16	0.221	24	0.250	22	0.263	20	0.265	14	0.267	10
0.201	20	0.236	25	0.286	23	0.331	21	0.331	16	0.298	10
0.233	24	0.293	27	0.311	23	0.358	22	0.349	17	0.325	11
0.294	26	0.315	28	0.334	24	0.415	21	0.410	16	0.339	12
0.335	27	0.350	29	0.441	22	0.480	20	0.468	15	0.397	12
0.369	25	0.386	29	0.530	20	0.558	17	0.569	14	0.573	10
0.422	25	0.422	28	0.608	19	0.618	17	0.630	13	0.652	9
0.567	24	0.564	27	0.663	19	0.770	15	0.775	11	0.770	8
0.680	21	0.675	25	0.725	17	0.844	13	0.851	9	0.843	7
0.774	19	0.773	22	0.818	16	0.882	11	0.894	8	0.891	5
0.855	17	0.854	20	0.906	13	0.934	9	0.921	5	0.920	4
0.932	15	0.933	17	0.968	11	0.964	7	0.965	6	0.971	4

**Table E 3. The influence the sizes of the orifice plates on the temperature reduction of the cold tube.**

**Given ;**

Orifice plates ( $d/D$ ) = 0.4  $D$  to 0.9 $D$

Number of nozzles ( $N$ ) = 4 inlet nozzles

Pressure at the inlet of the vortex tube ( $P_i$ ) = 3.5 bar (gage)

Temperature at the inlet of the vortex tube ( $T_i$ ) = 29 °C

Temperature reduction at the cold tube ( $\Delta T_c = T_i - T_c$ )

Cold mass fraction ( $\mu_c$ )

$d/D = 0.4$		$d/D = 0.5$		$d/D = 0.6$		$d/D = 0.7$		$d/D = 0.8$		$d/D = 0.9$	
$\mu_c$	$\Delta T_c$ (°C)	$\mu_c$	$\Delta T_c$ (°C)	$\mu_c$	$\Delta T_c$ (°C)	$\mu_c$	$\Delta T_c$ (°C)	$\mu_c$	$\Delta T_c$ (°C)	$\mu_c$	$\Delta T_c$ (°C)
0.036	13	0.049	16	0.048	11	0.059	10	0.058	8	0.066	6
0.072	17	0.101	20	0.108	14	0.113	14	0.116	12	0.132	9
0.146	20	0.151	23	0.162	18	0.168	16	0.178	15	0.193	13
0.193	23	0.202	25	0.210	22	0.212	19	0.219	16	0.235	15
0.237	25	0.248	27	0.247	25	0.251	20	0.262	17	0.295	16
0.294	28	0.303	29	0.309	26	0.309	22	0.317	18	0.327	16
0.329	29	0.328	30	0.336	27	0.366	23	0.371	19	0.377	16
0.402	29	0.405	30	0.399	26	0.403	23	0.403	20	0.408	16
0.452	27	0.453	29	0.459	26	0.471	24	0.472	18	0.469	14
0.515	26	0.508	28	0.532	25	0.533	20	0.551	14	0.558	12
0.557	25	0.548	27	0.555	24	0.569	17	0.577	13	0.590	11
0.606	24	0.600	26	0.588	21	0.614	15	0.626	12	0.649	9
0.630	23	0.636	24	0.637	18	0.723	13	0.720	10	0.713	8
0.839	16	0.829	19	0.814	14	0.768	11	0.778	9	0.778	7
0.930	12	0.921	15	0.907	10	0.921	8	0.932	5	0.921	4

APPENDIX C  
THE PUBLISHED PAPER



สัมมนาวิชาการวิศวกรรมเครื่องกล  
แห่งประเทศไทยครั้งที่ ๑๓

**NMEC13<sup>th</sup>**  
National Mechanical Engineering Conference

บทความทางวิชาการ เล่มที่ ๒/๒

จัดโดย

เครือข่ายวิศวกรรมเครื่องกล

ดำเนินงานโดย

ภาควิชาวิศวกรรมเครื่องกล

คณะวิศวกรรมศาสตร์

สถาบันเทคโนโลยีพระจอมเกล้า

เจ้าคุณทหารลาดกระบัง

วันที่ ๒-๓ ธันวาคม ๒๕๕๒

# การศึกษาสมรรถนะเชิงทดลองของท่อ Ranque-Hilsch Vortex An Experimental Performance Study of a Ranque-Hilsch Vortex Tube

พงษ์เจต พรหมวงศ์ และ สมิทธิ์ เอี่ยมสอาด  
ภาควิชาวิศวกรรมเครื่องกล คณะวิศวกรรมศาสตร์ สถาบันเทคโนโลยีพระจอมเกล้าเจ้าคุณทหารลาดกระบัง  
ถ.ฉลองกรุง เขตลาดกระบัง กรุงเทพฯ 10520  
โทร 66(2)326-9987, โทรสาร66(2)326-9053, E-Mail: kppcngje@kmitl.ac.th

### บทคัดย่อ

การศึกษาและทดลองถึงสมรรถนะการทำความเย็นของทอว์ร์เทกซ์ (Ranque-Hilsch Vortex Tube) ได้ทำการทดลองกับทอว์ร์เทกซ์แบบไหลสวนทางกัน (Counter flow vortex) และทำการศึกษถึงผลกระทบอัตราส่วนของแผ่นออริฟิสต่อขนาดทอว์ร์เทกซ์ที่มีผลต่อสมรรถนะการทำความเย็นภายในทอว์ร์เทกซ์และสัดส่วนมวลของอากาศเย็น (Cold factor) ซึ่งในทดลองได้ทำการเลือกใช้แผ่นออริฟิสขนาด  $d/D = 0.1, 0.12, 0.16, 0.25$  และ  $0.5$  โดยพบว่าที่  $d/D = 0.25$  จะมีผลต่อสมรรถนะทำความเย็นภายในทอว์ร์เทกซ์และสัดส่วนมวลของอากาศเย็น(Cold factor)มากที่สุด

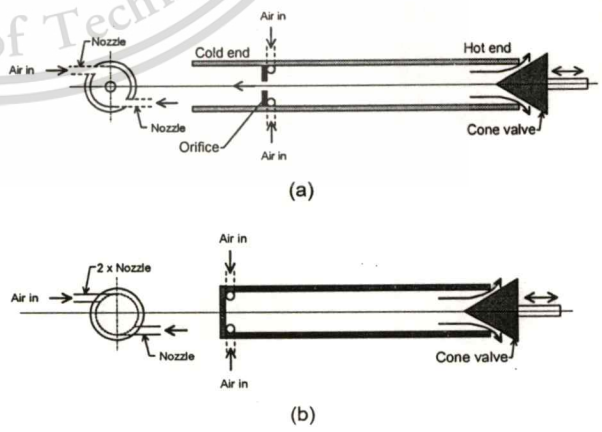
### Abstract

This paper concerns a cooling performance study of Ranque-Hilsch Vortex tubes. The vortex is a device used to separate a compressed gas stream into a cold stream and a hot one. Effects of ratios of orifice to tube diameter on a cooling performance are examined for the counter flow vortex-tube type. The results show that the orifice of  $d/D = 0.16-0.25$  gives the highest cooling performance.

### 1. บทนำ

ทอว์ร์เทกซ์เป็นอุปกรณ์ที่สามารถทำการผลิตอากาศร้อนและอากาศเย็นได้โดยที่ไม่มีการเคลื่อนที่และเมื่ออากาศที่ไหลอัดตัวผ่านรูหัวฉีด (Nozzle) เข้ามาในแนวเส้นสัมผัสกับมุมทอว์ร์เทกซ์ (Tangential Velocity) จะทำให้เกิดการเคลื่อนที่ในลักษณะการหมุนวน (Vortex) ภายในท่อเกิดขึ้น โดยที่อากาศบริเวณกลางท่อจะมีอุณหภูมิต่ำกว่าอุณหภูมิของอากาศที่ทางเข้าและส่วนอากาศบริเวณผนังท่อจะมีอุณหภูมิสูงกว่าอุณหภูมิของอากาศที่ทางเข้า ในการแยกอากาศเย็นและอากาศร้อนออกจากกัน สามารถทำได้โดยการติดตั้งแผ่นออริฟิสที่มีขนาดของเส้นผ่านศูนย์กลางเล็กกว่าทอว์ร์เทกซ์ในตำแหน่งที่ใกล้รูหัวฉีด (Nozzle) โดยที่อากาศเย็นที่บริเวณกลางท่อจะไหลออกผ่านแผ่นออริฟิสซึ่งอยู่ฝั่งตรงข้ามกับวาล์วควบคุมการไหล (Cone-shaped valve) ในขณะที่อากาศร้อนที่ผนังท่อจะไหลผ่านออกมาด้านวาล์วควบคุมการไหล (Cone-shaped valve) ดังที่แสดงในรูปที่ 1a ซึ่งปริมาณการไหลของอากาศร้อนและอากาศเย็นสามารถควบคุมได้โดยใช้วาล์วควบคุมดังกล่าว โดยทั่วไปทอว์ร์เทกซ์สามารถแบ่งออกได้เป็นสองแบบ แบบแรกเป็นการไหลแบบสวนทางกัน (Counter flow type) ซึ่งส่วนมากจะใช้เป็นรูปแบบอ้างอิงมาตรฐานและแบบที่สองเป็นการไหลแบบตามกันในทิศทางเดียว (Uniflow type) หรือการไหลแบบขนานกัน (Parallel flow type) ดังรูปที่ 1a และ 1b ตามลำดับ โดยทั่วไปชุดอุปกรณ์ทอว์ร์เทกซ์ได้ถูกนำไปใช้ในโรงงานและภาคอุตสาหกรรม โดยได้ทำการใช้ความเย็นที่ผลิตได้จากทอว์ร์เทกซ์มาใช้ในงานการหล่อเย็นชิ้นงานและเครื่องมือในงานกลึง งานกัด และงานเชื่อม ซึ่งเป็นที่นิยมมากในภาคอุตสาหกรรมเนื่องจากไม่ต้องทำการใช้สาร CFC ในการช่วยทำความเย็นโดยไม่เป็นมลพิษต่อสิ่งแวดล้อมและสามารถที่จะนำไปใช้งานในที่ต่างๆได้สะดวก

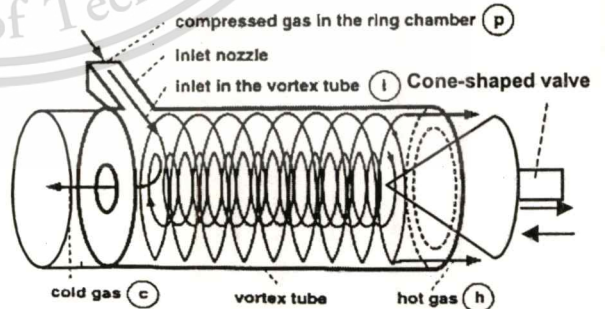
ริฟิสซึ่งอยู่ฝั่งตรงข้ามกับวาล์วควบคุมการไหล (Cone-shaped valve) ในขณะที่อากาศร้อนที่ผนังท่อจะไหลผ่านออกมาด้านวาล์วควบคุมการไหล (Cone-shaped valve) ดังที่แสดงในรูปที่ 1a ซึ่งปริมาณการไหลของอากาศร้อนและอากาศเย็นสามารถควบคุมได้โดยใช้วาล์วควบคุมดังกล่าว โดยทั่วไปทอว์ร์เทกซ์สามารถแบ่งออกได้เป็นสองแบบ แบบแรกเป็นการไหลแบบสวนทางกัน (Counter flow type) ซึ่งส่วนมากจะใช้เป็นรูปแบบอ้างอิงมาตรฐานและแบบที่สองเป็นการไหลแบบตามกันในทิศทางเดียว (Uniflow type) หรือการไหลแบบขนานกัน (Parallel flow type) ดังรูปที่ 1a และ 1b ตามลำดับ โดยทั่วไปชุดอุปกรณ์ทอว์ร์เทกซ์ได้ถูกนำไปใช้ในโรงงานและภาคอุตสาหกรรม โดยได้ทำการใช้ความเย็นที่ผลิตได้จากทอว์ร์เทกซ์มาใช้ในงานการหล่อเย็นชิ้นงานและเครื่องมือในงานกลึง งานกัด และงานเชื่อม ซึ่งเป็นที่นิยมมากในภาคอุตสาหกรรมเนื่องจากไม่ต้องทำการใช้สาร CFC ในการช่วยทำความเย็นโดยไม่เป็นมลพิษต่อสิ่งแวดล้อมและสามารถที่จะนำไปใช้งานในที่ต่างๆได้สะดวก



รูปที่ 1 พื้นฐานการทำงานของทอว์ร์เทกซ์ (1a) การไหลแบบสวนทางกัน (Counter flow type) และ (1b) การไหลแบบตามกัน (Uniflow type) หรือการไหลแบบขนานกัน (Parallel flow type)

ปรากฏการณ์การที่เกิดขึ้นภายในทอว์ออร์ทอกซ์ถูกค้นพบครั้งแรกในปี 1933 โดย George Ranque [1] ซึ่งเป็นผู้เชี่ยวชาญทางฟิสิกส์ โดยได้ทำการศึกษาปรากฏการณ์การแยกของพลังงาน (Energy Separation) ภายในทอว์ออร์ทอกซ์เป็นครั้งแรก โดยการปล่อยให้อากาศอัดตัวไหลผ่านเข้าไปในแนวสัมผัสกับทอว์ออร์ทอกซ์ ซึ่งพบว่าอากาศที่บริเวณผนังทอว์ออร์ทอกซ์มีความเร็วสูงกว่าอากาศบริเวณกลางทอว์ออร์ทอกซ์และนำผลที่ได้มาทำอุปกรณ์ทำความเย็น ในปี 1946 Rudolph Hillsch [2] เป็นวิศวกรชาวเยอรมันได้ทำการศึกษาทดลองโดยการเปลี่ยนความดันที่ทางเข้าและขนาดของทอว์ออร์ทอกซ์และทำการเปรียบเทียบกับทอว์ออร์ทอกซ์กับเครื่องทำความเย็นทั่วไป พบว่าทอว์ออร์ทอกซ์มีสมรรถนะทำความเย็นที่ต่ำกว่า โดยเฉพาะที่ความดันทางเข้าที่ต่ำกว่า ในปี 1950 Fulton [3] ได้พยายามศึกษาการแยกพลังงาน (Energy Separation) ภายในทอว์ออร์ทอกซ์ โดยสมมุติว่าผลจากการแลกเปลี่ยนพลังงานระหว่างอากาศใกล้แนวแกนกลางทอว์ออร์ทอกซ์จะมีความเร็วเชิงมุมที่สูงมาก (Higher angular velocity) และอากาศที่ใกล้บริเวณทอว์ออร์ทอกซ์จะมีความเร็วเชิงมุมที่ต่ำ (Lower angular velocity) เป็นผลให้ที่บริเวณแนวแกนทอว์ออร์ทอกซ์เพิ่มความเร่งของอากาศบริเวณขอบทอว์ออร์ทอกซ์ เมื่อเปรียบเทียบกับปัญหาการคำนวณทางคณิตศาสตร์ Fulton แนะนำเค้าโครงสำหรับรูปแบบการไหลภายในทอว์ออร์ทอกซ์ที่ประกอบด้วยท่อไหลในแนวรัศมี (Radial Flow) และการไหลในแนวแกนทอว์ออร์ทอกซ์ (Axial Flow) โดยได้มีทฤษฎีที่ต่างออกไป ซึ่งถูกพัฒนาโดยในปี 1951 Schultz-Grunow [4] ได้อธิบายการแยกพลังงาน (Energy Separation) โดยใช้ความรู้เกี่ยวกับการถ่ายเทความร้อนแบบปั่นป่วน (Turbulent heat transfer) ในการไหลที่แบ่งเป็นชั้นๆ ในปี 1957 Martynovskii และ Alekseev [5] ได้ทำการศึกษาการทดลองเกี่ยวกับความแตกต่างของโครงสร้างทอว์ออร์ทอกซ์ที่มีผลต่อความแตกต่างของอุณหภูมิระหว่างอากาศร้อนและอากาศเย็นมากที่สุดเท่าที่เป็นไปได้และทำการเปลี่ยนรูปแบบของหัวฉีด (Nozzle) เพื่อให้ได้รูปที่ดีที่สุด ในปี 1971 Williams [6] ได้ทำการเลือกใช้สารในการทดลองคือ แอมโมเนียมีเทนและคาร์บอนไดออกไซด์ พบว่าสัดส่วนการลดลงของอุณหภูมิจะขึ้นอยู่กับสัดส่วนของความดันที่ทางเข้า ในปี 1956-1957 Hartnett และ Eckert [7] ได้ทำการวัดอุณหภูมิและความดันที่จุดต่างๆ ภายในทอว์ออร์ทอกซ์ พบว่าความยาวของทอว์ออร์ทอกซ์มีผลอย่างมากต่อการแยกพลังงาน (Energy Separation) ภายในทอว์ออร์ทอกซ์และได้ทำการอธิบายไว้ถึงผลต่างของอากาศเย็นและอากาศร้อนและอัตราส่วนของความดันที่ทางเข้าและทางออกของทอว์ออร์ทอกซ์โดยจะขึ้นอยู่กับก๊าซที่ใช้ ในปี 1964 Linderstrom-Lang [8] ได้ทำการศึกษาถึงรายละเอียดในการประยุกต์ในการแยกของอากาศที่เป็นแบบอากาศผสม (Mixture Gas) กับขนาดของทอว์ออร์ทอกซ์ โดยแสดงให้เห็นว่าผลของการแยกอากาศขึ้นอยู่กับอัตราส่วนการไหลของมวลของอากาศร้อนและมวลของอากาศเย็นและผลที่เกิดขึ้นได้รับการยืนยัน ในปี 1977 Marshall [9] ได้ทำการเปลี่ยนของผสมและขนาดของทอว์ออร์ทอกซ์ต่างๆ ซึ่งแสดงให้เห็นว่าจุดวิกฤติของ Reynolds number มีผลต่อการแยกพลังงาน ในปี 1965 Takayama [10] ได้ทำการศึกษาถึงข้อมูลเกี่ยวกับประสิทธิภาพที่สูงขึ้นกับการแยกพลังงานจากการออกแบบทอว์ออร์ทอกซ์ที่เป็นมาตรฐานและสูตรสำหรับรูปแบบความเร็วและอุณหภูมิของอากาศที่ไหลในทอว์ออร์ทอกซ์และต่อมาในปี 1979 Takayama ได้เสนออิทธิพลของความชื้น

ของอากาศที่มีผลต่อการแยกพลังงาน (Energy Separation) โดยทำทดลองกับทอว์ออร์ทอกซ์ที่มีความชื้นของอากาศที่แตกต่างกันและพบว่าความชื้นมีผลต่อการแยกพลังงานในทอว์ออร์ทอกซ์ ในปี 1960 Deissler และ Perltmutter [11] ได้ทำการศึกษาการกระจายความเร็วอุณหภูมิและความดันในทอว์ออร์ทอกซ์แบบปั่นป่วน (Turbulent) กับการไหลในแนวรัศมีและแนวแกนในรูปแบบทางคณิตศาสตร์และได้ทำการแยกทอว์ออร์ทอกซ์เป็นพื้นที่ในแนวแกน (Core Region) และพื้นที่วงแหวน (Annular Region) และสรุปได้ว่าการไหลในพื้นที่ในแนวแกน (Core Region) จะทำให้เกิดงานเนื่องจากแรงเฉื่อยที่ของไหลบริเวณรอบนอก (Outer Region) กับผลของการแยกพลังงาน (Energy Separation) ในปี 1962 Erdelyi [12] มีข้อโต้แย้งเกี่ยวกับการสรุปของ Hillsch, Hartnett และ Eckert โดยอ้างว่าผลต่างของอุณหภูมิของอากาศร้อนและอากาศเย็นขึ้นอยู่กับชนิดของก๊าซที่ใช้และอัตราส่วนความดัน (Pressure ratio) ที่ทางเข้าและทางออกของทอว์ออร์ทอกซ์เท่านั้น ต่อมาในปี 1984 Stepphan [13] และคณะได้ทำการศึกษาการแยกของพลังงาน (Energy Separation) ในทอว์ออร์ทอกซ์ โดยอาศัยตัวแปรไร้มิติช่วยในการศึกษาผลจากการทดลอง ในปี 1985 นักสิทธิ์ คูวัฒนาชัย [14] ได้ทำการทดลองโดยการเปลี่ยนขนาดทอว์ออร์ทอกซ์แบบต่างๆ ที่มีผลต่อการกระจายอุณหภูมิที่ทอว์ออร์ทอกซ์ ในปี 1986 นราธิป นรเศรษฐพันธ์ และ พัฒนาเนตรสุวรรณ [15] ได้ทำการทดลองโดยการเปลี่ยนขนาดทอว์ออร์ทอกซ์แบบต่างๆ ที่มีผลต่อการกระจายอุณหภูมิที่ทอว์ออร์ทอกซ์ ในปี 1995 Cockerill [16] ทำการศึกษาถึงผลการเพิ่มจำนวนรูปหัวฉีดที่มีผลต่อการแยกพลังงานในทอว์ออร์ทอกซ์ ในปี 1999 พงษ์เจต พรหมวงศ์ [17] ทำการประยุกต์โดยใช้แบบจำลองทางคณิตศาสตร์ในการเขียนโปรแกรมทางคอมพิวเตอร์เพื่อช่วยในการทำนายปรากฏการณ์การไหลในทอว์ออร์ทอกซ์ของ Hartnett และ Eckert และต่อมาในปีเดียวกัน Frohlingsdorf และ Unger [18] ได้ทำการศึกษาการแยกของพลังงานภายในทอว์ออร์ทอกซ์ โดยได้ทำการใช้โปรแกรม CFX ช่วยในการศึกษาพฤติกรรมและทำการเพิ่มเติมของ Shear-stress-induced mechanical work ลงไป ซึ่งพบว่าผลที่ได้มีความใกล้เคียงกับการทดลองของ Bruun ในปี 1969



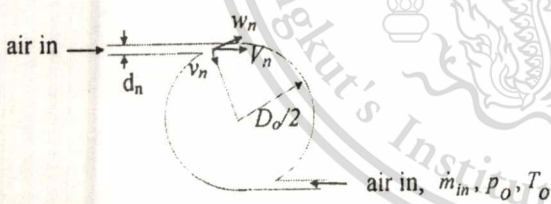
รูปที่ 2 ทอว์ออร์ทอกซ์แบบไหลสวนทางกัน (Counter flow type) โดยมี Cone-shaped valve ที่ปลายด้านนอกของอากาศร้อนและห้องหัวฉีด (Nozzle chamber)

ในรายงานฉบับนี้ทำการศึกษาถึงผลของการเปลี่ยนแผ่นอริฟิสขนาดต่างๆในการแยกอากาศเย็นและอากาศร้อนต่อสมรรถนะการทำ

ความเย็นที่ทอเวอร์เทกซ์ โดยทำการออกแบบทอเวอร์เทกซ์แบบ Counter flow และปรับค่าอัตราการไหลของอากาศที่ออกจากทอเวอร์เทกซ์โดยใช้ Cone-shaped Valve และมีจำนวน 2 หัวฉีดในการไหลเข้าทอเวอร์เทกซ์ตามรูปที่ 2 โดยข้อมูลทอเวอร์เทกซ์ถูกแสดงตามตารางที่ 1

## 2. ทฤษฎี

เมื่ออากาศถูกปล่อยอัดตัวผ่านเข้าไปในทอเวอร์เทกซ์ (Vortex chamber) ทำให้ความดันอากาศลดลงอย่างฉับพลันจนเข้าใกล้ความดันบรรยากาศและความเร็วของอากาศเข้าใกล้ความเร็วเสียง ทำให้มีแรงหนีศูนย์กลางบังคับให้การหมุนไปตามเส้นรอบวงของขอบท่อและบริเวณกลางท่อจะเป็นที่ว่างของอากาศและมีความถี่เชิงมุมที่สูงมาก ทำให้เกิดความเร็วจนเกิดการหมุนในแนวรัศมีของอนุภาคต่างๆจะมีค่าคงที่ ความเร็วในแนวสัมผัสมีค่าต่ำที่ชั้นในและมีความเร็วในแนวสัมผัสสูงที่ชั้นนอกใกล้บริเวณผนังท่อ ซึ่งเป็นการไหลแบบ irrotational เมื่อมีผลของการไหลที่มีความหนืดเข้ามาเกี่ยวข้องจะเกิดการแยกตัวของความเร็วของอนุภาคผ่านข้ามไปแนวรัศมีของท่อตามการขยายตัวของทอเวอร์เทกซ์ไปในท่อ ทำให้ชั้นความเร็วสูงไปเร่งชั้นความเร็วต่ำทำให้มีความเร็วเพิ่มขึ้น ซึ่งเป็นการไหลแบบ rotational จะเกิดการถ่ายเทพลังงานจลน์ออกจากแนวแกนท่อ และเมื่อมีการถ่ายเทพลังงาน (Energy transfer) จะทำให้เกิดความร้อนของชั้นนอกและความเย็นของชั้นใน ทำให้พลังงานหายไปในรูปแบบของความร้อน โดยการปรับอัตราการไหลที่วาล์วควบคุม (Cone-shaped valve) และพลังงานที่หายไปจากท่อเนื่องจากการหมุนชั้นในที่ได้รับความร้อน โดยอากาศเย็นจะไหลออกตรงข้ามด้าน Cone-shaped valve ตามรูปที่ 2



รูปที่ 4 อากาศที่ไหลผ่านเข้าหัวฉีดสู่ทอเวอร์เทกซ์

สัดส่วนมวลของอากาศเย็นเป็นค่าของอัตราการไหลของอากาศเย็นต่อค่าอัตราการไหลของอากาศที่ทางเข้า

$$x_c = \frac{\dot{m}_c}{\dot{m}_i} \quad (1)$$

เมื่อ  $\dot{m}_c$  และ  $\dot{m}_i$  เป็นอัตราการไหลโดยมวลของอากาศเย็น(kg/s) และอัตราการไหลโดยมวลของอากาศที่เข้าทอเวอร์เทกซ์(kg/s) และ  $x_c$  เป็นสัดส่วนมวลของอากาศเย็น

$$\Delta T_c = T_i - T_c \quad (2)$$

เมื่อ  $\Delta T_c$ ,  $T_i$  และ  $T_c$  เป็นผลความแตกต่างของการลดอุณหภูมิที่ด้านเย็นและอุณหภูมิทางเข้า(K), อุณหภูมิที่ทางเข้า(K) และอุณหภูมิที่ทางออกด้านเย็น (K)

$$Q_c = \dot{m}_c C_p (\Delta T_c) \quad (3)$$

เมื่อ  $Q_c$  และ  $C_p$  เป็นอัตราการทำความเย็นที่ทอเวอร์เทกซ์(J/kg) และค่าความจุความร้อนจำเพาะของพลังงาน(J/kg K)

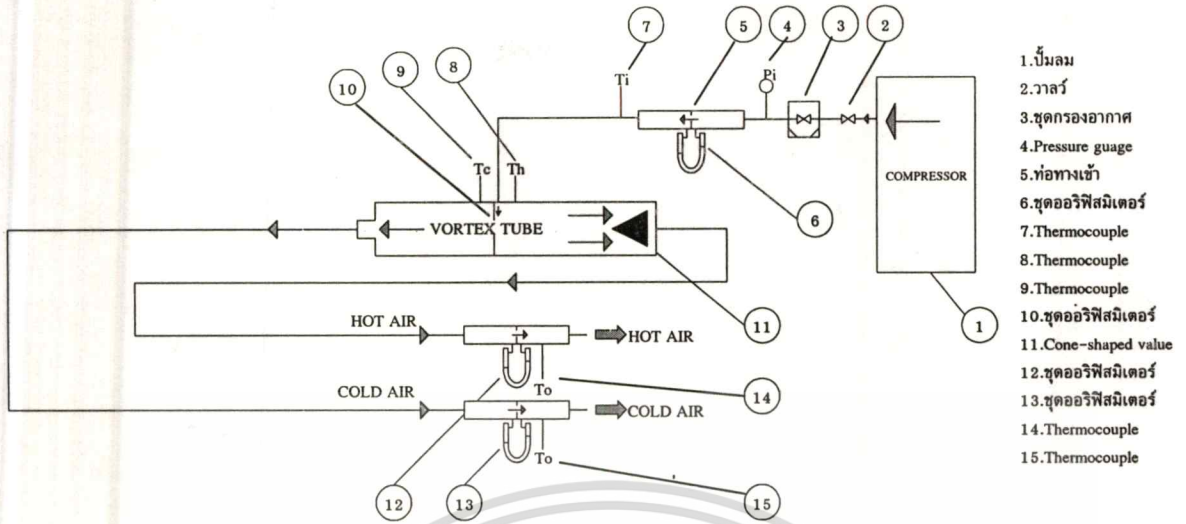
ตารางที่ 1 ข้อมูลสำหรับทอเวอร์เทกซ์

ลักษณะของท่อ	
ความยาวของท่อด้านร้อน, L (mm)	770
ขนาดเส้นผ่านศูนย์กลางท่อ, D (mm)	25.4, 31.5, 38.5
จำนวนหัวฉีดที่ทางเข้า	2
ขนาดเส้นผ่านศูนย์กลางหัวฉีดที่ทางเข้า, d (mm)	5, 6.5
ลักษณะการเปิดวาล์ว	
วาล์วควบคุม	Cone-shaped Valve
ขนาดของแผ่นออริฟิส (d/D)	0.1, 0.12, 0.16, 0.25, 0.5
คุณสมบัติของไหลที่ทางเข้า	
ของไหล	อากาศ
อุณหภูมิ, $T_i$ (K)	302
ความดันที่ทางเข้าก่อนหัวฉีด, $P_o$ (Bar)	2.0-6.0

ในชุดทดลองได้ทำการใช้ขนาดเส้นผ่านศูนย์กลางทอเวอร์เทกซ์ด้วยกัน 3 ขนาด แผ่นออริฟิส 4 ขนาด และจำนวนหัวฉีดที่ทางเข้า 2 หัว ตามตารางที่ 1 โดยโครงสร้างของชุดทอเวอร์เทกซ์เป็นรูปแบบที่กำหนดจาก Hilsch [2]

## 3. วิธีการทดลอง

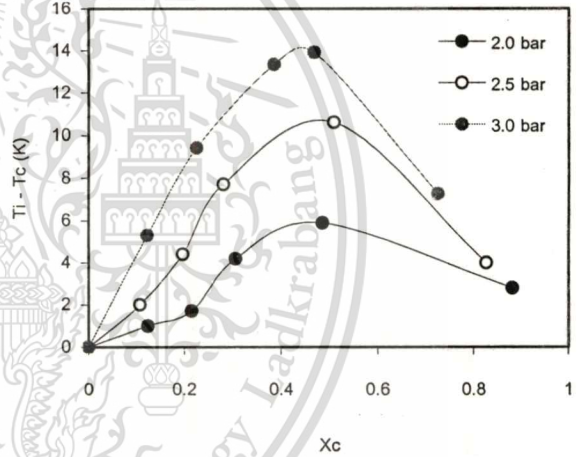
อุปกรณ์การทดลองสมรรถนะของทอเวอร์เทกซ์ตามรูปที่ 5 อากาศจะถูกอัดจากปั๊มลม(1)และไหลผ่านเข้าวาล์ว(2) ชุดวัดความดัน(3)และชุดกรองอากาศ(Air Filter)(4) เข้ามาที่ชุดออริฟิส(5) เพื่อทำการวัดค่าอัตราการไหลโดยมวลที่ทางเข้าก่อนเข้าสู่ทอเวอร์เทกซ์ อากาศจะถูกไหลอัดผ่านเข้าไปในแนวมุมสัมผัสกับผิวทอเวอร์เทกซ์(10) และทำให้เกิดการหมุนแบบวอร์เทกซ์เกิดขึ้นภายในท่อ โดยอากาศจะถูกขยายตัวในทอเวอร์เทกซ์และเกิดการแยกอากาศออกเป็นสองส่วนคืออากาศร้อนและอากาศเย็น อากาศเย็นจะไหลผ่านออกมาจากแผ่นออริฟิสที่ติดตั้งอยู่ใกล้ๆทางเข้าหัวฉีด (Nozzle) ในขณะที่อากาศร้อนจะไหลไปสู่ปลายอีกท่ออีกด้านหนึ่งที่มี Cone-shaped valve ติดตั้งอยู่ อัตราการไหลของอากาศร้อนและอากาศเย็นที่ออกจากทอเวอร์เทกซ์ จะถูกทำการปรับค่าโดยใช้ Cone-shaped valve ซึ่งค่าอัตราการไหลโดยมวลของอากาศร้อนและอากาศเย็นถูกทำการวัดโดยใช้ความดันตกคร่อมที่แผ่นออริฟิส(13)และ(15) และทำการวัดอุณหภูมิของอากาศทางเข้า อากาศทางเข้าและอากาศเย็นโดยใช้ Thermocouple (7) (8)และ(9)



รูปที่ 4 การทำงานของชุด Ranque-Hilsch Vortex tube

4. ผลการทดลองและวิจารณ์

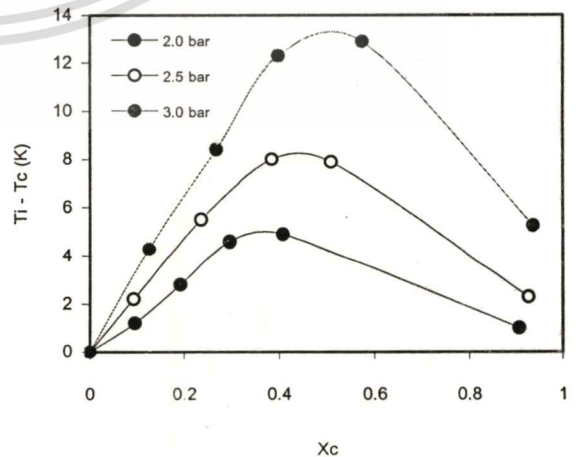
ในการทดลองได้ทำการใช้ชุดออร์บิสมิเตอร์วัดความดันและคำนวณหาค่าอัตราการไหลโดยมวลของทอว์ออร์ทกซ์ทั้งอากาศร้อนและอากาศเย็น ในการวัดอุณหภูมิของอากาศภายในทอว์ออร์ทกซ์จะทำการวัดโดยใช้ Thermocouple ทั้งอุณหภูมิที่ทางเข้า อุณหภูมิของอากาศร้อนและอากาศเย็นหลังจากอากาศที่ไหลผ่านออกจากแผ่นออร์บิสมิเตอร์ ในการทดลองได้ทำการทดสอบกับทอว์ออร์ทกซ์ขนาดเส้นผ่านศูนย์กลาง 25.4 31.5 และ 38.5 mm ที่ช่วงค่าความดัน 2.0-4.5 bar และที่ขนาดอัตราส่วนของแผ่นออร์บิสมิเตอร์เท่ากับ 0.1-0.5 เมื่ออากาศที่ไหลผ่านหัวฉีดเข้าสู่ทอว์ออร์ทกซ์ในแนวมุมสัมผัสกับท่อจะทำให้เกิดการหมุนวนภายในท่อ ซึ่งเกิดผลต่างของอุณหภูมิทั้งด้านอากาศร้อนและอากาศเย็นภายในทอว์ออร์ทกซ์และผลต่อสมรรถนะในการทำความเย็นที่ความดันช่วงต่างๆ ซึ่งแสดงความสัมพันธ์ดังรูปที่ 5-10



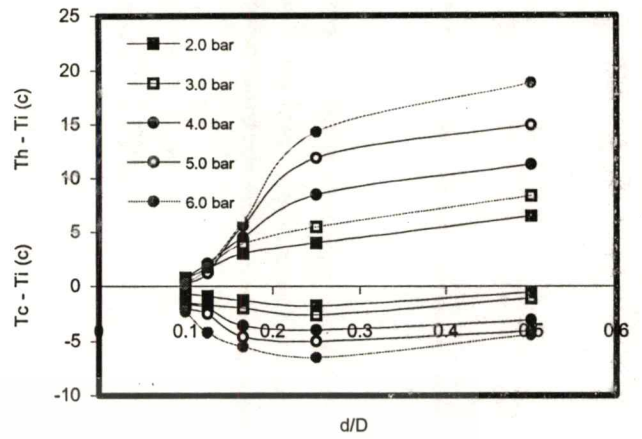
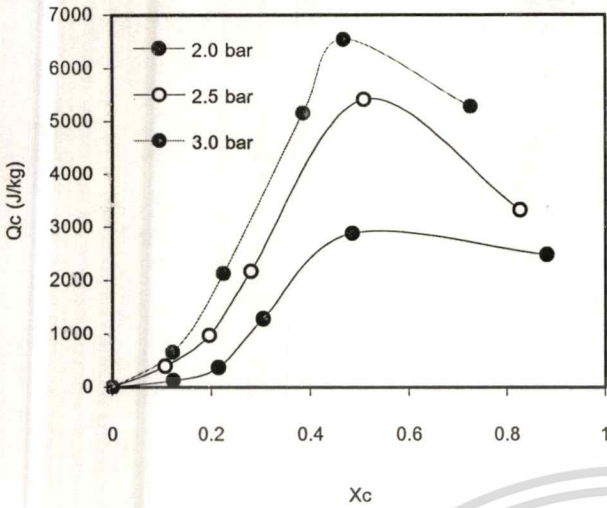
รูปที่ 5 การลดลงของอุณหภูมิด้านเย็น ( $T_i - T_c$ ) กับค่าสัดส่วนมวลของอากาศเย็น ( $x_c$ ) ที่ท่อขนาดเส้นผ่านศูนย์กลาง 25.4 mm

4.1 ผลกระทบของค่าสัดส่วนมวลของอากาศเย็นต่อค่าการลดลงของอุณหภูมิด้านเย็นในทอว์ออร์ทกซ์

ความสัมพันธ์ในรูปที่ 5 และ 6 พบว่าผลการลดลงของอุณหภูมิด้านเย็น ( $T_i - T_c$ ) กับค่าสัดส่วนมวลของอากาศเย็น ( $x_c$ ) ที่ค่าความดันที่เข้าทอว์ออร์ทกซ์ช่วงต่างๆ และทุกขนาดท่ออุณหภูมิจะลดลงสูงสุดที่สัดส่วนมวลของอากาศเย็นในช่วง 0.4-0.5 ซึ่งการลดลงของอุณหภูมิจะเพิ่มสูงขึ้นในช่วงค่าสัดส่วนมวลของอากาศเย็น ( $x_c$ ) เท่ากับ 0.1-0.5 และเริ่มที่จะลดลงภายหลังค่าสัดส่วนมวลของอากาศเย็น ( $x_c$ ) เท่ากับ 0.6 เมื่อความดันที่ทางเข้าสูงขึ้น ผลการลดลงของอุณหภูมิที่ด้านเย็นจะมีค่าสูงขึ้นตาม เนื่องจากค่าอัตราการไหลโดยมวลที่ไหลเข้าหัวฉีดมีความเร็วที่สูงขึ้น ทำให้การหมุนวนภายในทอว์ออร์ทกซ์แรงขึ้นและมีผลให้ที่ผิวท่อมีแรงเสียดทานที่สูงขึ้นความร้อนจึงสูงขึ้นตามในขณะที่กลางแกนท่อมีการลดลงของอุณหภูมิที่สูงขึ้น ผลความสัมพันธ์ในรูปที่ 5 และ 6 ที่ความดัน 3.0 bar จะมีค่าการลดลงของอุณหภูมิที่ด้านเย็นสูงสุดเท่ากับ 14 K ในขณะที่ความดัน 2.0 bar จะมีค่าการลดลงของอุณหภูมิสูงสุดเท่ากับ 6 K

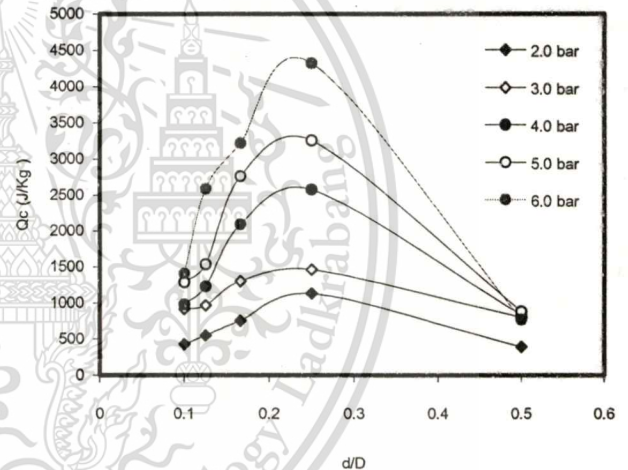
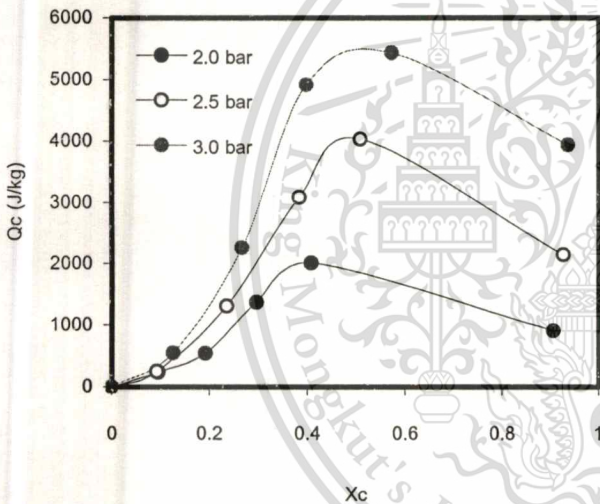


รูปที่ 6 การลดลงของอุณหภูมิด้านเย็น ( $T_i - T_c$ ) กับค่าสัดส่วนมวลของอากาศเย็น ( $x_c$ ) ที่ท่อขนาดเส้นผ่านศูนย์กลาง 31.5 mm



รูปที่ 7 สมรรถนะในการทำความเย็น ( $Q_c$ ) กับค่าสัดส่วนมวลของอากาศเย็น ( $x_c$ ) ที่ท่อขนาดเส้นผ่านศูนย์กลาง 25.4 mm

รูปที่ 9 การลดลงของอุณหภูมิด้านเย็น ( $T_c - T_i$ ) และการเพิ่มขึ้นของอุณหภูมิด้านร้อน ( $T_h - T_i$ ) กับขนาดแผ่นออร์ฟิสที่ท่อ 38.5 mm



รูปที่ 8 สมรรถนะในการทำความเย็น ( $Q_c$ ) กับค่าสัดส่วนมวลของอากาศเย็น ( $x_c$ ) ที่ท่อขนาดเส้นผ่านศูนย์กลาง 31.5 mm

รูปที่ 10 สมรรถนะในการทำความเย็น ( $Q_c$ ) กับขนาดแผ่นออร์ฟิสที่ท่อขนาดเส้นผ่านศูนย์กลาง 38.5 mm

**4.2 ผลกระทบของค่าสัดส่วนมวลของอากาศเย็นต่อค่าสมรรถนะในการทำความเย็นของท่อวอร์เทกซ์**

ความสัมพันธ์ของสมรรถนะในการทำความเย็น ( $Q_c$ ) ของท่อวอร์เทกซ์กับค่าสัดส่วนมวลของอากาศเย็น ( $x_c$ ) พบว่าความดันของวอร์เทกซ์ทุกช่วงและขนาดของท่อวอร์เทกซ์ 25.4, 31.5 mm สามารถทำความเย็นได้สูงสุดที่ค่าสัดส่วนมวลของอากาศเย็น ( $x_c$ ) เท่ากับ 0.4-0.5 โดยในการเพิ่มขึ้นของสมรรถนะในการทำความเย็น ( $Q_c$ ) จะสูงขึ้นในช่วงค่าสัดส่วนมวลของอากาศเย็น ( $x_c$ ) เท่ากับ 0.1-0.5 และเริ่มที่จะลดลงภายหลังค่าสัดส่วนมวลของอากาศเย็น ( $x_c$ ) เท่ากับ 0.6 จากความสัมพันธ์ในรูปที่ 7 และ 8 สมรรถนะในการทำความเย็นของท่อวอร์เทกซ์จะลดลงตามขนาดของท่อวอร์เทกซ์ที่มีขนาดเพิ่มขึ้น โดยที่ความดัน 3.0 bar ขนาดเส้นผ่านศูนย์กลางท่อวอร์เทกซ์ 25.4 mm จะมีค่าสมรรถนะในการทำความเย็น ( $Q_c$ ) เท่ากับ 6,500 J/kg ในขณะที่ท่อ

วอร์เทกซ์ขนาด 31.5 mm จะมีค่าสมรรถนะในการทำความเย็น ( $Q_c$ ) เท่ากับ 5,400 J/kg เนื่องจากการเพิ่มของขนาดท่อที่ใหญ่ขึ้น ทำให้การหมุนวนภายในท่อวอร์เทกซ์ลดลง จึงทำให้ที่ผิวท่อมีแรงเสียดทานที่ต่ำลง ในขณะที่กกลางแกนท่อมีการลดลงของอุณหภูมิที่ต่ำลงเช่นกัน จึงทำให้ค่าสมรรถนะในการทำความเย็น ( $Q_c$ ) ของท่อวอร์เทกซ์ลดลงตาม

**4.3 ผลกระทบของค่าอัตราส่วนของแผ่นออร์ฟิสต่อค่าการลดลงของอุณหภูมิด้านเย็น ด้านร้อนและสมรรถนะในการทำความเย็นของท่อวอร์เทกซ์**

การลดลงของอุณหภูมิกับขนาดอัตราส่วนของแผ่นออร์ฟิส ในความสัมพันธ์ตามรูปที่ 9 และ 10 พบว่าเมื่อความดันที่ทางเข้าท่อวอร์เทกซ์มีค่าสูงขึ้น จะมีผลทำให้ค่าความผลต่างของอุณหภูมิด้านเย็นและอุณหภูมิด้านร้อนสูงขึ้นตาม ในขณะที่ค่าการผลต่างของอุณหภูมิด้าน

เย็นและอุณหภูมิด้านร้อนสูงขึ้นตาม ในขณะที่ค่าการผลต่างของอุณหภูมิด้านเย็น อุณหภูมิด้านร้อนและค่าสมรรถนะการทำความเย็นของทอว์เรทเทกซ์มีค่าเพิ่มขึ้นในช่วงที่ขนาดอัตราส่วนของแผ่นออริฟิสเท่ากับ 0.1 - 0.25 และมีค่าลดลงมาตามลำดับ พบว่าที่ค่าผลต่างของอุณหภูมิด้านเย็น อุณหภูมิด้านร้อนและค่าสมรรถนะการทำความเย็นของทอว์เรทเทกซ์มีค่าสูงสุดจะอยู่ในช่วงขนาดอัตราส่วนของแผ่นออริฟิสที่ 0.25 จะมีค่าผลต่างของอุณหภูมิด้านเย็น อุณหภูมิด้านร้อนเพิ่มขึ้นเท่ากับ 15 K และค่าสมรรถนะการทำความเย็นของทอว์เรทเทกซ์เท่ากับ 4,500 J/kg ที่ค่าความดัน 6.0 bar ที่ขนาดทอว์เรทเทกซ์เส้นผ่านศูนย์กลาง 38.5 mm เนื่องจากอากาศเย็นที่ไหลผ่านขนาดแผ่นออริฟิสที่ 0.5 จะมีอากาศเย็นไหลเข้าความสะอาดที่สุด ในขณะที่ขนาดอัตราส่วนของแผ่นออริฟิสต่างๆมีอากาศร้อนบางส่วนไหลออกทางด้านเย็น ทำให้อากาศร้อนเข้าไปผสมกับอากาศเย็นจึงทำให้มีผลต่างของอุณหภูมิลดลงและค่าสมรรถนะการทำความเย็นของทอว์เรทเทกซ์ลดลงตาม

## 5. สรุปการทดลอง

ผลการทดลองสมรรถนะการทำความเย็นของทอว์เรทเทกซ์ พบว่าการทำความเย็นสูงสุดในทอว์เรทเทกซ์มีค่าเท่ากับ 6,500 J/kg ผลต่างของอุณหภูมิด้านเย็นมีค่าเท่ากับ 14 K และผลต่างของอุณหภูมิด้านร้อนมีค่าเท่ากับ 20 K ซึ่งขึ้นอยู่กับขนาดเส้นผ่านศูนย์กลางของทอว์เรทเทกซ์ที่มีขนาดที่ลดลง ความดันที่ทางเข้าที่มีค่าสูงขึ้นและขนาดอัตราส่วนของแผ่นออริฟิสที่เหมาะสม ในการทดลองพบว่าขนาดแผ่นออริฟิสที่เหมาะสมจะอยู่ในช่วง  $d/D$  0.16-0.25 เนื่องจากเป็นช่วงที่ได้ค่าการทำความเย็นและผลต่างของการลดลงของอุณหภูมิในทอว์เรทเทกซ์ขนาด 38.5 mm มากที่สุด และผลต่างความเย็นที่ได้รับสามารถที่จะนำไปใช้ในงานในอุตสาหกรรมได้หลายประเภท เช่น งานหล่อเย็นวัสดุในงานกลึง งานตัดวัสดุ ซึ่งสามารถใช้น้ำยาหล่อเย็นได้โดยไม่ต้องมีผลต่อสิ่งแวดล้อมและนำไปใช้ในสถานที่ต่างๆได้สะดวก ซึ่งจากงานที่ทดลองมาจำเป็นที่จะต้องทำการเปลี่ยนค่า ขนาดทอว์เรทเทกซ์ ความดันทางเข้า และขนาดแผ่นออริฟิสเพื่อสามารถที่นำไปใช้ในงานที่เหมาะสมต่อไป

## 6. กิตติกรรมประกาศ

งานวิจัยฉบับนี้ทำไปได้ด้วยดีต้องขอขอบคุณ นาย เทพฤทธิ์ ชื่นโชคสันต์ นาย วรวิฑูร์ โควานิชเจริญ นาย วรวิฑูร์ ภูทองคำ นาย ชาลีเทพพิมล นาย สุริโย รักษาการ และ นาย กฤษกร ธนจตุพิท ที่ช่วยในการเก็บข้อมูลของงานในบทความฉบับนี้

## หนังสืออ้างอิง

- [1] George's Ranque, (1933), Experiences sur la détente giratoire productions simultanees d'un echappement d'air chaud et d'un echappement d'air froid, Journal of physic Radium, Paris 4, pp.112-114.
- [2] Rudolph Hilsch, (1947), The Use of the Expansion of Gases in a Centrifugal Field as Cooling Process, The review of scientific instruments, pp.108-113.

- [3] Fulton, C.D., (1950), Ranque's tube, ASRE Refrigeration Engineering 5, pp.473-479.
- [4] Schultz-Grunow, F. (1951), Turbulenter Warmedurchgang im Zentrifugalfeld, Forsch. Ing.Wes.Vol.17, No 3, pp.66-76.
- [5] Martynovskii and Alekseev, (1957), Investigation of the vortex thermal separation effect of gases and vapour, Soviet Phys.tech.Phys 1, pp.233.
- [6] Williams, A. (1971), The cooling of methane with vortex tubes, Journal of Mechanical Engineering Science Volume 13 No.6, pp.365-375.
- [7] Hartnett J.P., and Eckert, E.R.G. (1957), Experimental Study of the Velocity and Temperature Distribution in a High-Velocity Vortex-Type Flow, Tran. ASME 79, pp.751-758.
- [8] Linderstrom-Lang. C.U. (1964), Gas separation in the Ranque-Hilsch vortex tube, Int. Journal of Heat Mass Transfer 7, pp.1200-1206.
- [9] Marshall, J. (1977), Effect of operation condition, 'Physical size and flow characteristic an the gas separation performance of a Linderstrom-Lang vortex tube, International Journal Heat and Mass Transfer, 20, pp.227-231.
- [10] Takayama, H. (1965), Studies on vortex tube, Buil. JSME, pp.443- 440.
- [11] Deissier, R.G. and Pertmutter, M. (1960), Analysis of the flow and energy separation in a vortex tube, International Journal of Heat Mass Transfer 1, pp.173-191.
- [12] Erdelyi, J. (1962), Wirkung des Zentrifugalfeldes auf Warmezustand der Gase Erklarung der Ranque Erschemung, Forsch, Inq Wes.28, pp.181-186.
- [13] Stephan, K., lin, S., Durst, M., Hanng, P., and Scher, D. (1984), A similarity relation for energy separation and vortex tube, International Journal of Heat Mass Transfer 27(6), pp. 911-920.
- [14] นักสิทธิ์ คุ้มพัฒนาชัย (1985), ทอว์เรทเทกซ์, วิศวกรรมสารแห่งประเทศไทย, มิถุนายน
- [15] นราธิป นรเศรษฐพันธ์ และ พัฒนา เนตรสุวรรณ (1986), การทำความเย็นโดยลมหมุน, วิทยานิพนธ์, สถาบันเทคโนโลยีพระจอมเกล้าธนบุรี
- [16] Cockerill, T. (1995), Ranque-Hilsch Vortex Tubes, Ph.D. Thesis, University of Sunderland
- [17] Promvong, P. (1999), Numerical Simulation of Turbulent Compressible Vortex-Tubes Flow, ASME/JSME Fluid Engineering
- [18] Frohlingsdorf, W. and Unger, H. (1999), Numerical investigations of the compressible flow and the energy separation in the Ranque-Hilsch vortex tube, International Journal of Heat and Mass Transfer 42, pp.415-422.

## AUTHOR BIOGRAPHY

<b>Name</b>	Mr. Smith Eiamsa-ard
<b>Date of Birth</b>	15 September 2516
<b>Degree</b>	Bachelor degree of Mechanical Engineering (2535-2538) Mahanakorn University of Technology
<b>Office</b>	Mahanakorn University of Technology



### Researches Previous

- 1."The Curve through Extrema of an Underdamped Free Vibration", The 11<sup>th</sup> Conference of Mechanical Engineering Network of Thailand, 23-24 November 2540
- 2."A Belt-Type Oil Film Remover for Confined Water Reservoir", The 12<sup>th</sup> Conference of Mechanical Engineering Network of Thailand, 11-13 November 2541
- 3."An Experimental Performance Study of a Ranque-Hilsch Vortex Tube" The 13<sup>th</sup> Conference of Mechanical Engineering Network of Thailand, 2-3 December 2542
- 4."An Experimental Performance Study of Particle Classification in Hydro-cyclone", The 13<sup>th</sup> Conference of Mechanical Engineering Network of Thailand, 2-3 December 2542
- 5."Effects of Heat Transfer on Aluminum Alloy", The 13<sup>th</sup> Conference of Mechanical Engineering Network of Thailand, 2-3 December 2542